

**CORRELATION OF FINITE ELEMENT FREE VIBRATION
PREDICTIONS USING RANDOM VIBRATION
TEST DATA**

JEFFREY A. CHAMBERS

Bachelor of Science in Aerospace Engineering
Tri-State University
May, 1989

submitted in partial fulfillment of requirements for the
degree

MASTER OF SCIENCE IN ENGINEERING MECHANICS

at the

CLEVELAND STATE UNIVERSITY

June, 1994

This thesis has been approved for the
DEPARTMENT OF ENGINEERING MECHANICS and
the College of Graduate Studies by

Paul X. Bellini

Dr. Paul X. Bellini / Thesis Committee Chairperson

Department of Engineering Mechanics

05/31/94

Date

Paul A. Bosela

Dr. Paul A. Bosela / Department of Engineering Technology

5/31/94

Date

Majid Rashidi

Dr. Majid Rashidi / Department of Mechanical Engineering

05-31-94

Date

Omar M. Ibrahim

Dr. Omar M. Ibrahim / Structural Dynamics Engineer

Analex Corporation

05/31/94

Date

ACKNOWLEDGEMENTS

I would like to acknowledge the efforts of my entire thesis committee; Dr. Bellini, Dr. Bosela, Dr. Rashidi, and Dr. Ibrahim. All have been very supportive and giving of their time in helping to advance the development of my thesis topic. I would like to extend special thanks to Dr. Bellini for his conscientious help during both my thesis research and supporting course work. Additionally, I would like to thank those people at NASA Lewis Research Center who have given freely of their time to aid in the development of this thesis.

**CORRELATION OF FINITE ELEMENT FREE VIBRATION
PREDICTIONS USING RANDOM VIBRATION
TEST DATA**

JEFFREY A. CHAMBERS

ABSTRACT

Finite element analysis is regularly used during the engineering cycle of mechanical systems to predict the response to static, thermal, and dynamic loads. The finite element model (FEM) used to represent the system is often correlated with physical test results to determine the validity of analytical results provided. Results from dynamic testing provide one means for performing this correlation. One of the most common methods of measuring accuracy is by classical modal testing, whereby vibratory mode shapes are compared to mode shapes provided by finite element analysis. The degree of correlation between the test and analytical mode shapes can be shown mathematically using the cross orthogonality check.

A great deal of time and effort can be exhausted in generating the set of test acquired mode shapes needed for the

cross orthogonality check. In most situations response data from vibration tests are digitally processed to generate the mode shapes from a combination of modal parameters, forcing functions, and recorded response data.

An alternate method is proposed in which the same correlation of analytical and test acquired mode shapes can be achieved without conducting the modal survey. Instead a procedure is detailed in which a minimum of test information, specifically the acceleration response data from a random vibration test, is used to generate a set of equivalent local accelerations to be applied to the reduced analytical model at discrete points corresponding to the test measurement locations. The static solution of the analytical model then produces a set of deformations that once normalized can be used to represent the test acquired mode shapes in the cross orthogonality relation.

The method proposed has been shown to provide accurate results for both a simple analytical model as well as a complex space flight structure.

TABLE OF CONTENTS

Chapter	Page
I. INTRODUCTION	
1.1 Background	1
1.2 Objective	4
1.3 Scope	6
II. THEORETICAL DEVELOPMENT	
2.1 Fundamental Dynamic Relationships	8
2.2 Preparation of Model	10
2.3 Calculation of Static Mode Shapes	16
2.4 Correlating the Mode Shapes	22
2.5 Automating the Process	24
III. CORRELATION PROCESS	
3.1 Demonstration I	27
3.2 Demonstration II	48
IV. DISCUSSION	
4.1 Summary and Conclusions	76
4.2 Recommendations for Further Study	78
REFERENCES	80

APPENDICES

A - MSC/NASTRAN DMAP Listing	81
B - Cantilevered Beam Model	88
C - STDCE Experiment Package	110

LIST OF TABLES

Table		Page
I.	Comparison of Analytical and Test Eigenproblem Results	35
II.	Peak Response Values	42
III.	Response Amplification Values	43
IV.	Acceleration Orientations	44
V.	Equivalent Local Accelerations	45
VI.	Peak Response Data at Selected Frequencies	69
VII.	Response Amplification Values at Selected Frequencies	70
VIII.	Accelerometer/Node Association	73

LIST OF FIGURES

Figure		Page
2.1	Typical Response PSD Plot	15
3.1	Cantilevered Beam Analytical Model	28
3.2	High Fidelity Cantilevered Beam Model	34
3.3	Comparison of Test and Analytical Frequencies - Cantilevered Beam Model	36
3.4	Excitation PSD at Large Mass	37
3.5	Response PSD at One-Third Span	39
3.6	Response PSD at Two-Thirds Span	40
3.7	Response PSD at Full Span	41
3.8	STDCE Flight Experiment Structure	50
3.9	STDCE Flight Experiment Structure	51
3.10	STDCE Flight Experiment Structure - Finite Element Model	52
3.11	STDCE Flight Experiment Structure - Finite Element Model	53
3.12	STDCE Flight Experiment Structure Random Vibration Test Levels	55
3.13	STDCE Flight Experiment Structure Response Accelerometer Locations	56
3.14	STDCE Flight Experiment Structure Mode 1 - 66.5 Hz	58
3.15	STDCE Flight Experiment Structure Mode 2 - 71.1 Hz	59
3.16	STDCE Flight Experiment Structure Mode 3 - 88.1 Hz	60

3.17	STDCE Flight Experiment Structure Mode 4 - 108.3 Hz	61
3.18	STDCE Flight Experiment Structure Mode 5 - 112.7 Hz	62
3.19	STDCE Flight Experiment Structure Mode 6 - 122.2 Hz	63
3.20	STDCE Flight Experiment Structure Mode 7 - 163.2 Hz	64
3.21	STDCE Flight Experiment Structure Mode 8 - 186.6 Hz	65
3.22	Sample Control and Response Measurements	67
3.23	Comparison of Test and Analytical Frequencies	71

NOMENCLATURE

A	Cross sectional area
a	Local acceleration
B	Damping matrix
C	Cross orthogonality matrix
D	Intermediate matrix
E	Modulus of elasticity (flexural)
$F(t), F$	Dynamic force vector
f	Cyclic frequency
G	Intermediate matrix
g	Acceleration due to gravity
I	Identity matrix
I	Bending moment of inertia
K	Stiffness matrix
L	Element length
M	Mass matrix
PSD	Power spectral density
Q	Response amplification factor
$S(\omega)$	Power Spectral Density function
v	Displacement
$X(t), X$	Generalized displacement
x	Displacement

α	Frequency response function
λ	Eigenvalue
ν	Poisson's ratio
ρ	Mass density
ϕ	Eigenvector or eigenvector matrix
ω	Circular frequency

Subscripts

A	Analytical related matrix
a	Active set
f	Displacement set
G	Generalized matrix
I	Input
O	Output
o	Omitted set
s	Iteration
T	Test related matrix

CHAPTER I

INTRODUCTION

1.1 Background

During the engineering development cycle of structural/mechanical systems, finite element models are often used to provide insight into the static and dynamic response characteristics of the system. Given the broad assumptions made during the finite element modeling process, there is a need to verify the accuracy of the modeling techniques employed. The validity of these math models is usually substantiated through static or dynamic tests conducted on the engineered system. Results taken from these physical tests are compared with analytical results provided by the finite element model (FEM) under the same boundary and loading conditions.

Probably one of the most common methods used to validate a finite element model is through the use of modal testing and

correlation [1]. With this technique, the physical test specimen is fixtured to represent its working environment, or may be suspended in such a manner as to simulate free restraint condition, and is subjected to a known forced excitation (or simultaneous excitations). The response of the system to this excitation is measured at various points about the structure. The response data gathered is then analyzed by making a transformation from physical (spacial) coordinates to modal coordinates and the frequency response characteristics of the system are generated mathematically by observing the relationships between the forcing functions, response data, and known modal parameters. This allows the generation of mode shapes at resonant frequencies of the structure that can be compared to the frequencies and mode shapes provided by the analytical model.

The mode shapes generated from the physical test can be mathematically compared to those from analysis by a number of methods, with one of the more popular being the cross orthogonality relation

$$[C]_{ij} = [\phi_A]^T [M_A] [\phi_T] \quad (1.1)$$

where $[C]_{ij}$ is the cross orthogonality matrix correlating the i -th analytical mode shape with the j -th test mode shape [2]. Matrices $[\phi_A]$ and $[\phi_T]$ represent the assemblage of analytical and test acquired mode shapes, respectively, while $[M_A]$ is the analytically derived mass matrix.

Under ideal correlation where the test and analysis mode shapes correlate identically, the resulting cross orthogonality matrix appears as a unit diagonal matrix. Under more realistic situations where the degree of correlation is less than ideal, the degree of variation between the two sets of mode shapes is identified by the density and magnitude of the off-diagonal terms appearing in the cross orthogonality matrix. Generally, satisfactory correlation is obtained if the cross orthogonality matrix possesses no off-diagonal terms exceeding 0.20 indicating twenty percent miscorrelation between the i -th analytical and j -th test mode shapes.

Unfortunately, the process of modal testing can be quite expensive and time consuming. It is not uncommon for the modal test to consume many hundreds or thousands of man-hours to set up, conduct, and post-process the data. It also requires the use of specialized digital processing equipment and software that may not always be available to the engineer. This can make the correlation process somewhat prohibitive for smaller scale engineering projects.

The process of correlating a finite element model can be optimized if it may be done without the testing required with the modal technique. In the case of space flight hardware, this optimization could be realized if the frequency response information needed from the test article could be provided by means of the random vibration data that is normally acquired during the flight qualification process. Random vibration

testing is usually required in the engineering process to prove the system's structural and functional survivability when subjected to the anticipated flight environment. This is in sharp contrast to the modal technique which is necessitated by the desire to validate the analytical assumptions. Consequently if the engineering assumptions can be quantified by the random vibration test, additional resources need not be allocated for a separate modal survey.

Normally, the random vibration response data is not accepted as valid correlation input since it only shows the existence of resonance but in its raw form does not provide any insight into the mode shape present at the resonant frequency. In essence, the resonant frequency indicated by the random response data may ideally match a frequency provided by analysis yet contain a completely different mode of vibration.

1.2 Objective

Consider a scenario in which the random vibration data gathered at a discrete number of spatial locations on the test article is reduced to provide peak response and amplification data for a limited number of primary frequencies indicated by the test data and assumed to correspond with predetermined analytical frequencies. These analytical frequencies at which correlation is sought could be selected from the free

vibration analysis to represent the fundamental system frequencies. This can easily be accomplished by selecting modes in which there is significant mass participation. Assuming that for any of these predetermined frequencies if the structure were subjected to static loads equivalent to those generated by the flight random vibration environment, some sort of deflected shape could be expected. It stands to reason therefore that since the random vibration test provides local accelerations at discrete spacial locations and frequencies the analyst should be able to surmise a deflected shape for any of the resonant frequencies chosen from the test data.

Given Power Spectral Density (PSD) output from a random vibration test, peak response and amplification values can be extracted for any number of selected frequencies. By use of basic dynamic relationships, this response and amplification data can be used to generate equivalent local accelerations corresponding to the accelerometer locations and directions monitored during the testing event. Assuming that these equivalent local accelerations possess the proper orientations and magnitudes, when applied to the FEM and a static analysis performed, a static deformation is produced resembling the mode shape expected at the frequency from which the response values were taken. This static deformation can then be mass normalized in the same manner as an eigenvector would be to form a static or 'pseudo' mode shape. This static mode shape

can then be used in the cross orthogonality correlation, taking the place of the test acquired mode shape that would have been generated via the modal technique. By carrying out this procedure, a set of static mode shapes can be generated from the frequency response characteristics of the physical model without the need for any additional testing above that done in the normal flight qualification process.

1.3 Scope

This thesis provides a detailed method for accomplishing the dynamic to static transformation which allows for the generation of the static or 'pseudo' mode shapes.

The equations governing the correlation process, from the basic eigenproblem through the cross orthogonality check are outlined to examine their relevance to the process. A discussion is also presented on the preparation of both the analytical model and random vibration test data. This includes the reduction of the analytical model to those same degrees of freedom observed in the vibration test as well as the reduction of the random vibration data to the parameters required in the calculations. The calculation of the static mode shapes, their mass normalization, and comparison with the mode shapes provided by the free vibration analysis is presented in detail.

Lastly, the correlation process is demonstrated in full

for both a simplistic cantilevered beam model as well as for an actual article of space flight hardware. The results of both examples indicate that the process generates accurate system mode shapes and provides a greatly abbreviated correlation method.

CHAPTER II

THEORETICAL DEVELOPMENT

2.1 Fundamental Dynamic Relationships

The basic response characteristics (for both free and forced vibration) of a mechanical system can be expressed by means of the frequency response function (FRF). This mathematical relation contains the mass, stiffness, and damping properties of the system and can be used to evaluate the frequency of vibration as well as the relative displacements of the points within the system. In terms of the spacial model, the mechanical system is described by mass, stiffness, and damping properties

$$[M] \{\ddot{x}\} + [B] \{\dot{x}\} + [K] \{x\} = \{F(t)\} \quad (2.1)$$

Considering the response to be a time varied function and with the presence of damping the complete solution to be complex, the FRF of the mechanical system can be written in

terms of the modal properties of frequencies and eigenvectors (mode shapes).

$$x(t) = xe^{i\omega t} \quad (2.2)$$

$$(-\omega^2 [M] + i\omega [B] + [K]) xe^{i\omega t} = Fe^{i\omega t} = F(t) \quad (2.3)$$

$$\alpha_{ij}(\omega) = \left(\frac{X_j}{F_k} \right) = \sum_{r=1}^N \frac{(\phi_j)_r (\phi_k)_r}{(K_r - \omega^2 M_r) + i(\omega B_r)} \quad (2.4)$$

The preceding FRF represents a single term in the complete FRF matrix that describes all modal properties of the system. Ewins [1] provides a detailed development of the FRF and its relevance in vibration testing.

The response of the system to random excitation is a function of the total FRF and the source excitation. If this input excitation is a time varied function of acceleration and is considered to be a random process with a uniform spectral density, $S_I(\omega)$, then the spectral density response, $S_O(\omega)$, may be represented by the following function

$$S_O(\omega) = |\alpha(\omega)|^2 S_I(\omega) \quad (2.5)$$

Given the Power Spectral Density (PSD) function above [3], it is evident that the response of a mechanical system to a random excitation is dependent upon the full complement of frequency response functions used to describe the mechanical

system. Realization of this dependency enables the transformation from random response characteristics back to static response characteristics as proposed in the correlation process. In the modal method, the frequency response function is operated on directly to provide the system mode shapes. The process to be developed uses the response as provided by Equation 2.5 to generate the system mode shapes. It is important to note, however, that the response provided by the random response function contains all of those same frequency response characteristics present in the modal method.

Although the origin, development, and theories behind the frequency response and power spectral density functions are very important in the analysis of dynamic systems, their direct applications have very little impact on the development of the process at hand. It is left up to the reader to become familiar and comfortable with the mathematical origins of these topics.

2.2 Preparation of Model

The correlation process deals with three varying levels of fidelity representing the same mechanical system. The physical test specimen represents a continuum system while the analytical model represents the continuum system through significantly reduced degrees of freedom. Thirdly, the

testing process gathers response data at a discrete number of points (and directions) that represents still yet a further reduction in the active degrees of freedom when compared with the already reduced analytical model. Consequently in working with the analytical and test models there needs to exist a correspondence for those active degrees of freedom coincident to both. Generally this means that the positioning of accelerometers on the physical specimen are judiciously selected so that the response measurements can accurately represent the dominant response characteristics of the structure. The positioning of these accelerometers can be greatly aided by studying the predictions provided by the analytical model. The analysis can provide great insight into the system modes containing significant amounts of mass participation as well as indicating spacial locations where maximum dynamic deflections occur. Using this information to place the accelerometers increases the likelihood of observing the peak response characteristics during the testing event.

However, in the reverse process of applying measured data to the analytical model in performing the correlation process, it is also desirable to reduce the many degrees of freedom present in the model to those same degrees of freedom which were measured in test. Doing so allows a one-to-one correlation between the analytical and physical properties. When using MSC/NASTRAN for the analysis, this reduction in active degrees of freedom can be accomplished through Guyan

(static condensation), Generalized Dynamic Reduction, or component modal synthesis. The Guyan reduction method will be used throughout this work. In the terminology of MSC/NASTRAN [4] the degrees of freedom in the displacement set $\{x_r\}$ are partitioned into the active set $\{x_a\}$ and the omitted set $\{x_o\}$. The active set is that set remaining after condensation on which the analysis is performed. Partitioning of the spacial system is performed such that properties of the full structure are maintained after condensation. In short, the reduction of the free vibration problem is done in the following manner

$$[M_{ff}]\{\ddot{x}\} + [B_{ff}]\{\dot{x}\} + [K_{ff}]\{x_f\} = \{0\} \quad (2.5)$$

$$\begin{bmatrix} K_{aa} & K_{ao} \\ K_{oa} & K_{oo} \end{bmatrix} \begin{Bmatrix} x_a \\ x_o \end{Bmatrix} = \begin{Bmatrix} 0 \\ 0 \end{Bmatrix} \quad (2.6)$$

$$[K_{aa}]\{x_a\} + [K_{ao}]\{x_o\} = \{0\} \quad (2.7)$$

$$[K_{oa}]\{x_a\} + [K_{oo}]\{x_o\} = \{0\} \quad (2.8)$$

$$[G_{oa}] = -[K_{oo}]^{-1}[K_{oa}] \quad (2.9)$$

$$\{x_o\} = [G_{oa}]\{x_a\} \quad (2.10)$$

$$\{x_f\} = \begin{Bmatrix} x_a \\ x_o \end{Bmatrix} = \begin{bmatrix} [I] \\ [G_{oa}] \end{bmatrix} \{x_a\} \quad (2.11)$$

$$\begin{bmatrix} [I] \\ [G_{oa}] \end{bmatrix}^T [-\omega^2 [M_{ff}] + i\omega [B_{ff}] + [K_{ff}]] \begin{bmatrix} [I] \\ [G_{oa}] \end{bmatrix} \{x_a\} = \{0\} \quad (2.12)$$

which results in the final set of equations for the reduced model (system)

$$[-\omega^2 [M_{aa}] + i\omega [B_{aa}] + [K_{aa}]] \{x_a\} = \{0\} \quad (2.13)$$

For a forced vibration problem, the static condensation presented above takes some liberties with the time dependency of the force vectors involved. But for the free vibration problems presented in the correlation problem, these assumptions pose no degradation in the solution process. Therefore, the Guyan Reduction methods used by MSC/NASTRAN can be used without concern. Alternately, Generalized Dynamic Reduction may also be employed (which retains all factors in the force vectors) with the same results being obtained. Regardless of the method employed, either method allows for the reduction from the full set of active degrees of freedom to a set corresponding with the test measurement points and directions.

During the testing event, acceleration response data are

gathered and processed to provide a set of PSD curves for each accelerometer on the test specimen as well as those accelerometers mounted on fixturing which provide a control feedback loop to the excitation equipment. These PSD curves generally appear as shown in Figure 2.1, one existing for each DOF recorded, providing acceleration response data in terms of acceleration squared per unit frequency (g^2/Hz) versus cyclic frequency (Hz). When biaxial or triaxial accelerometers are used, two or three such PSD curves appear for the same discrete spacial location at which the accelerometer is attached. This enables the engineer to observe response in up to three translational directions at any given point on the structure. In general, only translational accelerations are measured since the measurement, processing, and application of rotational accelerations is seldom used.

The random response data can provide a means of identifying principle modes of vibration. Each set of data (in reference to a given excitation) can be evaluated to indicate principle modes excited by the input energy. Generally, the response data can indicate a primary mode of vibration by numerous appearances of distinct peaks at the same frequency. Once a number of these modes have been identified as being primary system modes or local modes of interest, the peak values for each can be recorded from the set of PSD curves. Amplification data can be calculated from the response data at each of these frequencies by dividing the

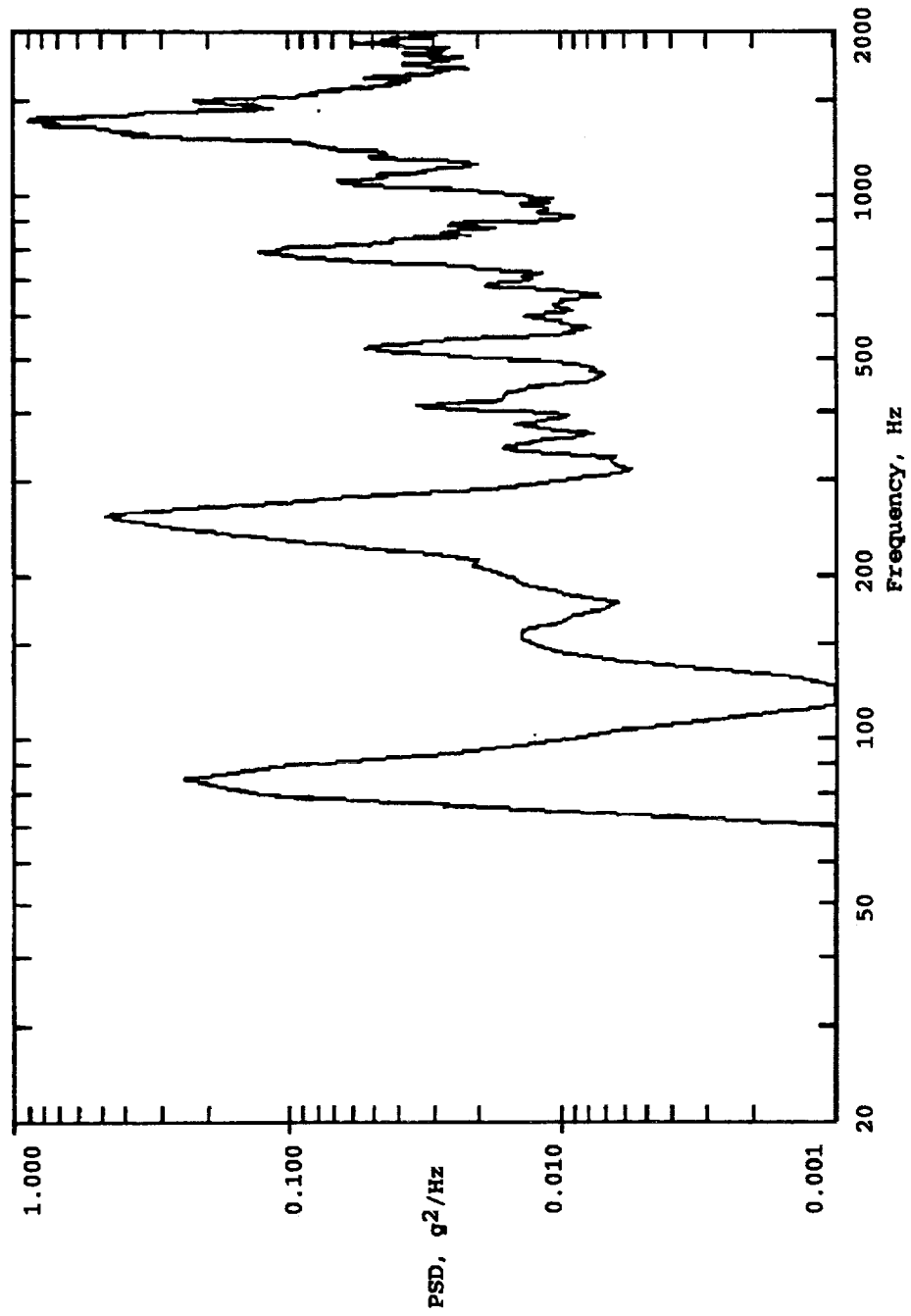


FIGURE 2.1
Typical Response PSD Plot

response PSD by the input PSD (from the control accelerometers). For a given DOF and frequency the associated amplification, or quality factor, may be calculated as

$$Q_i = \frac{PSD_{resp}}{PSD_{input}} \quad (2.14)$$

2.3 Calculation of Static Mode Shapes

Once the test data has been reduced to a set of frequencies, peak PSD and amplification values, the corresponding static or 'pseudo' mode shapes can be calculated using the analytical model.

With the reduction of the analytical model to the degrees of freedom measured in test, as demonstrated earlier, the apparent mass and stiffness of the FEM are given by matrices $[M_{aa}]$ and $[K_{aa}]$. In order to produce statically deformed shapes from this mass and stiffness, the peak PSD and amplification values must be transformed to equivalent local accelerations so that the static system of equations may be solved

$$[K_{aa}] \{x\}_i = [M_{aa}] \{a\}_i \quad (2.15)$$

where $\{x\}_i$ represents the static deflection, or static mode shape, resulting from the application of the equivalent local

accelerations $\{a\}_i$. The vector of equivalent local accelerations $\{a\}_i$ can be assembled from the individual peak PSD and amplification values for each DOF present. The transformation from dynamic response to equivalent local acceleration is performed by use of Mile's equation [5]

$$a_i = \pm 3.0g \sqrt{\left(\frac{\pi}{2}\right) Q_i PSD_i f} \quad (2.16)$$

where a_i = equivalent local acceleration
 g = acceleration due to gravity
 Q_i = amplification factor from test
 PSD_i = peak PSD value from test
 f = frequency (cyclic) of interest
 i = degree of freedom

This local acceleration term, a_i , represents the equivalent acceleration obtained for a single degree of freedom on the test article at a single frequency point. If the article is instrumented with five triaxial accelerometers, then there will be fifteen such local accelerations calculated and assembled to form a single acceleration vector, $\{a\}_i$. Likewise, if four frequencies are chosen for correlation, there will be four acceleration vectors, $\{a\}_i$, assembled from the test data.

The PSD and amplification factors involved come from test data at a specific frequency value that may or may not be

identical to the frequency indicated by analysis but at which the correlation is sought. To prevent introduction of error from the test sequence (in reference to the frequency discrepancies) it is preferable to use the frequency (f) as provided by analysis. In other words, the correlation is always going to be less than ideal since the test and analysis models will never be identical. The intended purpose of the correlation process is to compare the mode shapes of the two and therefore it is desirable to avoid introducing additional error into the calculations. A comparison of test and analysis frequencies can be made on a much smaller scale as will be demonstrated later. For this reason, the analytical frequencies are used in the calculation of the equivalent local accelerations.

One last step is required in the preparation of the test data. The response data coming from test is assumed to be in the proper relative magnitudes but contains no information concerning the orientation, or direction, of the acceleration. Some insight is needed to orient the applied accelerations so that they are meaningful in the solution of the static system of equations. The orientation of each acceleration can be taken from the corresponding degree of freedom of the eigenvector as predicted by the normal modes analysis. The analytical eigenvector for each mode to be correlated can easily be reduced to a directional vector containing positive or negative values of unity to give the accompanying

acceleration vector the proper orientation at the reduced nodal degrees of freedom.

From the static equations, the deformed shape, $\{x\}_i$, resulting from the application of the equivalent local accelerations is performed by pre-multiplying both sides of the static equation by the inverse of the reduced stiffness matrix $[K_{aa}]$.

$$[K_{aa}]^{-1} [K_{aa}] \{x\}_i = [K_{aa}]^{-1} [M_{aa}] \{a\}_i \quad (2.17)$$

$$\{x\}_i = [K_{aa}]^{-1} [M_{aa}] \{a\}_i \quad (2.18)$$

This statically deformed shape is not unlike a raw eigenvector having unbounded magnitudes of its components, and may appear somewhat meaningless when first observed. However, just as in an eigenanalysis, this deformed shape can be mass normalized to provide the static or 'pseudo' mode shape.

$$\{\phi_T\}_i = \frac{\{x\}_i}{\sqrt{\{x\}_i^T [M_{aa}] \{x\}_i}} \quad (2.19)$$

Ideally, it would appear that the series of equations shown above could be applied consecutively for all the vectors of equivalent local accelerations representing the modes desired to be correlated. But in fact if this were carried out consecutively for a number of modes, it becomes evident that the lower order modes have a large influence on the

subsequent modes derived. The higher order modes exhibit strong content of the lower modes, with the lowest mode exhibiting the greatest influence.

To carry out the correlation process for modes other than the lowest analytical mode presented, the influence of each successive mode must be removed from the active set of equations. This is easily performed by applying classical matrix deflation techniques [6] to the system of equations. Letting

$$[D]_i = [K_{aa}]_i^{-1} [M_{aa}]_i \quad (2.20)$$

and

$$\{x\}_i = [D]_i \{a\}_i \quad (2.21)$$

Then by classical matrix deflation techniques, the apparent mass and stiffness of the system excluding the effects of vectors just iterated upon are established by

$$[D]_{i+1} = [D]_i - \frac{1}{\lambda_i} \left(\frac{\{\phi\}_i \{\phi\}_i^T [M_{aa}]_i}{\{\phi\}_i^T [M_{aa}]_i \{\phi\}_i} \right) \quad (2.22)$$

where λ_i and $\{\phi\}_i$ are the eigenvalue and eigenvector as provided by analysis, not test. Using the analytical values again keeps the active mass and stiffness from becoming contaminated with the error introduced by test. Also note

that to prevent the introduction of error, the eigenvalue and eigenvector taken from analysis must be accurate enough to prevent affecting downstream calculations.

If the analytical eigenvector is mass normalized as part of its original processing, the denominator in the right side of the equation takes on the value of unity by definition. This allows the further simplification to

$$[D]_{i+1} = [D]_i - \frac{1}{\lambda_i} \{\phi\}_i \{\phi\}_i^T [M_{aa}] \quad (2.23)$$

The solution of the second deflected shape in the series is then

$$\{x\}_{i+1} = [D]_{i+1} \{a\}_{i+1} \quad (2.24)$$

This deformed shape is also mass normalized with respect to the analytical reduced mass matrix to complete the iteration and all subsequent static mode shapes are iterated upon in the same manner.

It is important to reiterate that each successive mode shape appearing in the analytical results must be swept from the mass and stiffness matrices for the calculation of higher order modes, even if that particular mode is not one to be correlated. That is to say that if it is sought to correlate the first, third, and fourth analysis modes, the second mode must be swept from the system before the third and fourth eigenvectors are calculated. Otherwise the presence of the

second mode will heavily influence the latter static mode shapes.

2.4 Correlating the Mode Shapes

When all of the static mode shapes desired for correlation have been calculated, the degree at which they match the analytical mode shapes can be evaluated using any number of methods, e.g. Modal Assurance Criterion, Cross Orthogonality Criterion, etc. For the sake of demonstration purposes, the cross orthogonality method has been chosen in this thesis work. The cross orthogonality method can be expressed by

$$[C] = [\phi_A]^T [M_{aa}] [\phi_T] \quad (2.25)$$

Where $[\phi_A]$ is a matrix formed by assembling the eigenvectors from analysis and $[\phi_T]$ is the matrix formed by assembling the static or 'pseudo' mode shapes as calculated by the process outlined above. The cross orthogonality matrix is a square matrix where the diagonal terms represent the orthogonality condition between each of the analytical and test eigenvectors. If the i -th analysis eigenvector is identical to the i -th test (pseudo) eigenvector, the i -th diagonal term in $[C]$ would be unity.

$$\{\phi_A\}_i^T [M_{aa}] \{\phi_T\}_i = 1.0 \quad (2.26)$$

Therefore anything less than unity on the diagonal indicates some level of skew between the analysis and test eigenvectors.

The off-diagonal terms represent the orthogonality condition between the i -th analytical and j -th test eigenvectors. By the principal of orthogonality, two eigenvectors from the same eigenproblem must be perpendicular, or orthogonal, to each other. Mathematically

$$\{\phi_A\}_i^T [M_{aa}] \{\phi_T\}_j = 0.0 \quad (2.27)$$

Therefore for ideal correlation between the analytical and test models, the cross orthogonality matrix would appear as a unit diagonal matrix. Realistically, where the correlation between the analytical and test models is not ideal the diagonal terms will become less than unity while the off-diagonal terms will increase from zero. If the correlation experienced is less than acceptable, the finite element model can be 'tuned' to gain more accurate distributions of mass and stiffness. Iterations on the FEM can be followed by recalculation of the static modes shapes and the cross orthogonality matrix. The vibration testing need only be conducted once since the same data is used for each iteration on the finite element model. Usually, satisfactory correlation has been achieved when the absolute values of diagonal terms are greater than 0.90 and the

absolute values of the off-diagonal terms are limited to 0.20 or less. These limits are usually applied for those modes deemed principal system modes or for local modes of particular interest.

2.4 Automating the Process

A Direct Matrix Abstraction Program (DMAP) alter has been written for Version 67.5 of MSC/NASTRAN [7] to carry out the sequence of operations presented above. This DMAP alter uses the analytical model, once reduced with Guyan or Generalized Dynamic Reduction, to calculate the static mode shapes in the same run sequence as a free vibration analysis is performed. The DMAP statements are compiled in the MODERS module where MSC/NASTRAN performs the real eigenvalue analysis. The user is required to input matrices assembled from the vectors of peak PSD and amplification values (Q) as well as a listing of the analytical modes to be correlated. Peak PSD and amplification values are entered via the DMI bulk data entry cards (PSD and QUAL) while the list of modes to be correlated are entered via a DTI entry (MODELST). The user is also required to input several constant parameters to describe the acceleration due to gravity (GRAV), maximum number of modes predicted by analysis (NMAX), number of modes to be matched (NMODES), and number of reduced degrees of freedom (NTEST).

The latter three values are used for partitioning the various matrices assembled internal to MSC/NASTRAN. The user is also required to disable the internal resequencing routine within MSC/NASTRAN so that no transformation between the internal and external node numbering schemes is implemented. This helps to prevent application of the external accelerations to wrong internal degrees of freedom.

The DMAP alter recovers the reduced analytical mass and stiffness matrices, M_{aa} and K_{aa} , as well as the eigenvalue and eigenvector matrices from the modal analysis. These eigenvalue and eigenvector matrices are partitioned and reduced for the modes to be correlated as indicated in the DTI MODELST entry. The reduced eigenvector matrix is partitioned term by term and the directional orientation of each DOF is determined. A matrix (NDIR) is then assembled using these directional orientations. The test data is then read and the equivalent local acceleration matrix is formed by using Mile's relation with the information provided.

The static mode shapes are calculated and mass normalized as demonstrated earlier. After each static mode shape is calculated, the influence of the corresponding analytical mode shape is swept from the reduced mass and stiffness matrices. Any intermediate modes not chosen for correlation are also swept from the system before subsequent higher order static mode shapes are calculated. The resulting matrix of static mode shapes (PHITST) is automatically printed for the user.

Lastly, the reduced analytical eigenvector, reduced analytical mass, and static mode shape matrices are used to perform the system cross orthogonality calculation. The resulting cross orthogonality matrix (COC) is also printed for the user.

A complete listing of the DMAP alter is given in Appendix A.

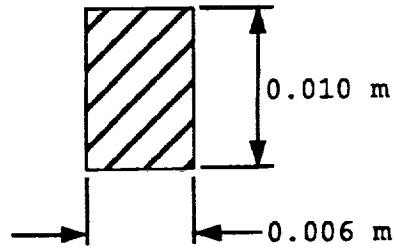
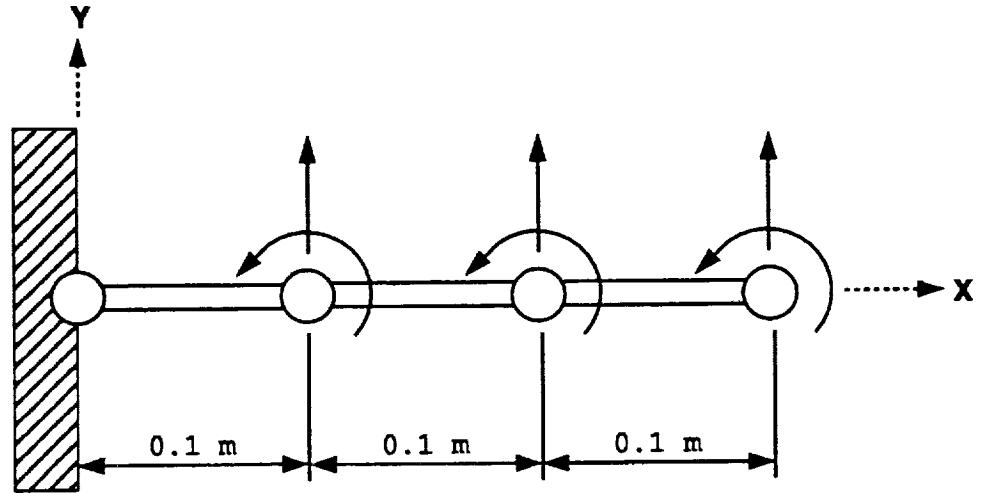
CHAPTER III

CORRELATION PROCESS

3.1 Demonstration I

For purposes of developing the correlation process, a simple cantilevered beam model was used as the baseline system. The analytical model is a cantilevered beam as shown in Figure 3.1 consisting of four (4) nodes with two degrees of freedom per node, one translational and one rotational. The nodes are connected by three Bernoulli-Euler beam elements with consistent mass and stiffness [8] as given below

$$[M_i] = \left(\frac{\rho AL}{420} \right) \begin{bmatrix} 156 & 22L & 54 & -13L \\ 22L & 4L^2 & 13L & -3L^2 \\ 54 & 13L & 156 & -22L \\ -13L & -3L^2 & -22L & 4L^2 \end{bmatrix} \quad (3.1)$$



$$E = 70.0 \text{ MPa}$$

$$\nu = 0.33$$

$$\rho = 2700 \text{ kg/m}^3$$

$$I = 5.0 \times 10^{-10} \text{ m}^4$$

$$A = 6.0 \times 10^{-5} \text{ m}^2$$

FIGURE 3.1
Cantilevered Beam Analytical Model

$$[K_i] = \left(\frac{EI}{L^3} \right) \begin{bmatrix} 12 & 6L & -12 & 6L \\ 6L & 4L^2 & -6L & 2L^2 \\ -12 & -6L & 12 & -6L \\ 6L & 2L^2 & -6L & 4L^2 \end{bmatrix} \quad (3.2)$$

Substituting the geometric properties of the beam, assembling the connectivity, and condensing out degrees of freedom associated with the cantilevered restraint, the mass and stiffness matrices appear as follows

$$[M_{aa}] = 3.85 \times 10^{-5} \begin{bmatrix} 312.00 & 0.00 & 54.00 & -1.30 & 0.00 & 0.00 \\ 0.00 & 0.08 & 1.30 & -0.03 & 0.00 & 0.00 \\ 54.00 & 1.30 & 312.00 & 0.00 & 54.00 & -1.30 \\ -1.30 & -0.03 & 0.00 & 0.08 & 1.30 & -0.03 \\ 0.00 & 0.00 & 54.00 & 1.30 & 156.00 & -2.20 \\ 0.00 & 0.00 & -1.30 & -0.03 & -2.20 & 0.04 \end{bmatrix} \quad (3.3)$$

$$[K_{aa}] = \begin{bmatrix} 840.00 & 0.00 & -420.00 & 21.00 & 0.00 & 0.00 \\ 0.00 & 2.80 & -21.00 & 0.70 & 0.00 & 0.00 \\ -420.00 & -21.00 & 840.00 & 0.00 & -420.00 & 21.00 \\ 21.00 & 0.70 & 0.00 & 2.80 & -21.00 & 0.70 \\ 0.00 & 0.00 & -420.00 & -21.00 & 420.00 & -21.00 \\ 0.00 & 0.00 & 21.00 & 0.70 & -21.00 & 1.40 \end{bmatrix} \quad (3.4)$$

For free-vibration, the basic eigenproblem can be given as

$$[M_{aa}] \{\ddot{x}\} + [K_{aa}] \{x\} = \{0\} \quad (3.5)$$

Assuming the solution is harmonic in nature,

$$x_i = X \cos(\omega t - \alpha) \quad (3.6)$$

$$\dot{x}_i = -\omega X \sin(\omega t - \alpha) \quad (3.7)$$

$$\ddot{x}_i = -\omega^2 X \cos(\omega t - \alpha) \quad (3.8)$$

Therefore the complete solution is

$$-\omega^2 X \cos(\omega t - \alpha) [M_{aa}] + X \cos(\omega t - \alpha) [K_{aa}] = \{0\} \quad (3.9)$$

$$[[K_{aa}] - \omega^2 [M_{aa}]] \{X\} \cos(\omega t - \alpha) = \{0\} \quad (3.10)$$

$$[[K_{aa}] - \omega^2 [M_{aa}]] \{X\} = \{0\} \quad (3.11)$$

For which the nontrivial solution is

$$\det[[K_{aa}] - \omega^2 [M_{aa}]] = 0 \quad (3.12)$$

Using inverse iteration [6] as the solution scheme and the Rayleigh quotient to force convergence of the eigenvalue

$$[D]_1 = [K_{aa}]_1^{-1} [M_{aa}]_1 \quad (3.13)$$

$$\{v_{s+1}\} = [D]_1 \{x_s\} \quad (3.14)$$

$$\{x_{s+1}\} = \frac{\{v_{s+1}\}}{\sqrt{\{v_{s+1}\}^T [M_{aa}] \{v_{s+1}\}}} \quad (3.15)$$

and the associated eigenvalue is

$$\lambda_{s+1} = \frac{\{v_{s+1}\} [M_{aa}] \{x_s\}}{\{v_{s+1}\} [M_{aa}] \{v_{s+1}\}} \quad (3.16)$$

Upon satisfactory convergence of the eigenvalue, the final eigenvector can be normalized with respect to the system mass (mass normalization).

$$\{\phi_A\}_i = \frac{\{v_{s+1}\}}{\sqrt{\{v_{s+1}\}^T [M_{aa}] \{v_{s+1}\}}} \quad (3.17)$$

Subsequent eigenvectors and eigenvalues are found in the same manner once the system is shifted to remove the influence of the present mode. Therefore

$$[D]_{i+1} = [D]_i - \frac{1}{\lambda_i} \{\phi_A\}_i \{\phi_A\}_i^T [M_{aa}] \quad (3.18)$$

Performing the series of iterations on the analytical model produces the following results

$$\begin{bmatrix} \lambda_i \\ f_i \\ \{\phi_A\}_i \end{bmatrix} = \begin{bmatrix} 329.8 & 1.304e4 & 1.041e5 & 5.278e5 & 1.870e6 & 7.430e6 \\ 2.89 & 18.36 & 51.35 & 115.6 & 217.6 & 433.8 \\ 1.5021 & -5.3845 & 6.7827 & 2.4709 & 2.7984 & 2.3954 \\ 27.358 & -53.667 & -50.501 & -315.713 & 521.238 & 245.673 \\ 4.9630 & -3.8654 & -5.9809 & 1.1416 & -4.9303 & 3.7505 \\ 39.591 & 90.048 & -38.548 & 323.470 & 342.850 & 690.579 \\ 9.0740 & 9.1282 & 9.1159 & -9.8090 & -10.6002 & 19.9162 \\ 41.635 & 145.594 & 241.534 & -418.042 & -702.697 & 1990.912 \end{bmatrix} \quad (3.19)$$

The validity of the eigenvectors calculated can be reinforced by examining the orthogonality conditions present. By definition of mass orthonormality, the eigenvectors associated with distinct eigenvalues must satisfy the following relation

$$[\phi]^T [M] [\phi] = [I] \quad (3.20)$$

where [I] is the real identity matrix. Carrying out the operation

$$[\phi_A]^T [M_{aa}] [\phi_A] = \begin{bmatrix} 1.0000 & 0.0000 & 0.0000 & 0.0000 & 0.0000 & 0.0000 \\ 0.0000 & 1.0000 & 0.0000 & 0.0000 & 0.0000 & 0.0000 \\ 0.0000 & 0.0000 & 1.0000 & 0.0000 & 0.0000 & 0.0000 \\ 0.0000 & 0.0000 & 0.0000 & 1.0000 & 0.0000 & 0.0000 \\ 0.0000 & 0.0000 & 0.0000 & 0.0000 & 1.0000 & 0.0000 \\ 0.0000 & 0.0000 & 0.0000 & 0.0000 & 0.0000 & 1.0000 \end{bmatrix} \quad (3.21)$$

All errors in the orthogonality test were on the order of 10^{-7} indicating that the eigenvectors satisfy the

orthonormality constraint.

The test or physical system for this demonstration problem was simulated with a higher fidelity model (to imitate a continuum system). An MSC/NASTRAN model was created with sixty-one nodes, again with two degrees of freedom per node, and sixty CBAR structural elements. Coupled mass formulation was employed as in the analytical model. This model is shown in Figure 3.2.

Initially, a normal modes analysis was performed on this 'test' model to compare the resulting frequencies with those from the lower fidelity analytical model. The comparison of eigenvalues and cyclic frequencies is shown in Table I.

As can be seen in the comparison, the lower fidelity analysis model is significantly over-stiffened in the higher modes. The stiffening effect of the analytical model is shown graphically in Figure 3.3. The systematic deviation from the ideal line shows the uniform mathematical stiffening created by the dramatic reduction in degrees of freedom associated with the analytical model.

The eigenanalysis of the 'test' model was followed with a random vibration analysis. The original model was augmented by attaching a large (5000 kg) mass to the support node applying a random acceleration excitation (Figure 3.4) to this mass. The excitation was applied in the translational (Y) direction to force bending response in the beam.

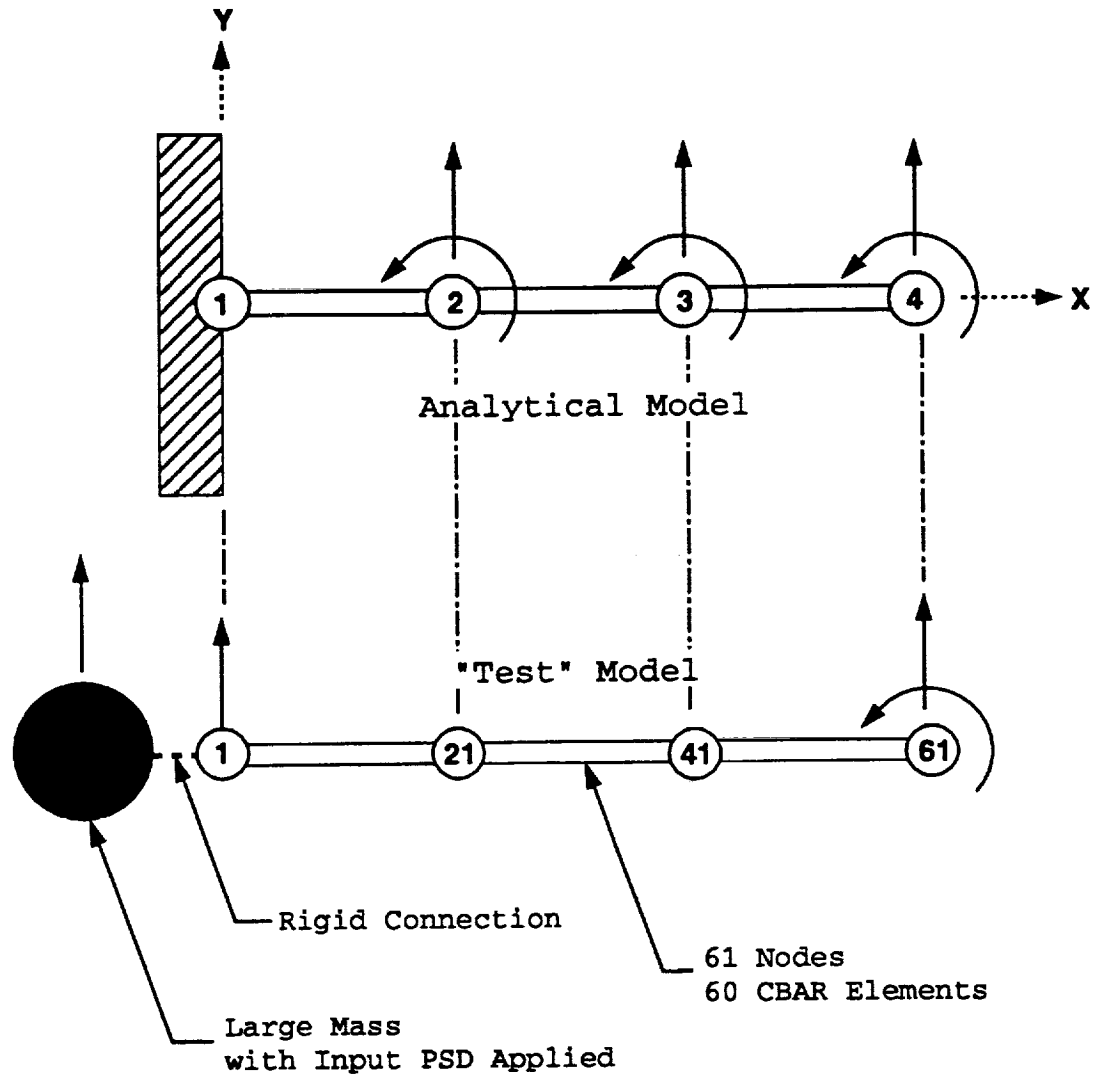


FIGURE 3.2
High Fidelity Cantilevered Beam Model

TABLE I.
Comparison of Analytical and Test Eigenproblem Results

Node	Eigenvalue		Frequency (Hz)		
	Anal.	Test	Anal.	Test	%Diff
1	329.8	329.7	2.89	2.89	0.00
2	13305.3	12950.1	18.36	18.11	-1.42
3	104.1e3	101.5e3	51.35	50.71	-1.25
4	527.8e3	389.9e3	115.6	99.37	-14.0
5	186.9e4	106.5e4	217.6	164.3	-24.5
6	743.0e4	237.8e4	433.8	245.4	-43.4

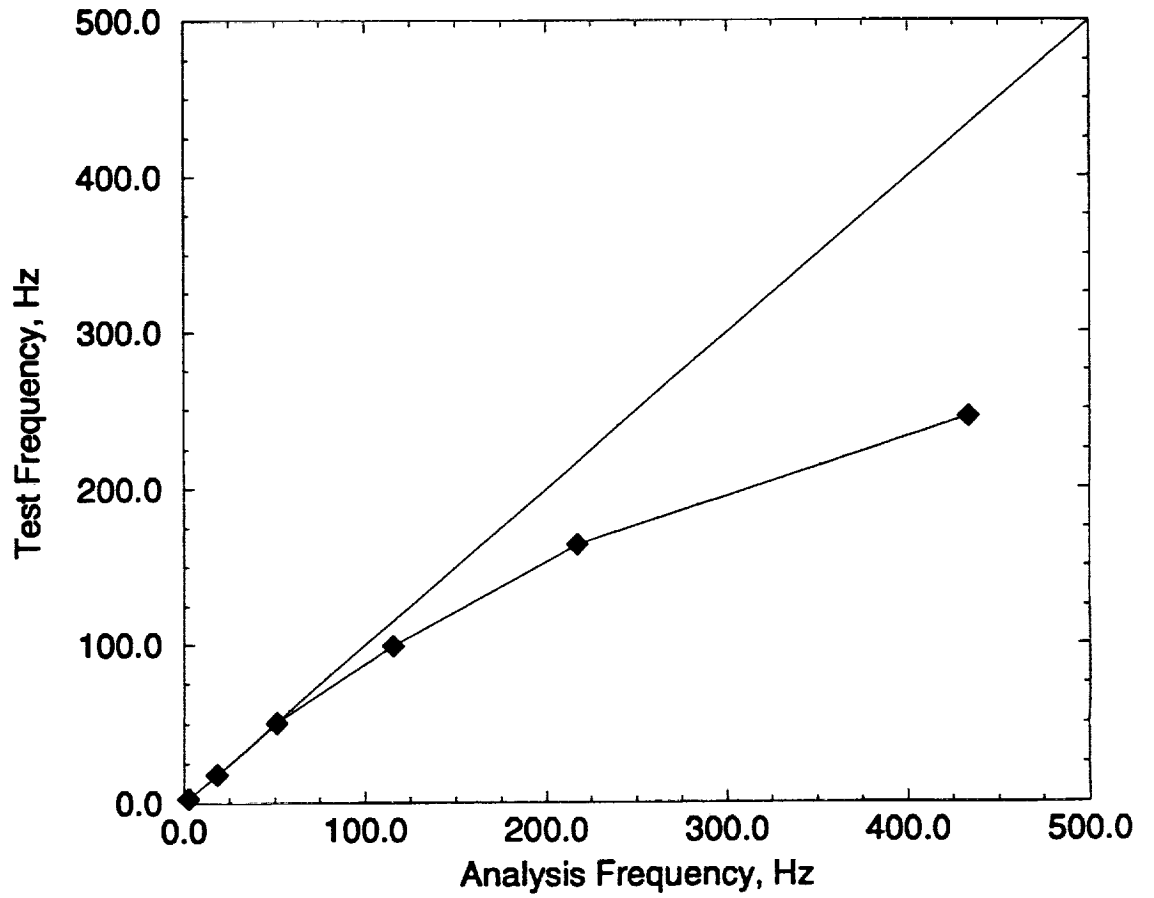


FIGURE 3.3
Comparison of Test and Analytical Frequencies - Cantilevered
Beam Model

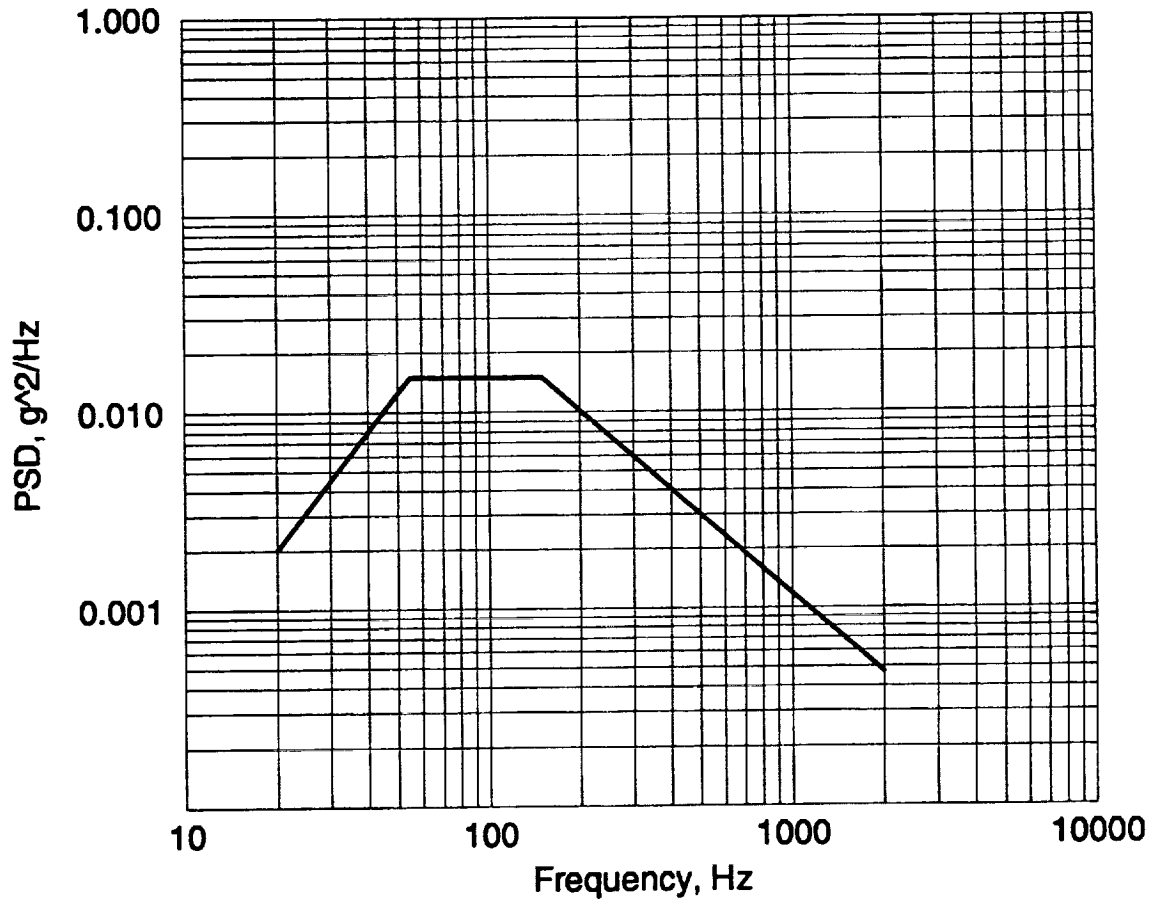


FIGURE 3.4
Excitation PSD at Large Mass

Structural damping equal to ten percent of critical damping ($Q = 5$) was included in the structure and was held constant throughout the frequency range of zero to two thousand Hertz. The translational response Power Spectral Densities were recovered at the three nodes corresponding to the node locations present in the analysis model (excluding the support node). These PSD plots are shown in Figures 3.5, 3.6 and 3.7. The peak response values at resonant frequencies were recorded from the analysis and are summarized in Table II.

By dividing each of the response predictions by the input (control) acceleration, the response amplification values can likewise be tabulated for each active degree of freedom. This set of amplification factors is shown in Table III.

Referring to the matrix of eigenvectors from the analytical model (see Eq. 3.19) the directional attributes of each DOF in each mode can be determined. The nodal directional coefficients are shown in Table IV.

Using Mile's relation as presented earlier, the combination of peak response, amplification, and orientation are used to establish the set of equivalent local accelerations. Note that the frequencies established by the analytical model are used in the calculation of these accelerations. These accelerations are shown in Table V.

Applying these equivalent local accelerations to the analytical model using the process outlined earlier and mass

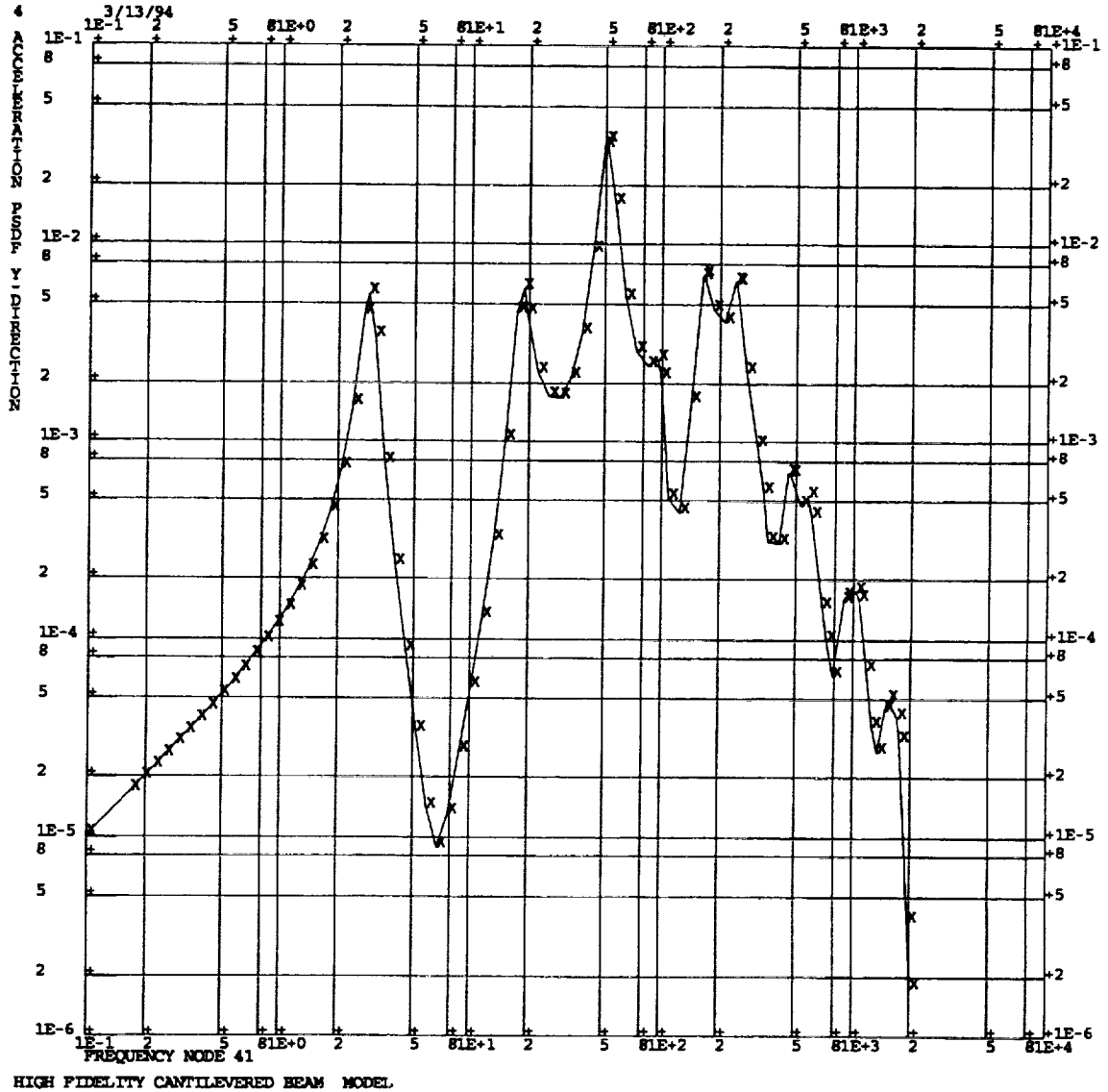


FIGURE 3.6
Response PSD at Two-Thirds Span

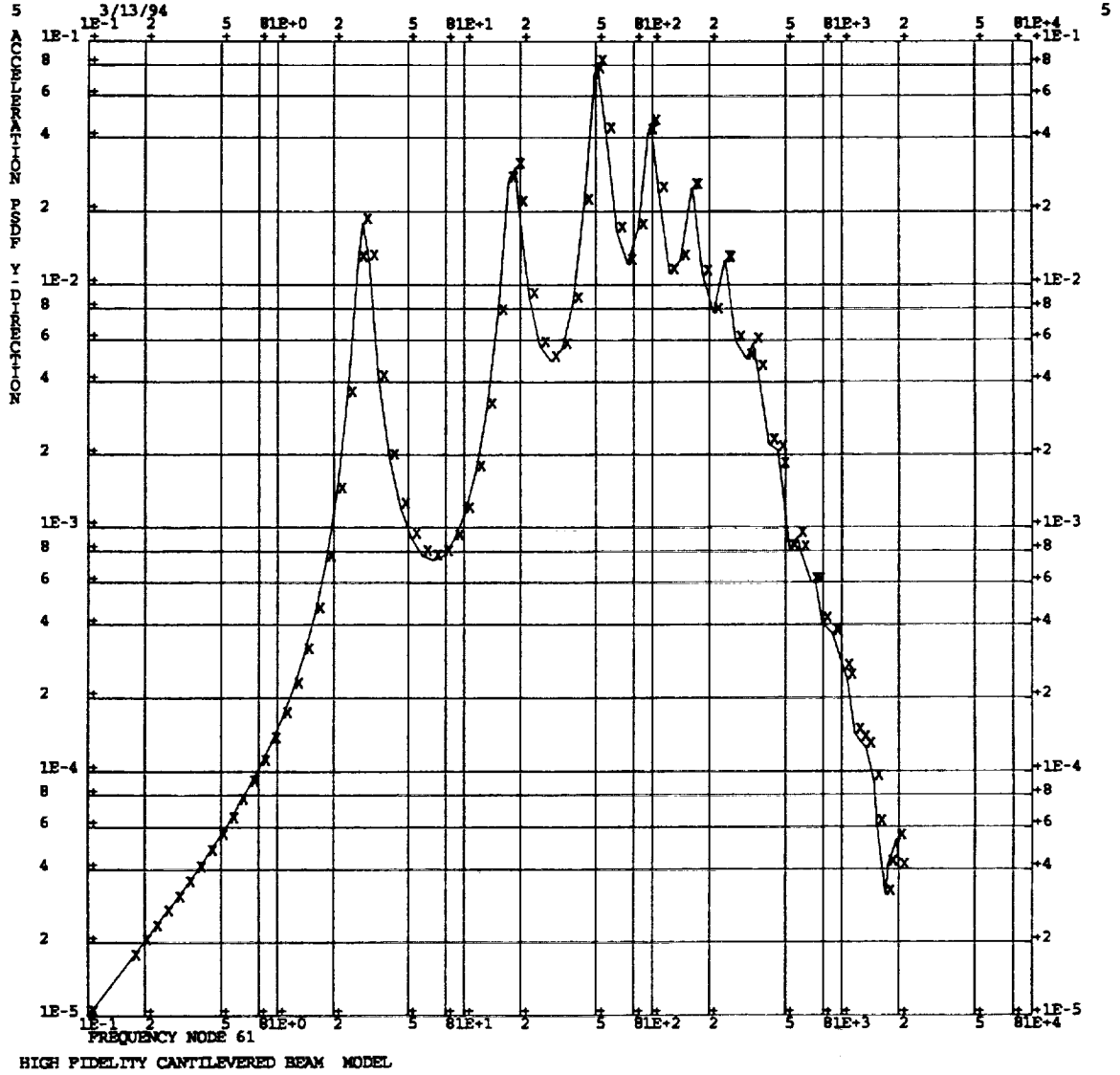


FIGURE 3.7
Response PSD at Full Span

TABLE II.
Peak Response Values

Freq/DOF	Peak PSD Values (g^2/Hz)					
	2.89	18.11	50.71	99.37	164.3	245.4
Input	2.890e-4	1.881e-3	1.300e-2	1.500e-2	1.288e-2	5.290e-3
21T2	8.689e-4	1.029e-2	4.675e-2	4.908e-3	9.372e-3	1.919e-3
21R3	0.0	0.0	0.0	0.0	0.0	0.0
41T2	5.595e-3	5.950e-3	3.365e-2	2.146e-3	6.995e-3	6.339e-3
41R3	0.0	0.0	0.0	0.0	0.0	0.0
61T2	1.799e-2	3.012e-2	8.031e-2	4.531e-2	2.477e-2	1.243e-2
61R3	0.0	0.0	0.0	0.0	0.0	0.0

TABLE III.
Response Amplification Values

Freq/ DOF	Response Amplification Values					
	2.89	18.11	50.71	99.37	164.3	245.4
21T2	3.001	5.470	3.596	0.327	0.728	0.363
21R3	0.0	0.0	0.0	0.0	0.0	0.0
41T2	19.360	3.163	2.588	0.143	0.143	1.198
41R3	0.0	0.0	0.0	0.0	0.0	0.0
61T2	62.249	16.013	6.178	3.021	1.923	2.350
61R3	0.0	0.0	0.0	0.0	0.0	0.0

TABLE IV.
Acceleration Orientations

Freq/ DOF	Acceleration Orientations					
	2.89	18.11	50.71	99.37	164.3	245.4
21T2	1.0	-1.0	1.0	1.0	1.0	1.0
21R3	1.0	-1.0	-1.0	-1.0	1.0	1.0
41T2	1.0	-1.0	-1.0	1.0	-1.0	1.0
41R3	1.0	1.0	-1.0	1.0	1.0	1.0
61T2	1.0	1.0	1.0	-1.0	-1.0	1.0
61R3	1.0	1.0	1.0	-1.0	-1.0	1.0

TABLE V.
Equivalent Local Accelerations

Freq/ DOF	Equivalent Local Accelerations (m/s ²)					
	2.89	18.36	51.35	115.6	217.6	433.8
21T2	3.203	-37.498	108.375	15.892	44.932	20.269
21R3	0.0	0.0	0.0	0.0	0.0	0.0
41T2	20.637	-21.682	-78.007	6.949	-33.536	66.956
41R3	0.0	0.0	0.0	0.0	0.0	0.0
61T2	66.356	109.761	186.174	-146.719	-118.754	131.292
61R3	0.0	0.0	0.0	0.0	0.0	0.0

normalizing each resulting vector with respect to the reduced analytical mass matrix, the following static mode shapes can be derived.

$$\begin{bmatrix} \lambda_i \\ f_i \\ \{\phi_T\}_i \end{bmatrix} = \begin{bmatrix} 329.8 & 1.331e4 & 1.041e5 & 5.278e5 & 1.870e6 & 7.430e6 \\ 2.89 & 18.36 & 51.35 & 115.6 & 217.6 & 433.8 \\ 1.473 & -5.322 & 6.819 & 2.306 & 3.525 & -2.395 \\ 27.046 & -52.912 & -48.600 & -353.950 & 576.020 & -245.673 \\ 4.940 & -3.934 & -6.018 & 1.962 & -3.009 & -3.751 \\ 40.083 & 88.439 & -34.436 & 331.998 & 591.330 & -690.579 \\ 9.128 & 9.251 & 8.940 & -7.070 & -1.709 & -19.916 \\ 42.523 & 149.021 & 230.603 & -189.772 & 156.038 & -1990.91 \end{bmatrix} \quad (3.22)$$

As demonstrated earlier, the orthogonality condition of the eigenvectors calculated can be evaluated using Equation 3.20.

$$[\phi_T]^T [M_{aa}] [\phi_T] = \begin{bmatrix} 1.000 & 0.006 & 0.000 & 0.000 & 0.000 & 0.000 \\ 0.006 & 1.000 & 0.010 & -0.004 & 0.000 & 0.000 \\ 0.000 & 0.010 & 1.000 & 0.006 & 0.007 & 0.001 \\ 0.000 & -0.004 & 0.006 & 1.000 & -0.074 & -0.073 \\ 0.000 & 0.000 & 0.007 & -0.074 & 1.000 & -0.402 \\ 0.000 & 0.000 & 0.001 & -0.073 & -0.402 & 1.000 \end{bmatrix} \quad (3.23)$$

The orthogonality results shown above indicate that static eigenvectors calculated do experience some error, particularly with respect to the orthogonality between the fifth and sixth modes. The remaining modes appear to modestly satisfy the orthogonality constraint. The fifth and sixth

modes appear to be fairly orthogonal to the other four modes but do experience some degree of skew between each other.

Using the set of static eigenvectors and considering them to be the test acquired mode shapes, the cross orthogonality check can be performed.

$$[C] = \begin{bmatrix} 1.000 & 0.000 & 0.000 & 0.000 & 0.000 & 0.000 \\ 0.006 & 1.000 & 0.000 & 0.000 & 0.000 & 0.000 \\ 0.000 & 0.010 & 1.000 & 0.000 & 0.000 & 0.000 \\ 0.000 & -0.004 & 0.007 & 0.991 & 0.000 & 0.000 \\ 0.000 & 0.000 & 0.008 & -0.113 & 0.916 & 0.000 \\ 0.000 & 0.000 & -0.001 & 0.073 & 0.402 & -1.000 \end{bmatrix} \quad (3.24)$$

As can be seen, five out of the six modes correlate nearly identically. The fifth mode correlates to a lesser degree with the analytical modes as exhibited by the decreased diagonal term and the larger off-diagonal term. This indicates some level of skew from the adjacent eigenvectors. If the generalized stiffness for this mode is calculated

$$[K_G] = \{\phi\}^T [K_{aa}] \{\phi\} = \lambda \quad (3.25)$$

$$[K_G]_5 = \{\phi_{T5}\}^T [K_{aa}] \{\phi_{T5}\} = 2.776 \times 10^6 > 1.870 \times 10^6 \quad (3.26)$$

This shows that the fifth mode is predicted to be much stiffer than that predicted by analysis. By comparison, if the generalized stiffness of the sixth mode is calculated in the

same manner

$$[K_G]_6 = \{\phi_{T_6}\}^T [K_{aa}] \{\phi_{T_6}\} = 7.43024 \times 10^6 \approx 7.43020 \times 10^6 \quad (3.27)$$

This sixth mode shape is nearly identical to that predicted by analysis.

Overall this model would be considered to be well correlated even with the presence of the larger off-diagonal term relating to the fifth mode. Nearly ninety-one percent of the total effective mass is present in the first four modes correlated, with only four percent occurring in the fifth and sixth modes combined. This indicates that the principle vibratory modes are well represented by the static mode shapes that were generated by process.

Formatted input and output from the MSC/NASTRAN analyses of the high fidelity beam model are given in Appendix B.

3.2 Demonstration II

Although the process has been demonstrated on a small scale theoretical model, the entire process is intended to be used during the engineering development cycle. Therefore, the correlation process will also be applied to an actual space flight structure for which the finite element modeling and random vibration test sequences have already been performed.

The structure in question is a NASA space flight structure that flew aboard Space Shuttle Columbia during the First U.S. Microgravity Laboratory (USML-1) Spacelab Mission in 1992. The package is approximately 19 inches wide, 36 inches tall, 26 inches deep, and weighs approximately 300 pounds. The primary structural component is a large aluminum plate machined with integral stiffeners to form a waffleplate, or stiffened panel. This waffleplate supports various optical components and the experiment test chamber. The waffleplate is in turn supported by a framework of large channel sections running front to back at all four corners. The front and rear faces of the package are constructed of aluminum sheet that form shear panels to tie the various structural components together. Once mounted in the Spacelab module, the entire structure is supported by the front shear panel and four brackets attached to the primary channels at either of the four rear corners. Several photos of the flight system are shown in Figures 3.8 and 3.9.

An MSC/NASTRAN finite element model was constructed during the engineering design process to serve as both the dynamic and stress model for the system. Various views of this finite element model are shown in Figures 3.10 and 3.11. The model consists of plate and offset bar elements to form the waffleplate structure with concentrated masses used to represent those components attached to the waffleplate. The rest of the primary structure is modeled using beam elements

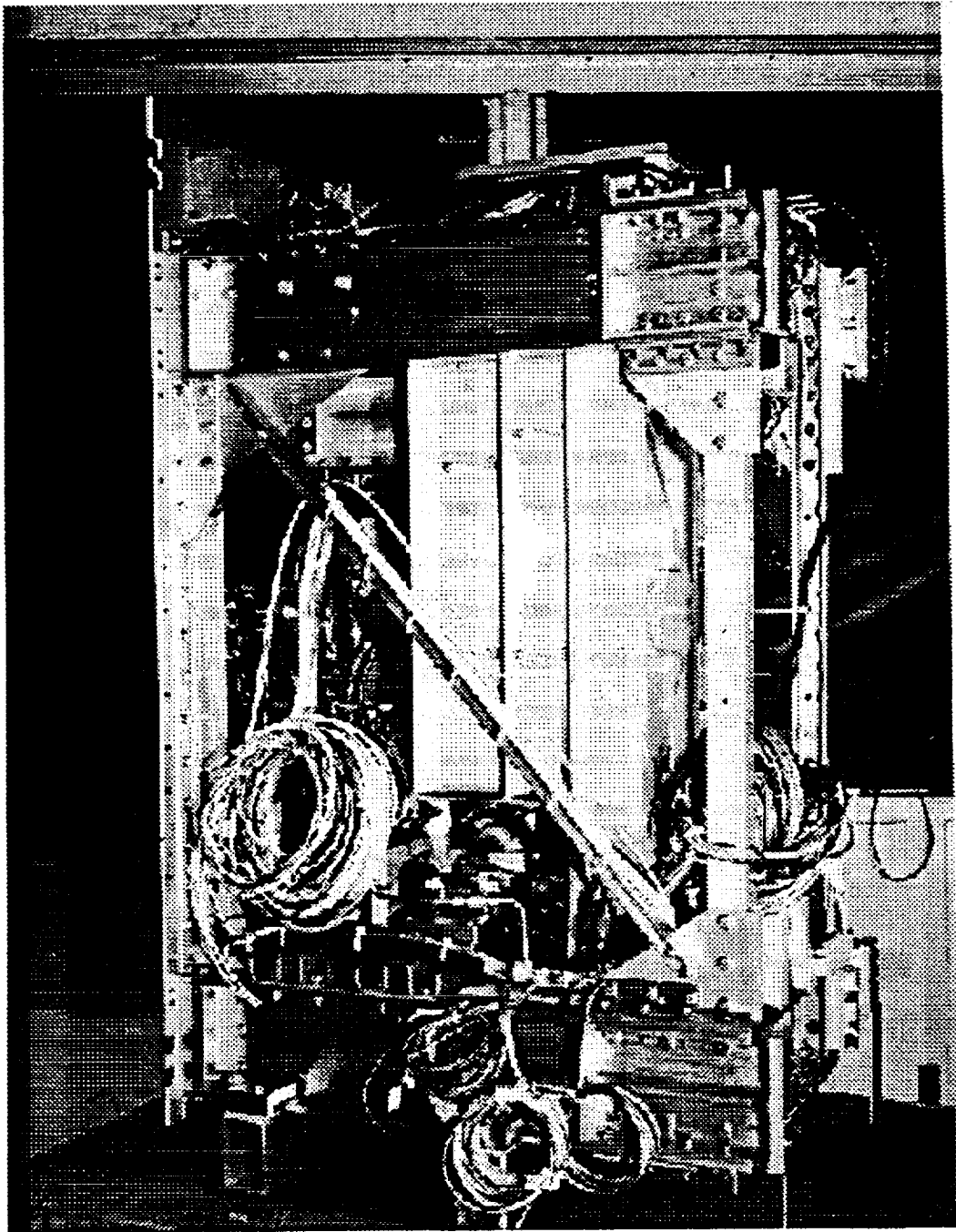


FIGURE 3.8
STDCE Flight Experiment Structure

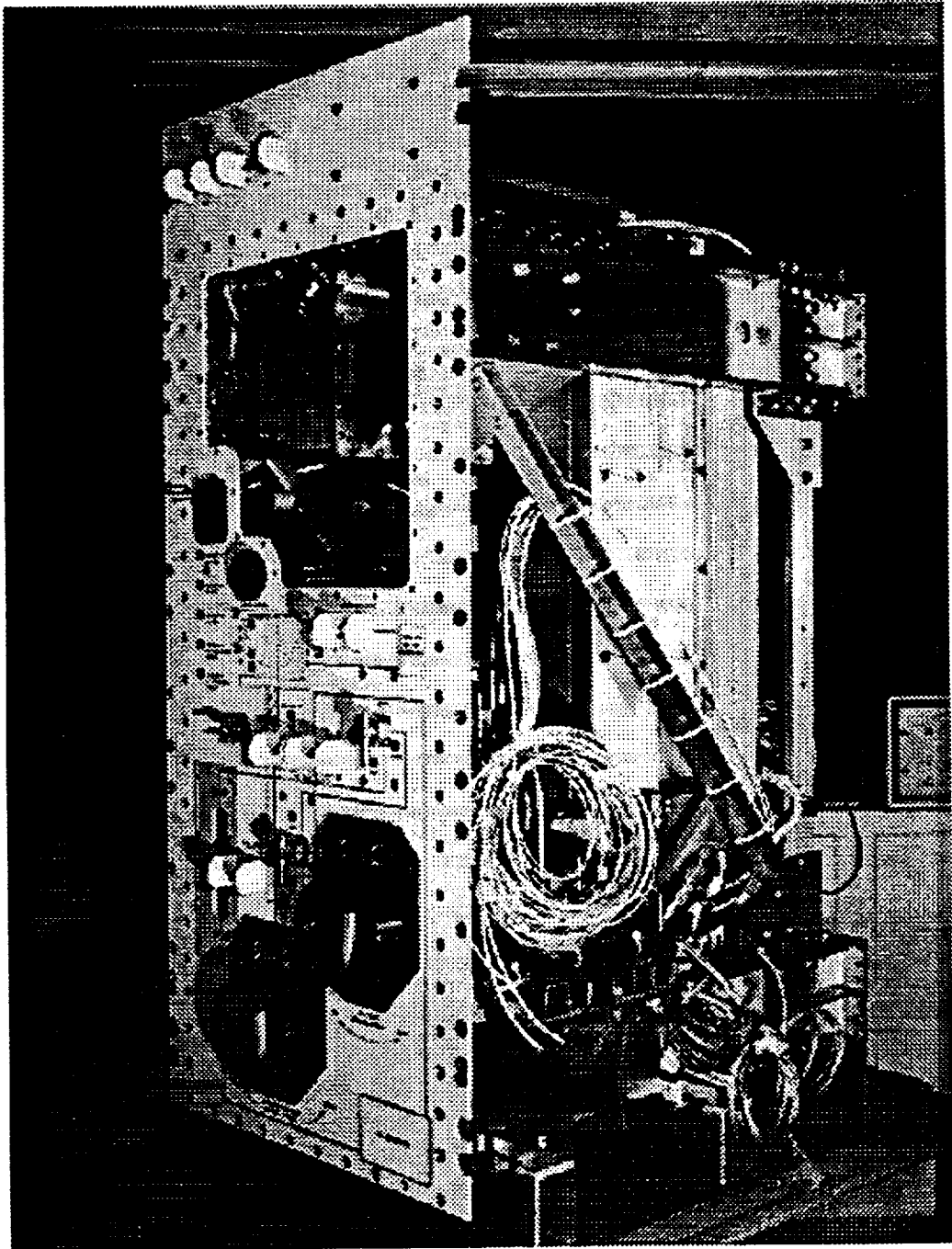


FIGURE 3.9
STDCE Flight Experiment Structure

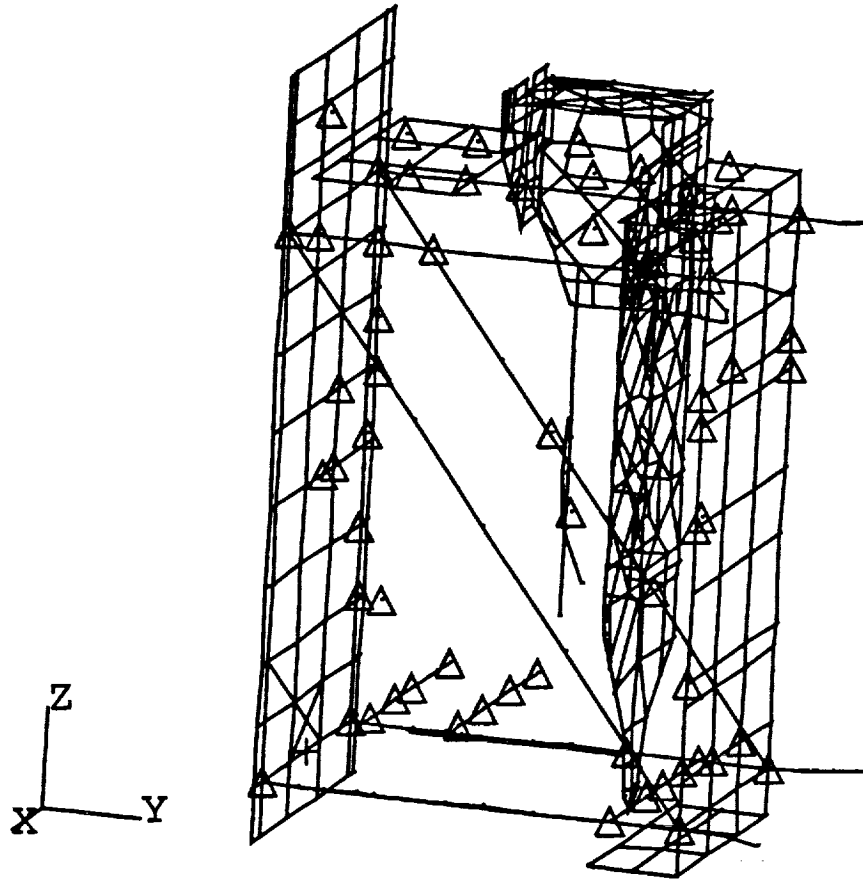


FIGURE 3.10
STDCE Flight Experiment Structure Finite Element Model

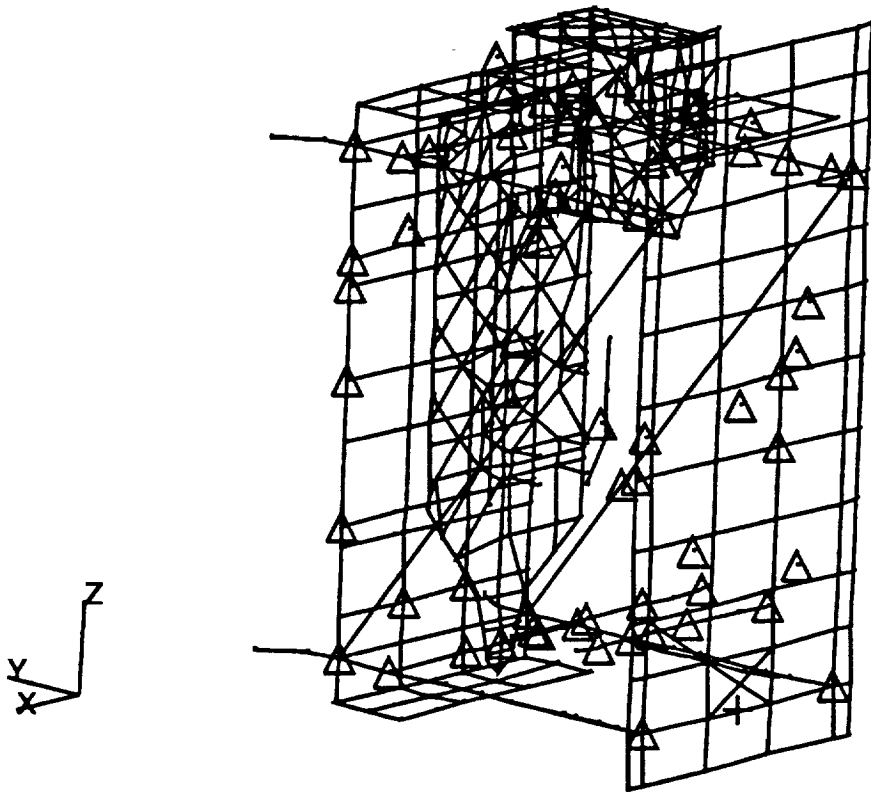


FIGURE 3.11
STDCE Flight Experiment Structure Finite Element Model

to represent the primary channel sections and various stiffeners, while plate elements to represent the front and rear shear panels. A separate study of the mass properties showed the model to conform well with the actual structure in both mass and center of gravity.

During the flight qualification process the Experiment Package was rigidly fixtured and subjected to random vibration testing at the maximum expected flight levels [9]. The input spectra are shown in Figure 3.12. Three separate tests were conducted, one in each of the three primary coordinate directions with single axis base excitation. Response acceleration measurements were taken at seven discrete locations on the structure. Four of the accelerometers were triaxial accelerometers intended to measure in-axis response as well as response in the two cross-axis directions. One accelerometer was biaxial and the last two accelerometers were uniaxial accelerometers mounted to the front and rear shear panels and intended to measure the out-of-plane panel response. The locations of these accelerometers are shown in Figure 3.13. The seven accelerometers together allowed response measurements in sixteen degrees of freedom. Input excitation was measured by four triaxial accelerometers attached to the test fixture, and the response of these four accelerometers was averaged to form the control feed-back scheme for the test.

To correlate this FEM, the model was first reduced to the

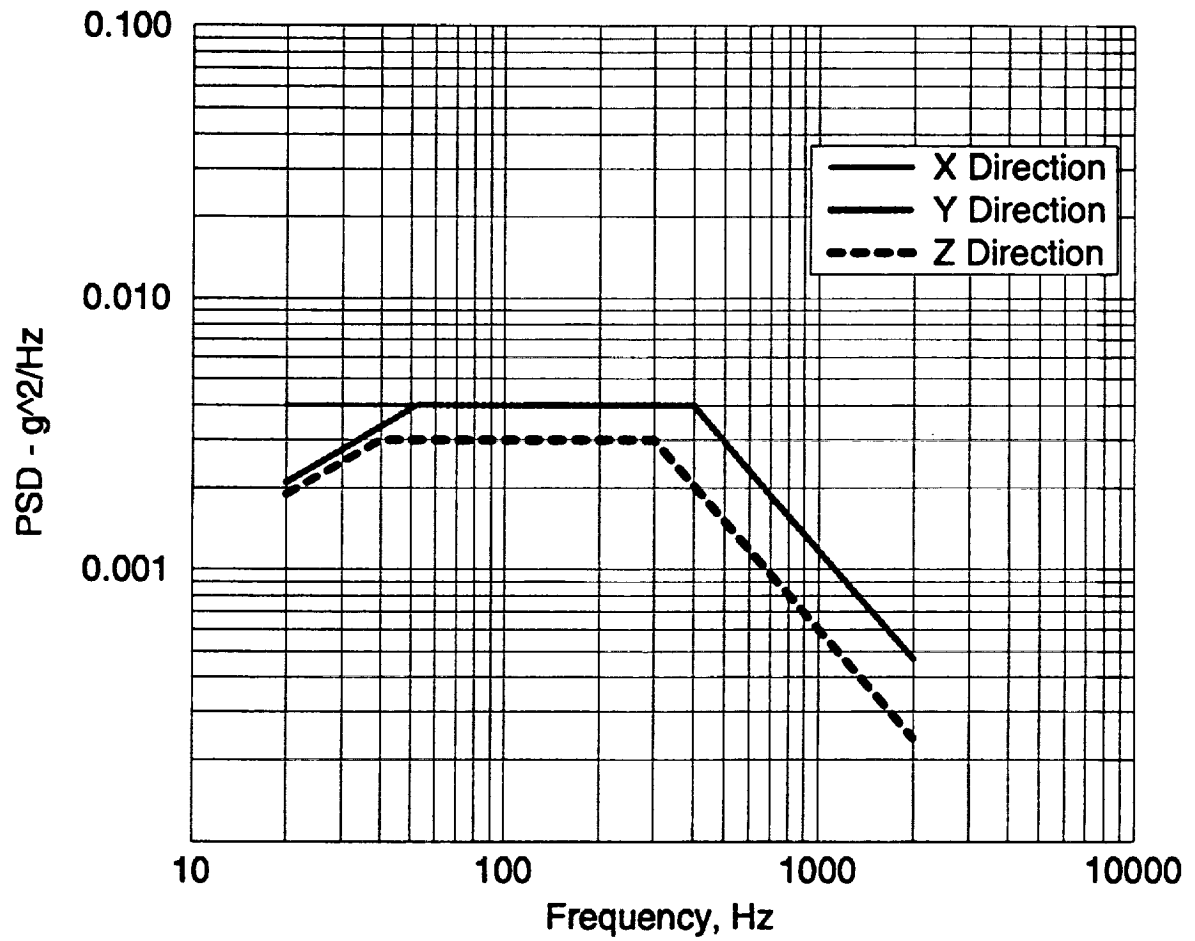


FIGURE 3.12
STDCE Experiment Structure Random Vibration
Test Levels

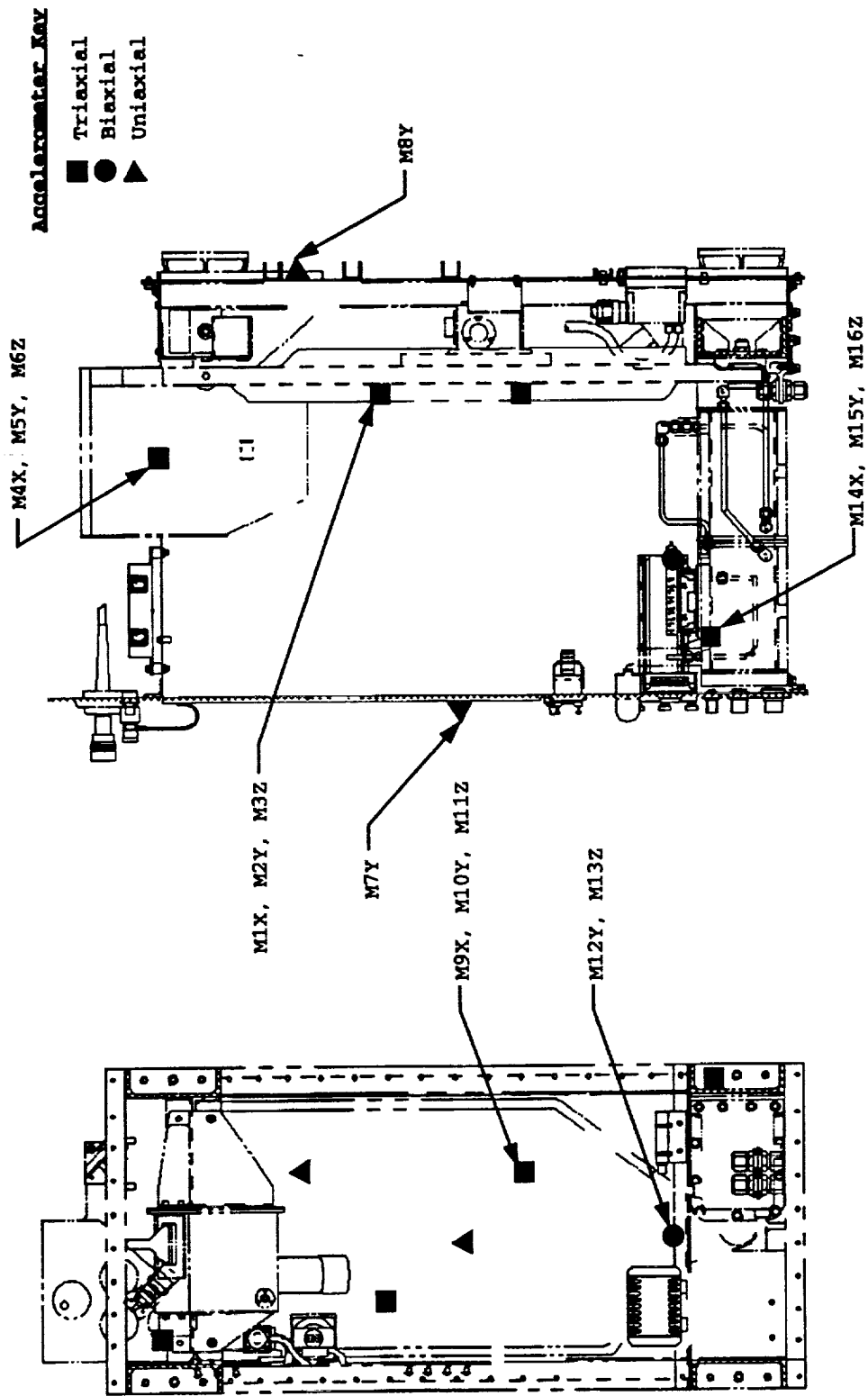


FIGURE 3.13
Response Accelerometer Locations

same sixteen degrees of freedom at which response data were measured during the vibration tests. This was done by including those degrees of freedom corresponding to the accelerometers (response only) in ASET1 bulk data entries and employing Guyan Reduction.

A preliminary modal analysis was conducted on the model to identify the principal modes of vibration. A separate MSC/NASTRAN alter [10] was employed in which the modal effective mass of each mode was calculated. This allows the analyst to determine which modes may be considered primary system modes and exclude from the correlation process local modes where negligible system mass participates. These neglected modes are often local plate modes or coupled modes where several modes of vibration are closely spaced. A frequency span from zero to two-hundred Hertz was swept for all modes within the range. A total of eight modes appeared in this range, varying from 66.5 to 186.7 Hertz. Mode shape plots for these modes are shown in Figures 3.14 through 3.21. These eight modes represent about forty-five, twenty-five, and forty-five percent of the total effective mass participation in the coordinate X, Y, and Z directions, respectively. Although these modes represent only a minority of the total effective mass, this frequency range in which they occur is suitable for correlating the model. Modes 1, 3, 4, 5, and 7 have been selected for correlation based on the large effective mass content in each of the modes. The second and

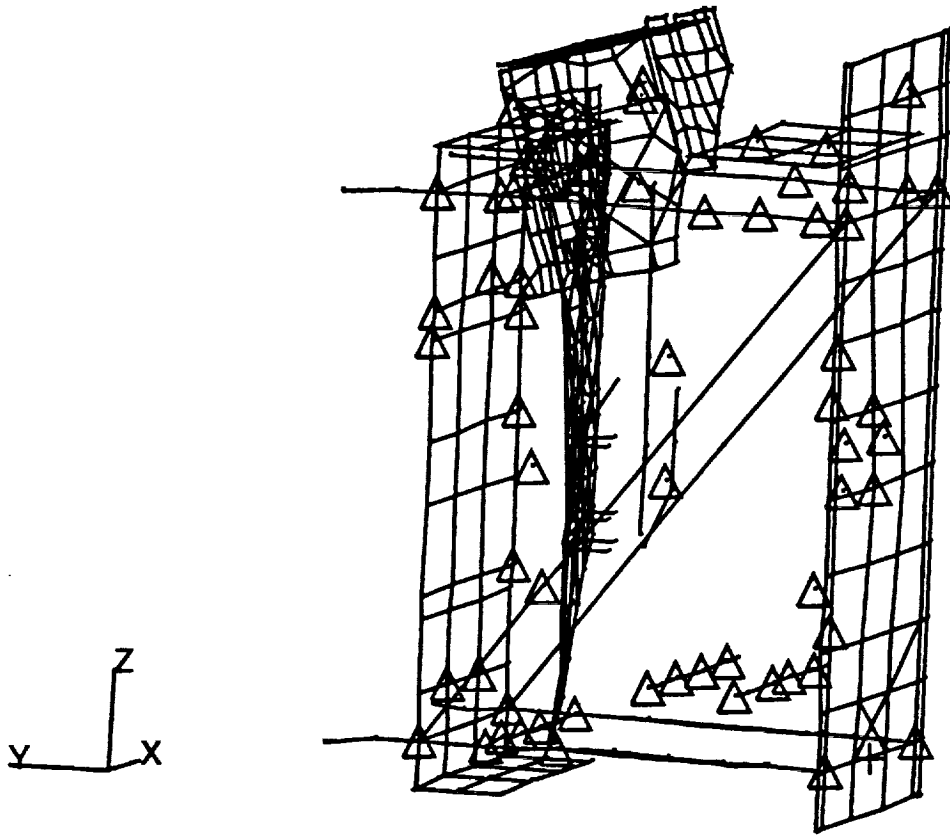


FIGURE 3.14
STDCE Experiment Package Mode 1 - 66.5 Hz

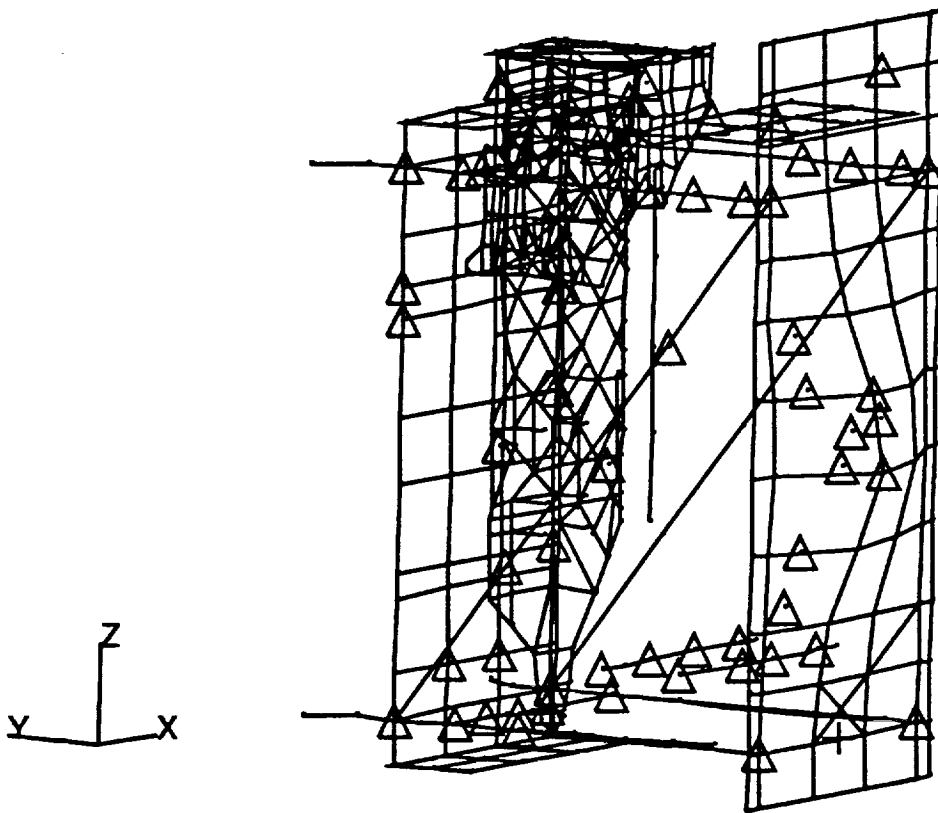


FIGURE 3.15
STDCE Experiment Package Mode 2 - 71.1 Hz

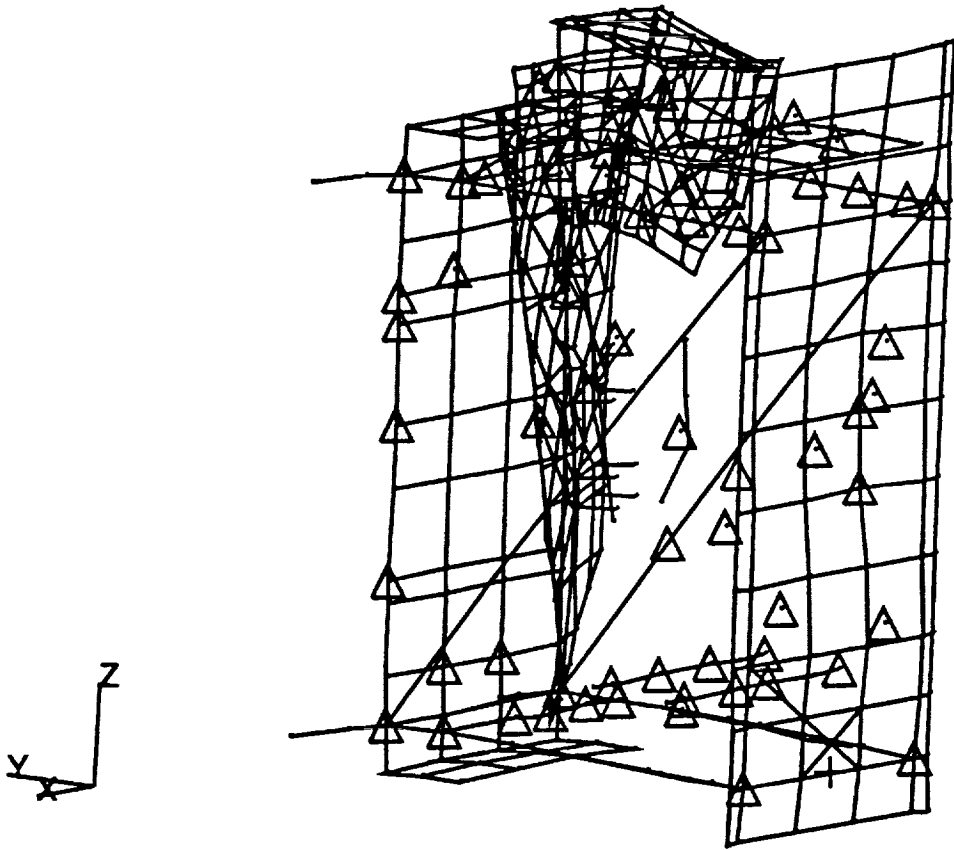


FIGURE 3.16
STDCE Experiment Package Mode 3 - 88.1 Hz

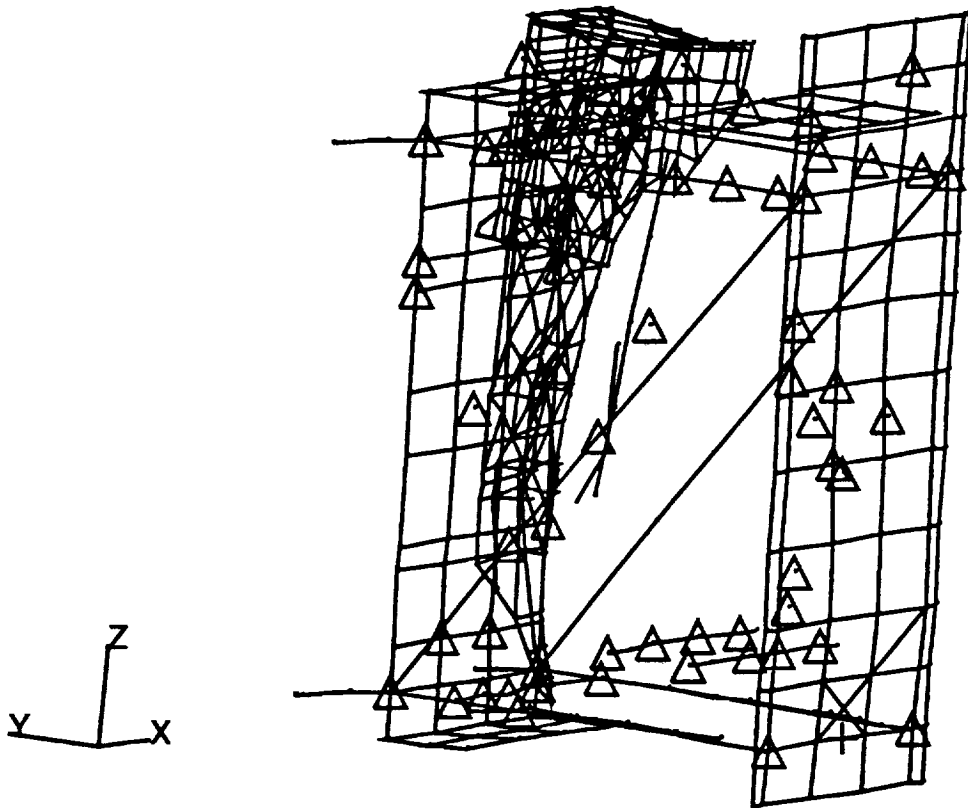


FIGURE 3.17
STDCE Experiment Package Mode 4 - 108.3 Hz

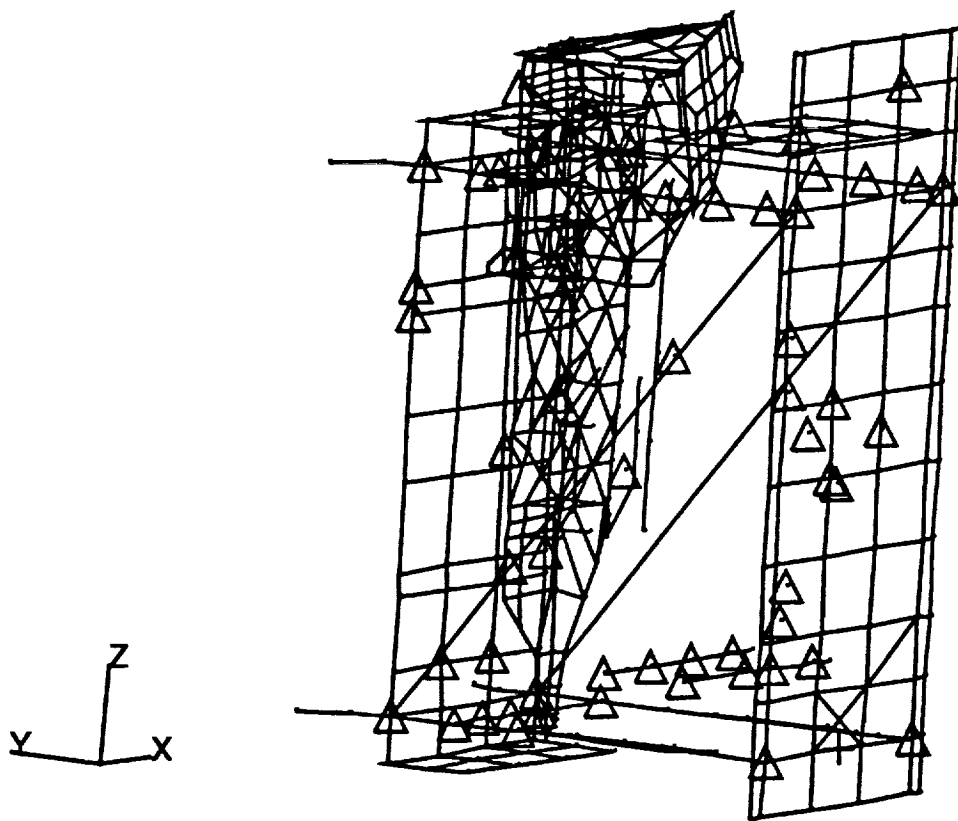


FIGURE 3.18
STDCE Experiment Package Mode 5 - 112.7 Hz

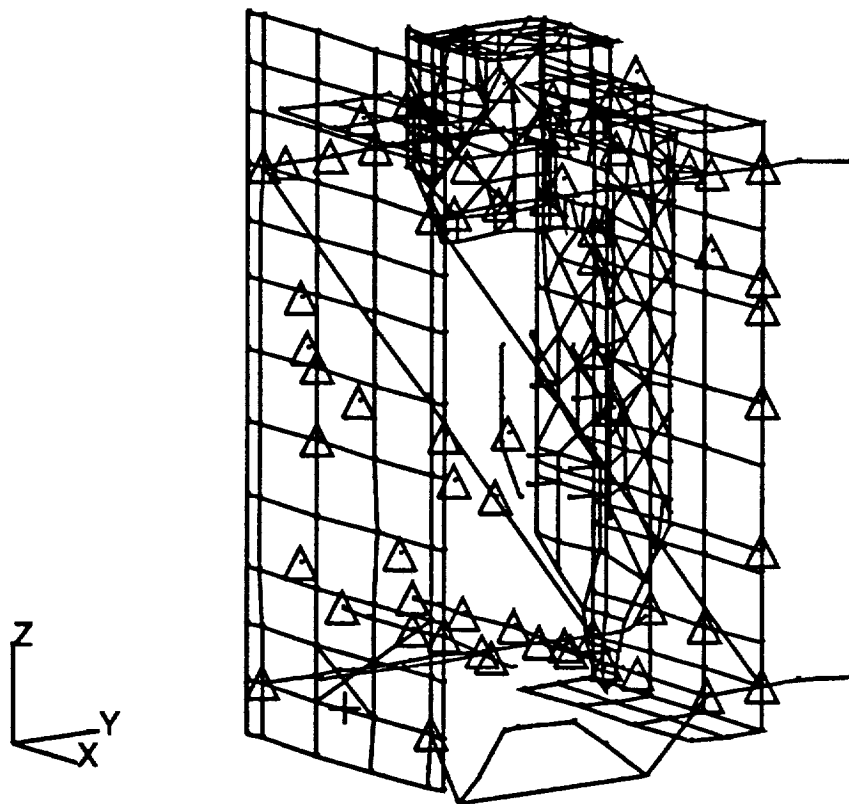


FIGURE 3.19
STDCE Experiment Package Mode 6 - 122.2 Hz

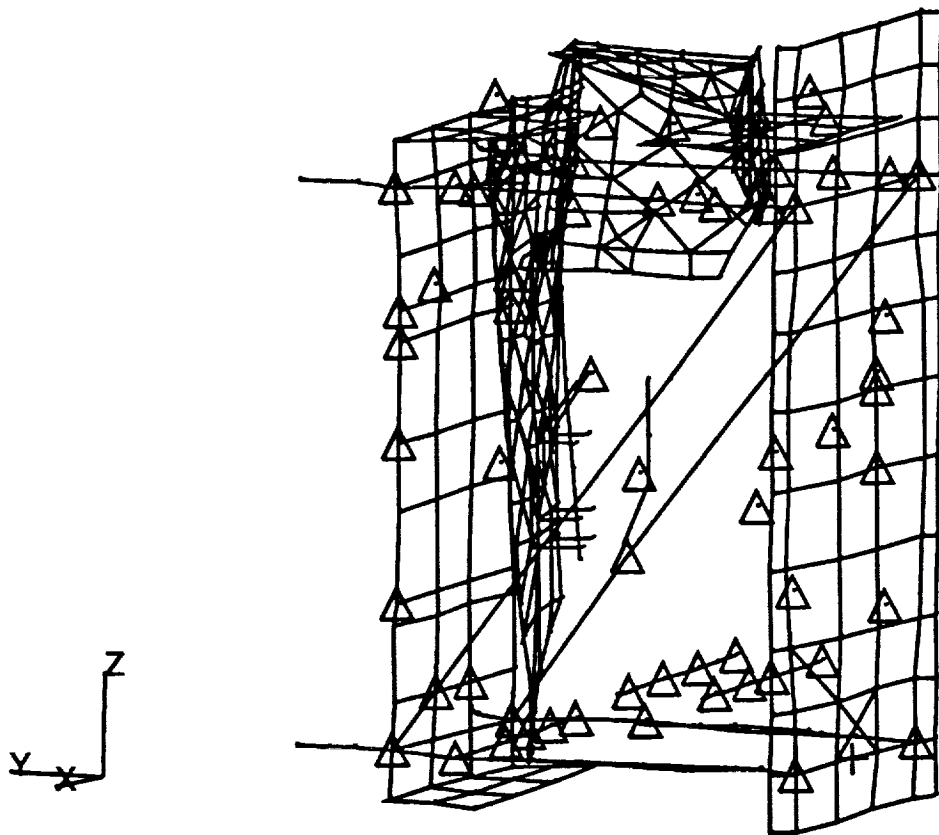


FIGURE 3.20
STDCE Experiment Package Mode 7 - 163.2 Hz

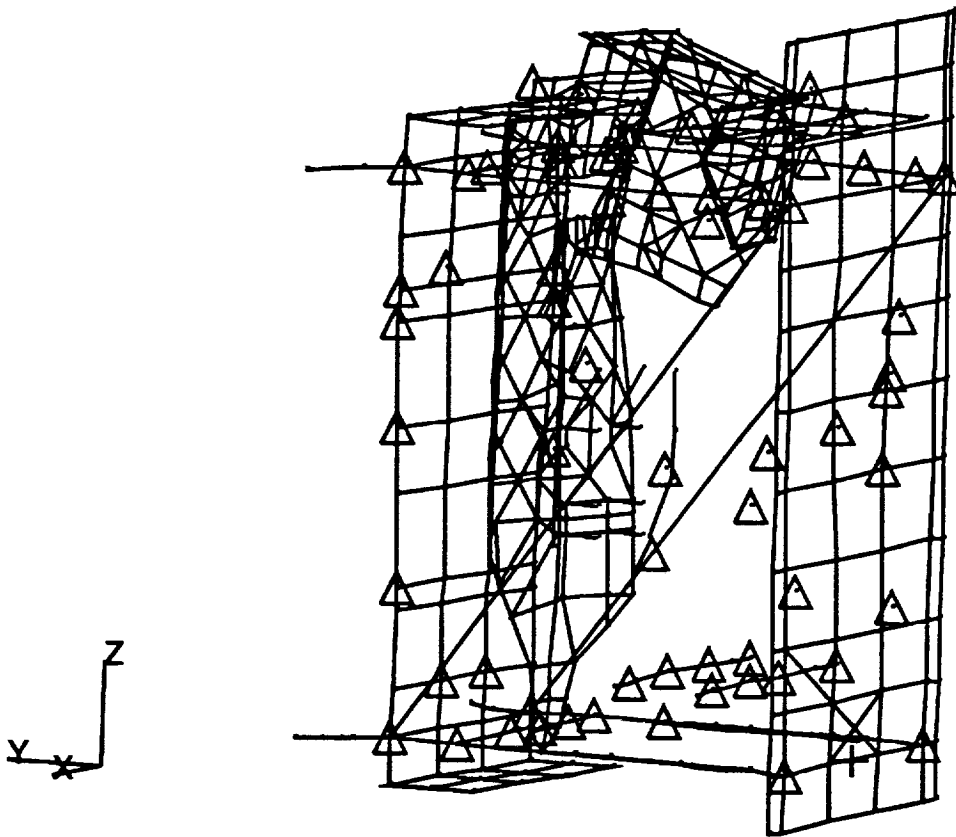


FIGURE 3.21
STDCE Experiment Package Mode 8 - 186.6

sixth modes were excluded from the correlation since they contain less than one percent of the total effective mass. The MSC/NASTRAN output listing for this effective mass analysis is given in Appendix C.

To proceed with the correlation process, the modes determined to be primary modes now need to be identified and separated in the random vibration test data. This can most easily be accomplished by examining and sorting the test data based on peak PSD values and the number of degrees of freedom where these values appear at the same frequency. Quite often one particular set of data, with respect to the excitation axis, provides a more discernable appearance of a fundamental mode more than the other sets of data. The set of data from which the data for the mode is taken doesn't necessarily coincide with the primary response direction (or effective mass direction) of the mode since the response mode may most easily be excited by cross-axis input (such as with a torsional mode). However, these strong system modes usually stand out markedly over the less effective or coupled system modes.

Figure 3.22 shows the averaged control and three response PSD plots corresponding to a single triaxial accelerometer affixed to the waffleplate. These plots were taken from the seventeen plots that make up the data set from the X-axis test. Here it is easy to see the existence of a resonance at 105.5 Hertz. The peak values at this frequency have been

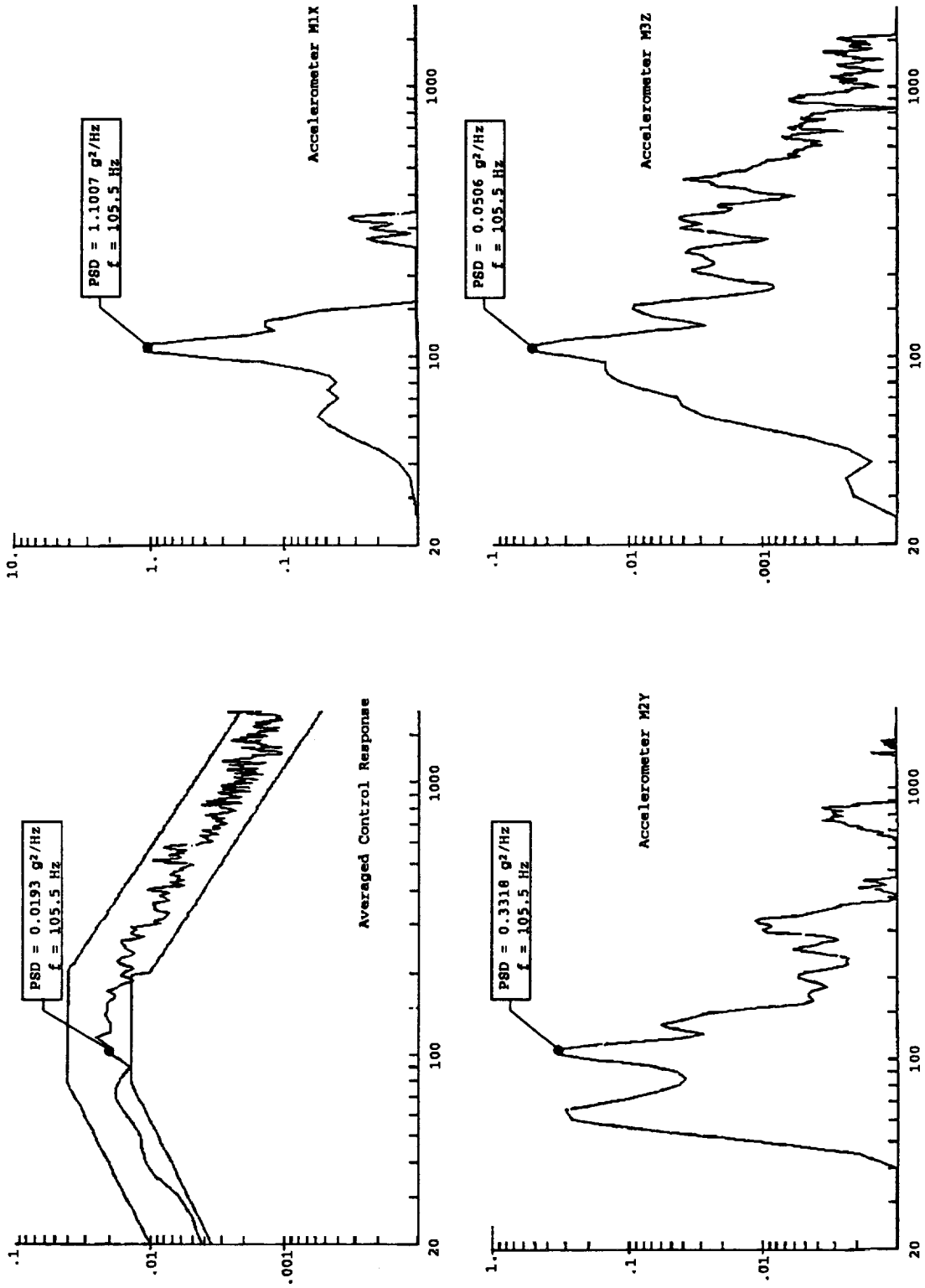


Figure 3.22
Sample Control and Response Measurements

indicated to illustrate how a data set is assembled. For the STDCE Experiment Package, the peak PSD response data for the five modes of interest has been reduced from the full complement of test data and is shown in Table VI.

Amplification values (Table VII) are computed in the same manner as demonstrated earlier using the control and response PSD values.

A graphical comparison of the selected test frequencies with the analytical frequencies is given in Figure 3.23. This shows the third mode (88.1 Hz) to be somewhat stiffened in the actual structure from what is predicted by analysis. The remaining modes are overly stiffened in the model as might be expected. These frequency differences may be the direct result from the reduction in active degrees of freedom in the model but may also be the result of effects not accounted for in the modeling and linear analysis, e.g. joint friction and other various nonlinear effects.

Before the PSD and amplification parameters can be used in the correlation process, they must be rearranged in the proper sequence to match the nodal numbering in the analytical model. This ensures that the resulting local accelerations are applied to the proper node and in the proper translational direction. With the MSC/NASTRAN nodal renumbering scheme deactivated, the system matrices are assembled and processed using the external node sequencing, relating the degrees of freedom with the nodes in ascending order. Therefore when the

TABLE VI.

Peak Response Data at Selected Frequencies.

ANAL. FREQ.	66.5	88.1	108.3	112.7	163.2
ANAL. ORDER	1	3	4	5	7
TEST FREQ.	65.2	92.1	95.4	105.5	134.8
M1X	0.0083	0.0049	0.0054	1.1007	0.3625
M2Y	0.4217	0.1695	0.1695	0.3318	0.0590
M3Z	0.0009	0.5623	0.6190	0.0506	0.0037
M4X	0.8254	0.0442	0.0402	0.1540	0.2054
M5Y	0.1957	0.0287	0.0301	0.2260	0.0301
M6Z	0.1695	0.4217	0.4870	0.1334	0.0422
M7Y	3.0142	0.2488	0.2738	0.0649	0.0001
M8Y	0.0301	0.0147	0.0169	0.0562	0.0162
M9X	0.0049	0.0054	0.0065	0.9085	0.1957
M10Y	0.1540	0.0590	0.0464	1.9573	0.0909
M11Z	0.0012	0.4642	0.5109	0.0075	0.0054
M12Y	0.0191	0.0249	0.0249	0.0029	0.0037
M13Z	0.0010	0.0866	0.0909	0.0075	0.0044
M14X	0.0010	0.0013	0.0026	0.1287	0.0442
M15Y	0.0165	0.0021	0.0020	0.0316	0.0079
M16Z	0.0002	0.0196	0.0178	0.0001	0.0001
CONTROL	0.0154	0.0095	0.0095	0.0193	0.0205

TABLE VII.

Response Amplification Values at Selected Frequencies

ANAL.FREQ.	66.5	88.1	108.3	112.7	16
ANAL.ORDER	1	3	4	5	7
TEST FREQ.	65.2	92.1	95.4	105.5	134.8
M1X	0.5390	0.5158	0.5684	57.0311	17.6829
M2Y	27.3831	17.8421	17.8421	17.1917	2.8780
M3Z	0.0584	59.1895	65.1579	2.6218	0.1805
M4X	53.5974	4.6526	4.2316	7.9793	10.0195
M5Y	12.7078	3.0211	3.1684	11.7098	1.4683
M6Z	11.0065	44.3895	51.2632	6.9119	2.0585
M7Y	195.7273	26.1895	28.8211	3.3627	0.0049
M8Y	1.9545	1.5474	1.7789	2.9119	0.7902
M9X	0.3182	0.5684	0.6842	47.0725	9.5463
M10Y	10.0000	6.2105	4.8842	101.4145	4.4341
M11Z	0.0779	48.8632	53.7789	0.3886	0.2634
M12Y	1.2403	2.6211	2.6211	0.1503	0.1805
M13Z	0.0065	9.1158	9.5684	0.3886	0.2146
M14X	0.0649	0.1368	0.2737	6.6684	2.1561
M15Y	1.0714	0.2211	0.2105	1.6373	0.3854
M16Z	0.0130	2.0632	1.8737	0.0052	0.0049

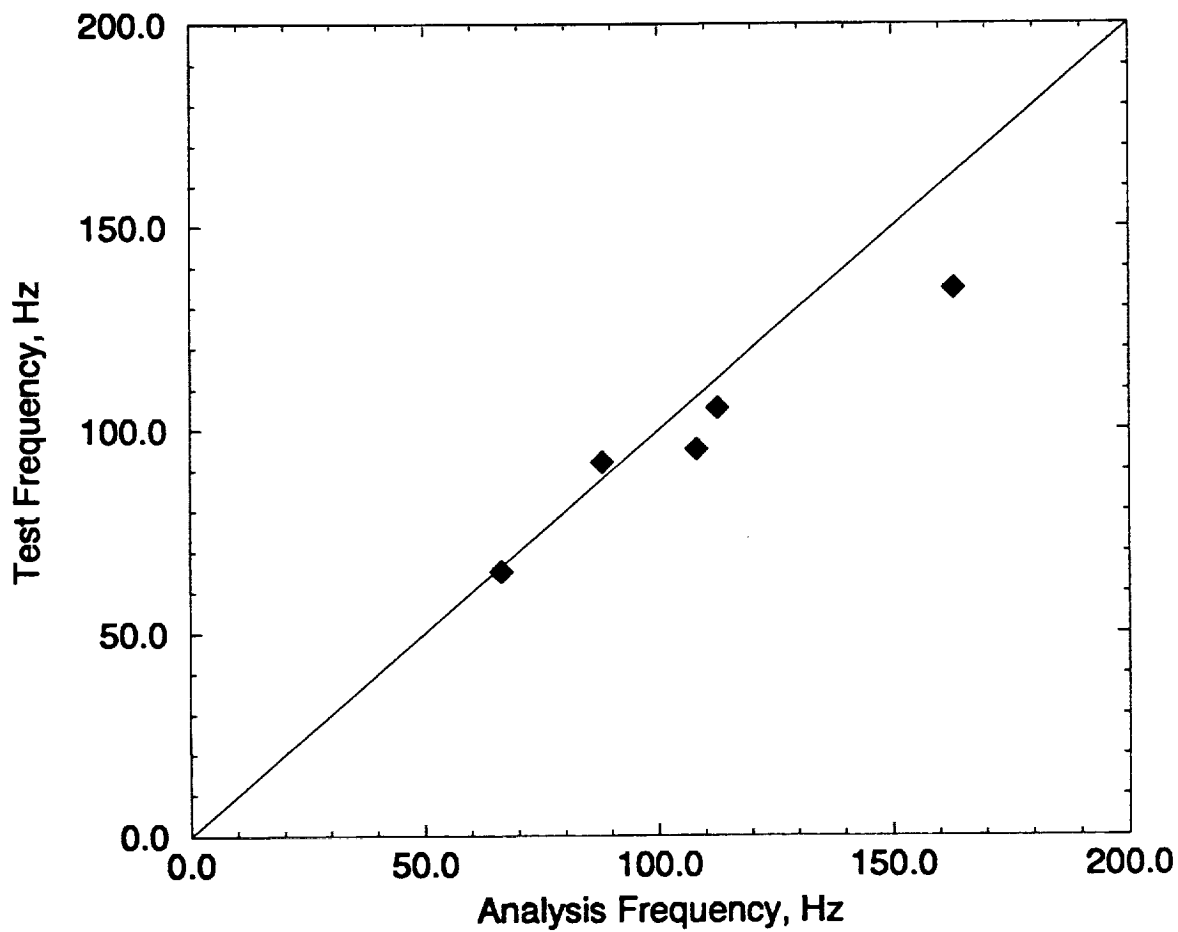


FIGURE 3.23
Comparison of Test and Analytical Frequencies

PSD and amplification values are prepared in the DMI entries, the values are entered according to the corresponding node numbers in ascending order. Table VIII shows the node and accelerometer association for the Experiment Package.

The results of the correlation run can be summarized in matrix form, one matrix each for the analytical mode shapes, calculated static mode shapes, and cross orthogonality results.

$$[\Phi_A] = \begin{bmatrix} -2.039e-2 & -1.393e-2 & 6.638e-2 & 7.351e-2 & 3.331e-1 \\ -2.974e-3 & 1.002e-1 & -2.645e-3 & 2.342e-2 & -1.359e-1 \\ 6.034e-3 & -5.098e-2 & 7.210e-3 & -1.024e-1 & 5.731e-1 \\ -2.683e-2 & -5.637e-2 & -2.737e-2 & -7.829e-2 & -7.658e-2 \\ 5.758e-1 & -2.385e-1 & 6.301e-2 & -1.077e-2 & -1.567e-2 \\ 5.161e-2 & 1.320e-1 & -1.262e-1 & -2.654e-2 & 1.524e-1 \\ -1.416e-1 & -4.459e-1 & 4.627e-1 & 2.350e-2 & -1.106e-1 \\ -2.892e-3 & 1.215e-1 & 1.237e-1 & 6.252e-1 & -1.946e0 \\ 2.595e-1 & 1.415e0 & 2.815e0 & 7.105e-1 & 1.224e0 \\ -5.351e-1 & -1.364e0 & 9.458e-1 & -3.395e-2 & -7.299e-2 \\ -1.232e-3 & 6.458e-2 & 9.748e-2 & 6.933e-1 & -1.896e0 \\ 2.029e0 & -7.294e-1 & 1.168e0 & -3.187e-1 & -7.265e-1 \\ -5.483e-1 & -1.418e0 & 9.204e-1 & 6.940e-2 & -6.299e-3 \\ 7.982e-1 & -1.101e0 & -1.111e0 & 4.579e0 & 1.422e0 \\ -4.164e-1 & 1.162e-1 & -6.254e-2 & -2.414e-2 & -7.733e-1 \\ -1.881e0 & -9.126e-1 & 6.913e-1 & 4.695e-2 & 3.628e-1 \end{bmatrix}$$

(3.28)

TABLE VIII.
Accelerometer/Node Association

Accel.	Node/DOF	Accel.	Node/DOF
M1X	603/T1	M9X	536/T1
M2Y	603/T2	M10Y	536/T2
M3Z	603/T3	M11Z	536/T3
M4X	744/T1	M12Y	224/T2
M5Y	744/T2	M13Z	224/T3
M6Z	744/T3	M14X	149/T1
M7Y	159/T2	M15Y	149/T2
M8Y	12/T2	M16Z	149/T3

$$[\Phi_T] = \begin{bmatrix} -1.147e-2 & -2.501e-2 & 4.464e-2 & -1.558e-1 & 3.548e-1 \\ -2.049e-1 & 1.026e-2 & -7.058e-2 & 5.764e-2 & -1.175e-1 \\ 2.179e-1 & -5.108e-2 & 7.808e-2 & -2.303e-1 & 4.065e-1 \\ 1.259e-1 & -6.862e-2 & -1.850e-2 & -1.566e-2 & -6.496e-2 \\ -7.776e-1 & -2.455e-1 & 5.173e-2 & -1.052e-3 & 1.244e-2 \\ 8.013e-2 & 1.543e-1 & -8.025e-2 & -5.418e-2 & 9.557e-2 \\ -1.591e-1 & -5.262e-1 & 3.218e-1 & 2.563e-2 & -2.090e-2 \\ -2.815e-1 & 6.603e-2 & 7.671e-2 & 1.157e0 & -1.913e0 \\ 3.011e-1 & 5.862e-1 & 2.757e0 & 3.358e-1 & 1.220e0 \\ -3.267e-1 & -1.578e0 & 9.239e-1 & 4.217e-2 & -3.074e-2 \\ -1.726e-1 & 1.607e-2 & 9.571e-2 & 1.205e0 & -1.964e0 \\ 1.975e0 & -1.029e0 & 1.157e0 & -2.162e-1 & -6.645e-1 \\ -1.826e-1 & -1.636e0 & 9.811e-1 & 1.260e-1 & -1.108e-1 \\ 1.775e0 & -6.563e-1 & -1.452e0 & 3.874e0 & 1.498e0 \\ -4.581e-1 & 1.318e-1 & -7.347e-2 & 4.477e-4 & -6.701e-1 \\ -1.426e0 & -1.048e0 & 6.569e-1 & -2.237e-1 & 4.127e-1 \end{bmatrix}$$

(3.29)

$$[C] = \begin{bmatrix} 0.9335 & 0.0000 & 0.0000 & 0.0000 & 0.0000 \\ -0.1854 & 0.9591 & 0.0000 & 0.0000 & 0.0000 \\ 0.0095 & -0.2819 & 0.9955 & 0.0000 & 0.0000 \\ 0.1223 & 0.0120 & -0.0661 & 0.9551 & 0.0000 \\ 0.1702 & 0.0143 & -0.0045 & -0.2811 & 0.9941 \end{bmatrix}$$

(3.30)

The process shows the model to correlate very well for the modes selected. The sparse content of off-diagonal terms and the relative magnitudes of the diagonal terms indicate acceptable correlation between the analytical model and physical system. The third and fifth analytical modes (second and fourth selected) correlate to a lesser degree than the other modes selected but still show satisfactory similarity.

Overall the analytical model may be considered to be a relatively good approximation of the mass and stiffness distributions of the continuum system. If a higher degree of correlation was sought, the model could be 'tuned' by adjusting mass and stiffness to provide more accurate mode shapes and frequencies.

CHAPTER IV

DISCUSSION

4.1 Summary and Conclusions

A method has been outlined for substantiating the free vibration predictions provided by finite element analysis using random vibration data acquired via dynamic testing. Power Spectral Density response data taken at a certain number of spacial locations on the structure and corresponding to a unique resonant frequency is used to generate a set of equivalent local accelerations that can be applied to a finite element model. Assuming that the finite element model is an accurate representation of the continuum system, and therefore possesses similar frequency response characteristics, these equivalent local accelerations deform the structure in a manner consistent with the mode of vibration from which they were derived. This statically deformed mode shape can then be compared with the free vibration mode shape at the

corresponding analytical frequency using modal techniques such as the cross orthogonality method.

The process has been applied to a simple cantilevered beam system using two analytical models: a high fidelity model to simulate the continuum system and a significantly lower fidelity model to serve as the analytical model. Through random response analysis, response Power Spectral Density and amplification levels were predicted over a large frequency range to serve as data that would be acquired during dynamic testing. These response levels were reduced at six frequencies corresponding to the natural frequencies of vibration predicted by the lower fidelity model. The reduced data was used to generate sets of equivalent local accelerations which were applied to the lower fidelity model. The resulting system of static equations were solved and six static deformations predicted, mass normalized, and compared to the eigenvectors provided by the previous modal analysis. Five of the six static mode shapes were found to correlate to a very high degree with the analytical eigenvectors.

The same correlation process was also applied to a NASA flight structure for which random vibration data had been acquired in the flight qualification process. Five primary system modes were chosen for correlation based on their mass participation content. Three of the five modes evaluated were found to correlate to a very high degree while the remaining two correlated to a lesser but still acceptable degree. The

correlation of these two modes could be significantly improved through the process of tuning the finite element model. The tuning process, however, is beyond the immediate scope of this thesis.

The results from both demonstrations indicate that the process can effectively be used to generate the mode shapes of the physical structure and thus correlate finite element results. The application of this process has the potential to substantially reduce the costs associated with correlating such models by eliminating the need for additional testing such as that required by classical modal techniques. All information required to complete the correlation process can be obtained during the normal flight qualification process.

4.2 Recommendations for Further Study

Even though the process developed here has been shown to provide sufficient correlation results, it has not been compared directly with results provided by alternate methods, e.g. modal testing. The full justification of merits provided by this method should be fully investigated by performing an accepted correlation procedure in parallel with the proposed procedure. Doing so would allow the comparison of test

acquired mode shapes from the two methods and also allow a characterization of the mathematical error that is introduced in the process that has been proposed.

REFERENCES

1. Ewins, D. J., "Modal Testing: Theory and Practice", Research Studies Press Ltd., Letchworth, Hertfordshire, England, 1984.
2. Payload Flight Equipment Requirements For Safety-Critical Structures, NASA JA-418, Revision A, Marshall Space Flight Center, Huntsville, Alabama, 1989.
3. Crandall, S. H., and Mark, W. D., "Random Vibration in Mechanical Systems", Academic Press, New York, New York, 1963.
4. Gockel, M. A., Editor, *MSC/NASTRAN - Handbook For Dynamic Analysis*, MacNeal-Schwendler Corporation, Los Angeles, California, 1983.
5. Harris, C. M., and Crede, C. E., "Shock And Vibration Handbook", Second Ed., McGraw-Hill, New York, New York, 1976.
6. Bathe, Klaus-Jorgen, "Finite Element Procedures In Engineering Analysis", Prentice-Hall, Englewood Cliffs, New Jersey, 1982.
7. *User's Manual - MSC/NASTRAN Version 67*, Volumes I and II, MacNeal-Schwendler Corporation, Los Angeles, California, 1991.
8. Craig, Roy R., Jr., "Structural Dynamics - An Introduction to Computer Methods", John Wiley and Sons, New York, New York, 1981.
9. Spacelab Payload Accommodations Handbook, NASA SLP/2104-2, Appendix B, Johnson Space Center, Houston, Texas, 1986.
10. Rose, T., *Alter to Compute Kinetic Energy and Effective Weight*, Proceedings of the MSC/NASTRAN World Users Conference, 1988.

APPENDIX A

MSC/NASTRAN DMAP LISTING


```

KSF, KVV, EDT, GEOM2S, GEOM3S, ECTS, EPTS, INDTA, KELM,
KDICT, GPECT, VELEM, EQEXINX, ECTX, BGPDTX, SILX,
GEOM4S, VGFS, SPECSEL, GPDTS, MELM, MDICT, GEOM1,
GEOM2, GEOM3, GEOM4, EPT, MPT, SLIST, VACOMPR,
$ DYNAMICS ONLY
  BGG, K4GG, MFF, MLR, MLL, MRR, CMLAMA, CMPHA, CMPHO,
  MLAA1, MR, GOAQ, KLA A, MLAA, MAA, MAR, MEA, BAA, K4AA,
  MGG,
$ PHASE 2
  PHA, LAMA, PHFA, LAMAF, PHSA, LAMAS,
$ PHASE 3
  PHG, PHQG, PUG, GPSF, OPHG1, OPHQG1, OPHEF1, OPHE1,
  OPHEE1, OPHEM1, OPHEG1, OPHEEM1, OPHEEG1, PHGPS,
  OPHNRGY, OPHGPFB, CASEDR, XYCDBDR, OPHGPS1,
$ EQUIV SCRATCH
  MCAA, MMAA, OLB, PCDB, VAFS, XYCDB, EDOMX, CASECC $
ALTER 36,36$
CALL MODERS MR, USET, DM, CASES, DYNAMICS, MMAA, MCAA, GPLS,
SILS, EED, EQEXINS, VACOMPR, DMI, DMINDX, DTI, DTINDX/
PHA,LAMA/
NORSET/ NOLSET/ 'MODES'/ ASING/ FALSE/ FALSE/ NOQSET $
COMPILE MODERS SOUIN=MSCSOU NOLIST NOREF
ALTER 1,1$
SUBDMAP MODERS MR, USET, DM, CASES, DYNAMICS, MMAA, MCAA,
GPLS, SILS, EED,
EQEXINS, VACOMPR, DMI, DMINDX, DTI, DTINDX/
PHIA,LAMA/
NORSET/ NOLSET/ READAPP/ ASING/ CYCLIC/ SECND/ NOQSET $
ALTER 84$
$ Input user specified response levels, amplification
$ levels, and listing of modes to be correlated. Input via
$ bulk data DMI and DTI cards.
DMIIN DMI,DMINDX/PSD,QUAL,,,,,,,,,$
DTIIN DTI,DTINDX/MODELST,,,,,,,,,$
TYPE PARM,,I,Y,NMODES$
TYPE PARM,,I,Y,NTEST$
TYPE PARM,,I,Y,NMAX$
TYPE PARM,,RS,Y,GRAV$
TYPE PARM,,I,N,COUNT=1$
TYPE PARM,,I,N,PART1$
TYPE PARM,,I,N,PART2$
TYPE PARM,,I,N,COUNT1$
TYPE PARM,,I,N,COUNT2$
TYPE PARM,,RS,N,PI2=1.57079633$
TYPE PARM,,CS,N,ALPHA$
TYPE PARM,,RS,N,RADI$
TYPE PARM,,CS,N,MRI$
FILE CP=OVRWRT/RP=OVRWRT/A11=OVRWRT/A12=OVRWRT$
FILE A21=OVRWRT/A22=OVRWRT/B11=OVRWRT/B12=OVRWRT$
FILE B21=OVRWRT/B22=OVRWRT/C11=OVRWRT/C12=OVRWRT$
FILE C21=OVRWRT/C22=OVRWRT/D11=OVRWRT/D12=OVRWRT$
FILE D21=OVRWRT/D22=OVRWRT/KINV=OVRWRT/DEF=OVRWRT$

```

```

FILE ACCEL=OVRWRT/ACCELI=OVRWRT/MODEI=OVRWRT$
FILE DEFT=OVRWRT/XMODE=OVRWRT/COC=OVRWRT$
$ Echo user input of response levels, amplification levels,
$ and modes to be correlated.
MATPRN PSD,QUAL//$
TABPT MODELST//$
$ Retrieve and equivalence analysis matrices. GDR
$ stiffness, GDR mass, eigenvectors, and eigenvalues.
EQUIVX KXX/KANL/ALWAYS$
EQUIVX MXX/MANL/ALWAYS$
EQUIVX PHIX/PHIANL/ALWAYS$
LAMX,,LAMA/LAMAT/-1$
MATPRN KANL,MANL,PHIANL,LAMAT//$
$ Partition eigenvector and eigenvalue matrices for the
$ modes to be correlated. Modes to be correlated are
$ identified by DTI entry MODELST. There may be at most
$ as many modes requested as the number specified by
$ NMODES.
EQUIVX LAMAT/LAMTMP/ALWAYS$
MATGEN ,/LAMDA/7/1/5$
MATGEN ,/PHIRED/7/NTEST/1$
COUNT=1$
DO WHILE (COUNT <= NMODES)$
  PARAML MODELST//'DTI'/COUNT/1//S,N,PART$
  PART1=PART-1$
  PART2=NMAX-PART$
  IF (PART = 1) THEN$
    MATGEN ,/CP/6/NMAX/PART/PART2$
    MATGEN ,/RP/6/NMAX/PART/PART2$
  ELSE$
    MATGEN ,/CP/6/NMAX/0/PART1/1/PART2$
    MATGEN ,/RP/6/NMAX/0/PART1/1/PART2$
  ENDIF$
  PARTN LAMTMP,,RP/LAMTP,A21,A12,A22/1$
  PARTN PHIX,CP,/PHITP,B21,B12,B22/1$
  IF (COUNT > 1) THEN$
    COUNT1=COUNT-1$
    TRNSP LAMDA/TEMP1$
    TRNSP LAMTP/TEMP2$
    APPEND TEMP1,TEMP2/TEMP3$
    TRNSP TEMP3/LAMDATX$
    EQUIVX LAMDATX/LAMDA/ALWAYS$
    APPEND PHIRED,PHITP/PHITX$
    EQUIVX PHITX/PHIRED/ALWAYS$
  ELSE$
    EQUIVX LAMTP/LAMDA/ALWAYS$
    EQUIVX PHITP/PHIRED/ALWAYS$
  ENDIF$
  COUNT=COUNT+1$
ENDDO$
MATPRN LAMDA,PHIRED//$
$ Create the nodal directional matrix NDIR by extracting

```

```

$ each term in PHIRED and selecting its directional
$ orientation (e.g. +1.0 or -1.0). Directional terms are
$ assembled in NDIR matrix of size [NTEST X NMODES].
EQUIVX PHIRED/NDIR/ALWAYS$
COUNT1=0$
DO WHILE (COUNT1 < NMODES)$
  MATGEN ,/CP/6/NMODES/COUNT1/1$
  COUNT2=0$
  DO WHILE (COUNT2 < NTEST)$
    MATGEN ,/RP/6/NTEST/COUNT2/1$
    PARTN NDIR,CP,RP/A11,A21,A12,AOLD/1$
    NORM AOLD/ANEW/$
    MERGE A11,A21,A12,ANEW,CP,RP/NDIR1/1$
    EQUIVX NDIR1/NDIR/ALWAYS$
    COUNT2=COUNT2+1$
  ENDDO$
  COUNT1=COUNT1+1$
ENDDO$
MATPRN NDIR//$
$ Create the nodal acceleration vector ACCEL for each mode
$ by extracting each term from NDIR, PSD, QUAL and LAMDA
$ then solving Miles equation.
MATGEN ,/ACCEL/7/NTEST/NMODES$
COUNT1=0$
DO WHILE (COUNT1 < NMODES)$
  MATGEN ,/CP/6/NMODES/COUNT1/1$
  MATGEN ,/CPL/6/5/2/1/2$
  MATGEN ,/RPL/6/NMODES/COUNT1/1$
  PARTN LAMDA,CPL,RPL/,,,FREQUI/1$
  COUNT2=0$
  DO WHILE (COUNT2 < NTEST)$
    MATGEN ,/RP/6/NTEST/COUNT2/1$
    PARTN NDIR,CP,RP/A11,A12,A21,NDIRI/1$
    PARTN PSD,CP,RP/B11,B12,B21,PSDI/1$
    PARTN QUAL,CP,RP/C11,C12,C21,QUALI/1$
    PARTN ACCEL,CP,RP/D11,D12,D21,DOLD/1$
    SMPYAD QUALI,PSDI,FREQUI,,,/RAD/3/1$
    PARAML RAD//'NULL'////S,N,NOPG$
    IF (NOPG = -1) THEN$
      RADI=0.0
    ELSE$
      PARAML RAD//'DMI'/1/1/S,N,RADI$
    ENDIF$
    RADI=(3.0*GRAV*SQRT(PI2*RADI))
    ALPHA=CMPLX(RADI)
    ADD NDIRI,/ACCELI/ALPHA$
    EQUIVX ACCELI/DNEW/ALWAYS$
    MERGE D11,D12,D21,DNEW,CP,RP/ACCEL1/1$
    EQUIVX ACCEL1/ACCEL/ALWAYS$
    COUNT2=COUNT2+1$
  ENDDO$
  COUNT1=COUNT1+1$

```

```

ENDDO$
MATPRN ACCEL//$
$ Perform the static solution [KANL]-1*[MANL]*{ACCEL} for
$ each mode selected to generate the 'psuedo' static mode
$ shapes. Each mode shape is mass normalized for the
$ correlation process. After each mode shape is generated
$ its influence in the remaining static solution is removed
$ by performing a deflation of the static matrix in the
$ form: [DEF]=[KANL]-1*[MANL] - (LAMDA)-1 *[PHITST]T
$ *[PHITST]* [MANL]. Intermediate modes not selected for
$ correlation are also swept from the system using the
$ corresponding mode shape provided by analysis.
MATGEN ,/KINV/7/NTEST/NMODES$
MATGEN ,/PHITST/7/NTEST/1$
MATGEN ,/MODEI/7/NTEST/1$
MATGEN ,/DEF/7/NTEST/NMODES$
MATGEN ,/DEFT/7/NTEST/NMODES$
SOLVE KANL,/KINV/3$
MPYAD KINV,MANL,/DEF/0/1$
COUNT=1$
COUNT1=1$
PARAML MODELST//'DTI'/COUNT1/1//S,N,PART$
DO WHILE (COUNT <= NMAX )$
  IF (COUNT = PART) THEN$
    MATMOD ACCEL,,,,,/ACCELI,/1/COUNT1$
    MPYAD DEF,ACCELI,/XMODE/0/1$
    SMPYAD XMODE,MANL,XMODE,,,/MFSQR/3/1///1/0/0$
    PARAML MFSQR//'DMI'/1/1/S,N,MR$
    MR=1.0/SQRT(MR)$
    MRI=CMPLX(MR)$
    ADD XMODE,/XTEMP/MRI$
    MESSAGE //'CALCULATION OF STATIC MODE SHAPE = '/PART$
    IF (COUNT = 1) THEN$
      EQUIVX XTEMP/PHITST/ALWAYS$
    ELSE$
      APPEND PHITST,XTEMP/XMODE$
      EQUIVX XMODE/PHITST/ALWAYS$
    ENDIF$
    MATMOD PHIANL,,,,,/MODEI,/1/COUNT$
    SMPYAD MODEI,MODEI,MANL,,,/NUMER/3///0/1/0$
    PARAML LAMAT//'DMI'/1/COUNT/S,N,EIGVAL$
    MESSAGE //'EIGENVALUE = '/EIGVAL$
    EIGVAL=-1.0/EIGVAL$
    ALPHA=CMPLX(EIGVAL)$
    ADD DEF,NUMER/DEFT/(1.0,0.0)/ALPHA/0$
    EQUIVX DEFT/DEF/ALWAYS$
    COUNT=COUNT+1$
    COUNT1=COUNT1+1$
    PARAML MODELST//'DTI'/COUNT1/1//S,N,PART$
  ELSE$
    MATMOD PHIANL,,,,,/MODEI,/1/COUNT$
    SMPYAD MODEI,MODEI,MANL,,,/NUMER/3/1///0/1/0$

```

```
PARAML LAMAT// 'DMI' /1/COUNT/S,N,EIGVAL$
EIGVAL=-1.0/EIGVAL$
ALPHA=CMLX(EIGVAL)$
ADD DEF,NUMER/DEFT/(1.0,0.0)/ALPHA/0$
EQUIVX DEFT/DEF/ALWAYS$
COUNT=COUNT+1$
ENDIF$
ENDDO$
MATPRN PHITST// $
$ Perform the Cross Orthogonality computation for the modes
$ selected. Orthogonality is provided by [PHIRED]^T*
$ [MANL]*[PHITST].
MATGEN ,/COC/7/NTEST/NMODES$
SMPYAD PHIRED,MANL,PHITST,,,/COC/3/1///1/0/0$
MATPRN COC// $
MESSAGE //'CROSS ORTHOGONALITY COMPUTATION COMPLETE'$
END$
```

APPENDIX B
CANTILEVERED BEAM MODEL

- Eigenvalue Analysis, Input
- Eigenvalue Analysis, Output (Abridged)
- Random Response Analysis, Input (Abridged)
- Random Response Analysis, Output (Abridged)

```

SOL 103
TIME 4
CEND
SEALL = ALL
SUPER = ALL
SET 100 = 21,41,61
TITLE = High Fidelity Cantilevered Beam Model
ECHO = SORT
SPC = 5
SUBCASE 1
  METHOD = 1
BEGIN BULK
PARAM  AUTOSPC YES
PARAM  COUPMASS 1
PARAM  WTMASS 1.
PARAM  GRDPNT 0
EIGR  1      SINV  0.      2000.      20 +      A
+      A MASS
PBAR  1      1      6.-5    5.-10
CBAR  1      1      1       2       1.      1.      0.
CBAR  2      1      2       3       1.      1.      0.
CBAR  3      1      3       4       1.      1.      0.
CBAR  4      1      4       5       1.      1.      0.
CBAR  5      1      5       6       1.      1.      0.
CBAR  6      1      6       7       1.      1.      0.
CBAR  7      1      7       8       1.      1.      0.
CBAR  8      1      8       9       1.      1.      0.
CBAR  9      1      9      10      1.      1.      0.
CBAR 10      1      10     11      1.      1.      0.
CBAR 11      1      11     12      1.      1.      0.
CBAR 12      1      12     13      1.      1.      0.
CBAR 13      1      13     14      1.      1.      0.
CBAR 14      1      14     15      1.      1.      0.
CBAR 15      1      15     16      1.      1.      0.
CBAR 16      1      16     17      1.      1.      0.
CBAR 17      1      17     18      1.      1.      0.
CBAR 18      1      18     19      1.      1.      0.
CBAR 19      1      19     20      1.      1.      0.
CBAR 20      1      20     21      1.      1.      0.
CBAR 21      1      21     22      1.      1.      0.
CBAR 22      1      22     23      1.      1.      0.
CBAR 23      1      23     24      1.      1.      0.
CBAR 24      1      24     25      1.      1.      0.
CBAR 25      1      25     26      1.      1.      0.
CBAR 26      1      26     27      1.      1.      0.
CBAR 27      1      27     28      1.      1.      0.
CBAR 28      1      28     29      1.      1.      0.
CBAR 29      1      29     30      1.      1.      0.
CBAR 30      1      30     31      1.      1.      0.
CBAR 31      1      31     32      1.      1.      0.
CBAR 32      1      32     33      1.      1.      0.
CBAR 33      1      33     34      1.      1.      0.

```

CBAR	34	1	34	35	1.	1.	0.
CBAR	35	1	35	36	1.	1.	0.
CBAR	36	1	36	37	1.	1.	0.
CBAR	37	1	37	38	1.	1.	0.
CBAR	38	1	38	39	1.	1.	0.
CBAR	39	1	39	40	1.	1.	0.
CBAR	40	1	40	41	1.	1.	0.
CBAR	41	1	41	42	1.	1.	0.
CBAR	42	1	42	43	1.	1.	0.
CBAR	43	1	43	44	1.	1.	0.
CBAR	44	1	44	45	1.	1.	0.
CBAR	45	1	45	46	1.	1.	0.
CBAR	46	1	46	47	1.	1.	0.
CBAR	47	1	47	48	1.	1.	0.
CBAR	48	1	48	49	1.	1.	0.
CBAR	49	1	49	50	1.	1.	0.
CBAR	50	1	50	51	1.	1.	0.
CBAR	51	1	51	52	1.	1.	0.
CBAR	52	1	52	53	1.	1.	0.
CBAR	53	1	53	54	1.	1.	0.
CBAR	54	1	54	55	1.	1.	0.
CBAR	55	1	55	56	1.	1.	0.
CBAR	56	1	56	57	1.	1.	0.
CBAR	57	1	57	58	1.	1.	0.
CBAR	58	1	58	59	1.	1.	0.
CBAR	59	1	59	60	1.	1.	0.
CBAR	60	1	60	61	1.	1.	0.
MAT1	1	7.+7		.333333	2700.		
GRID	1		0.	0.	0.		
GRID	2		.005	0.	0.		
GRID	3		.009999	0.	0.		
GRID	4		.014999	0.	0.		
GRID	5		.019998	0.	0.		
GRID	6		.024998	0.	0.		
GRID	7		.029997	0.	0.		
GRID	8		.034996	0.	0.		
GRID	9		.039996	0.	0.		
GRID	10		.044995	0.	0.		
GRID	11		.049995	0.	0.		
GRID	12		.054995	0.	0.		
GRID	13		.059994	0.	0.		
GRID	14		.064994	0.	0.		
GRID	15		.069993	0.	0.		
GRID	16		.074993	0.	0.		
GRID	17		.079992	0.	0.		
GRID	18		.084991	0.	0.		
GRID	19		.089991	0.	0.		
GRID	20		.09499	0.	0.		
GRID	21		.09999	0.	0.		
GRID	22		.10499	0.	0.		
GRID	23		.10999	0.	0.		
GRID	24		.114991	0.	0.		

GRID	25		.119991	0.	0.
GRID	26		.124991	0.	0.
GRID	27		.129992	0.	0.
GRID	28		.134992	0.	0.
GRID	29		.139992	0.	0.
GRID	30		.144992	0.	0.
GRID	31		.149992	0.	0.
GRID	32		.154993	0.	0.
GRID	33		.159993	0.	0.
GRID	34		.164993	0.	0.
GRID	35		.169994	0.	0.
GRID	36		.174994	0.	0.
GRID	37		.179994	0.	0.
GRID	38		.184994	0.	0.
GRID	39		.189994	0.	0.
GRID	40		.194995	0.	0.
GRID	41		.199995	0.	0.
GRID	42		.204995	0.	0.
GRID	43		.209996	0.	0.
GRID	44		.214996	0.	0.
GRID	45		.219996	0.	0.
GRID	46		.224996	0.	0.
GRID	47		.229997	0.	0.
GRID	48		.234997	0.	0.
GRID	49		.239997	0.	0.
GRID	50		.244997	0.	0.
GRID	51		.249998	0.	0.
GRID	52		.254998	0.	0.
GRID	53		.259998	0.	0.
GRID	54		.264998	0.	0.
GRID	55		.269999	0.	0.
GRID	56		.274999	0.	0.
GRID	57		.279999	0.	0.
GRID	58		.284999	0.	0.
GRID	59		.29	0.	0.
GRID	60		.295	0.	0.
GRID	61		.3	0.	0.
SPCADD	5	4	7		
SPCI	4	123456	1		
SPCI	7	1345	2	THRU	61
ENDDATA					

S

*	1.000000E+00	0.000000E+00	0.000000E+00	0.000000E+00	*
*	0.000000E+00	1.000000E+00	0.000000E+00	0.000000E+00	*
*	0.000000E+00	0.000000E+00	1.000000E+00	0.000000E+00	*

DIRECTION	MASS	X-C.G.	Y-C.G.	Z-C.G.
X	4.860000E-02	0.000000E+00	0.000000E+00	0.000000E+00
Y	4.860000E-02	1.500000E-01	0.000000E+00	0.000000E+00
Z	4.860000E-02	1.500000E-01	0.000000E+00	0.000000E+00

I(S)

*	0.000000E+00	0.000000E+00	0.000000E+00	*
*	0.000000E+00	3.644999E-04	0.000000E+00	*
*	0.000000E+00	0.000000E+00	3.644999E-04	*

I(Q)

*	0.000000E+00	*
*	3.644999E-04	*
*	3.644999E-04	*

Q

*	1.000000E+00	0.000000E+00	0.000000E+00	*
*	0.000000E+00	1.000000E+00	0.000000E+00	*
*	0.000000E+00	0.000000E+00	1.000000E+00	*

E I G E N V A L U E A N A L Y S I S S U M M A R Y (S T U R M I N V E R S E P O W E R)

N U M B E R O F E I G E N V A L U E S E X T R A C T E D

NUMBER OF TRIANGULAR DECOMPOSITIONS 12

TOTAL NUMBER OF VECTOR ITERATIONS 139

REASON FOR TERMINATION: ALL EIGENVALUES FOUND IN RANGE.

REAL EIGENVALUES

MODE NO.	EXTRACTION ORDER	EIGENVALUE	RADIANS	CYCLES	GENERALIZED MASS	GENERALIZED STIFFNESS
1	1	3.297383E+02	1.815870E+01	2.890047E+00	1.000000E+00	3.297383E+02
2	3	1.295013E+04	1.137986E+02	1.811161E+01	1.000000E+00	1.295013E+04
3	2	1.015311E+05	3.186395E+02	5.071305E+01	1.000000E+00	1.015311E+05
4	4	3.898836E+05	6.244066E+02	9.937740E+01	1.000000E+00	3.898836E+05
5	5	1.065417E+06	1.032190E+03	1.642782E+02	1.000000E+00	1.065417E+06
6	6	2.377510E+06	1.541918E+03	2.454038E+02	1.000000E+00	2.377510E+06
7	7	4.637981E+06	2.153597E+03	3.427556E+02	1.000000E+00	4.637981E+06
8	8	8.221040E+06	2.867236E+03	4.563347E+02	1.000000E+00	8.221040E+06
9	9	1.356334E+07	3.682844E+03	5.861428E+02	1.000000E+00	1.356334E+07
10	13	2.116403E+07	4.600438E+03	7.321825E+02	1.000000E+00	2.116403E+07
11	11	3.158487E+07	5.620042E+03	8.944575E+02	1.000000E+00	3.158487E+07
12	10	4.545033E+07	6.741686E+03	1.072973E+03	1.000000E+00	4.545033E+07
13	12	6.344779E+07	7.965412E+03	1.267735E+03	1.000000E+00	6.344779E+07
14	14	8.632777E+07	9.291273E+03	1.478752E+03	1.000000E+00	8.632777E+07
15	16	1.149042E+08	1.071934E+04	1.706036E+03	1.000000E+00	1.149042E+08
16	15	1.500549E+08	1.224969E+04	1.949599E+03	1.000000E+00	1.500549E+08

EIGENVALUE = 3.297383E+02

CYCLES = 2.890047E+00

REAL EIGENVECTOR NO. 1

POINT ID.	TYPE	T1	T2	T3	R1	R2	R3
1	G	0.0	0.0	0.0	0.0	0.0	0.0
21	G	0.0	1.501503E+00	0.0	0.0	0.0	2.735082E+01
41	G	0.0	4.961753E+00	0.0	0.0	0.0	3.958266E+01
61	G	0.0	9.072180E+00	0.0	0.0	0.0	4.162630E+01

EIGENVALUE = 1.295013E+04
 CYCLES = 1.811161E+01 2

POINT ID.	TYPE	T1	T2	T3	R1	R2	R3
1	G	0.0	0.0	0.0	0.0	0.0	0.0
21	G	0.0	-5.348792E+00	0.0	0.0	0.0	-5.330963E+01
41	G	0.0	-3.835341E+00	0.0	0.0	0.0	8.952410E+01
61	G	0.0	9.072219E+00	0.0	0.0	0.0	1.445746E+02

EIGENVALUE = 1.015311E+05
 CYCLES = 5.071305E+01 3

POINT ID.	TYPE	T1	T2	T3	R1	R2	R3
1	G	0.0	0.0	0.0	0.0	0.0	0.0
21	G	0.0	6.549566E+00	0.0	0.0	0.0	-5.142038E+01
41	G	0.0	-5.839239E+00	0.0	0.0	0.0	-3.542955E+01
61	G	0.0	9.072167E+00	0.0	0.0	0.0	2.373483E+02

EIGENVALUE = 3.898836E+05
 CYCLES = 9.937740E+01 4

POINT ID.	TYPE	T1	T2	T3	R1	R2	R3
1	G	0.0	0.0	0.0	0.0	0.0	0.0

21	G	0.0	1.775759E+00	0.0	0.0	0.0	0.0	0.0	0.0	-2.314598E+02
41	G	0.0	1.546072E+00	0.0	0.0	0.0	0.0	0.0	0.0	2.227602E+02
61	G	0.0	-9.072143E+00	0.0	0.0	0.0	0.0	0.0	0.0	-3.325212E+02

EIGENVALUE = 1.065417E+06
 CYCLES = 1.642782E+02 REAL EIGENVECTOR NO. 5

POINT ID.	TYPE	T1	T2	T3	R1	R2	R3
1	G	0.0	0.0	0.0	0.0	0.0	0.0
21	G	0.0	4.492882E+00	0.0	0.0	0.0	2.157620E+02
41	G	0.0	-4.578237E+00	0.0	0.0	0.0	2.118078E+02
61	G	0.0	-9.072212E+00	0.0	0.0	0.0	-4.275163E+02

EIGENVALUE = 2.377510E+06
 CYCLES = 2.454038E+02 REAL EIGENVECTOR NO. 6

POINT ID.	TYPE	T1	T2	T3	R1	R2	R3
1	G	0.0	0.0	0.0	0.0	0.0	0.0
21	G	0.0	6.183141E+00	0.0	0.0	0.0	-9.459785E+01
41	G	0.0	6.210276E+00	0.0	0.0	0.0	9.655643E+01
61	G	0.0	9.072327E+00	0.0	0.0	0.0	5.225280E+02

S

DIRECTION			MASS			X-C.G.			Y-C.G.			Z-C.G.		
MASS AXIS SYSTEM (S)			MASS			X-C.G.			Y-C.G.			Z-C.G.		
X	Y	Z												
*	1.000000E+00	0.000000E+00	0.000000E+00	0.000000E+00	0.000000E+00	*	0.000000E+00	0.000000E+00	0.000000E+00	0.000000E+00	0.000000E+00	0.000000E+00	0.000000E+00	0.000000E+00
*	0.000000E+00	1.000000E+00	0.000000E+00	0.000000E+00	0.000000E+00	*	0.000000E+00	0.000000E+00	0.000000E+00	0.000000E+00	0.000000E+00	0.000000E+00	0.000000E+00	0.000000E+00
*	0.000000E+00	0.000000E+00	1.000000E+00	0.000000E+00	0.000000E+00	*	0.000000E+00	0.000000E+00	0.000000E+00	0.000000E+00	0.000000E+00	0.000000E+00	0.000000E+00	0.000000E+00
	5.000005E+04						0.000000E+00	0.000000E+00	0.000000E+00	0.000000E+00	0.000000E+00	0.000000E+00	0.000000E+00	0.000000E+00
	5.000005E+04						-9.999845E-03	0.000000E+00	0.000000E+00	0.000000E+00	0.000000E+00	0.000000E+00	0.000000E+00	0.000000E+00
	5.000005E+04						-9.999845E-03	0.000000E+00	0.000000E+00	0.000000E+00	0.000000E+00	0.000000E+00	0.000000E+00	0.000000E+00

I(S)

*	0.000000E+00	0.000000E+00	0.000000E+00	0.000000E+00	*
*	0.000000E+00	1.607895E-03	0.000000E+00	0.000000E+00	*
*	0.000000E+00	0.000000E+00	1.607895E-03	0.000000E+00	*

I(Q)

*	0.000000E+00				*
*		1.607895E-03			*
*			1.607895E-03		*

Q

*	1.000000E+00	0.000000E+00	0.000000E+00	0.000000E+00	*
*	0.000000E+00	1.000000E+00	0.000000E+00	0.000000E+00	*
*	0.000000E+00	0.000000E+00	1.000000E+00	0.000000E+00	*

E I G E N V A L U E A N A L Y S I S S U M M A R Y (S T U R M I N V E R S E P O W E R)

NUMBER OF EIGENVALUES EXTRACTED 17

NUMBER OF TRIANGULAR DECOMPOSITIONS 13

TOTAL NUMBER OF VECTOR ITERATIONS 150

REASON FOR TERMINATION: ALL EIGENVALUES FOUND IN RANGE.

MODE NO.	EXTRACTION ORDER	EIGENVALUE	REAL EIGENVALUES				GENERALIZED MASS	GENERALIZED STIFFNESS
			RADIANS	CYCLES	X FOR	Y FOR		
1	1	1.064377E-13	3.262480E-07	5.192398E-08	1.000000E+00	1.064377E-13		
2	2	3.297385E+02	1.815870E+01	2.890048E+00	1.000000E+00	3.297385E+02		
3	3	1.295013E+04	1.137986E+02	1.811161E+01	1.000000E+00	1.295013E+04		
4	4	1.015311E+05	3.186395E+02	5.071305E+01	1.000000E+00	1.015311E+05		
5	5	3.898836E+05	6.244066E+02	9.937740E+01	1.000000E+00	3.898836E+05		
6	6	1.065417E+06	1.032190E+03	1.642782E+02	1.000000E+00	1.065417E+06		
7	7	2.377510E+06	1.541918E+03	2.454038E+02	1.000000E+00	2.377510E+06		
8	8	4.637981E+06	2.153597E+03	3.427556E+02	1.000000E+00	4.637981E+06		
9	9	8.221040E+06	2.867236E+03	4.563347E+02	1.000000E+00	8.221040E+06		
10	10	1.356334E+07	3.682844E+03	5.861428E+02	1.000000E+00	1.356334E+07		
11	14	2.116403E+07	4.600438E+03	7.321825E+02	1.000000E+00	2.116403E+07		
12	12	3.158487E+07	5.620042E+03	8.944575E+02	1.000000E+00	3.158487E+07		
13	11	4.545033E+07	6.741686E+03	1.072973E+03	1.000000E+00	4.545033E+07		
14	13	6.344779E+07	7.965412E+03	1.267735E+03	1.000000E+00	6.344779E+07		
15	15	8.632777E+07	9.291273E+03	1.478752E+03	1.000000E+00	8.632777E+07		
16	17	1.149042E+08	1.071934E+04	1.706036E+03	1.000000E+00	1.149042E+08		
17	16	1.500549E+08	1.224969E+04	1.949599E+03	1.000000E+00	1.500549E+08		

X Y - O U T P U T S U M M A R Y (A U T O R P S D F)

PLOT TYPE	CURVE FRAME NO.	CURVE ID.	RMS VALUE	NO. POSITIVE CROSSINGS		XMIN FOR ALL DATA		XMAX FOR ALL DATA		YMIN FOR ALL DATA		YMAX FOR ALL DATA	
				3	4	3	4	3	4	3	4		
PSDF ACCE	3	21(4)	1.600065E+00	4.820225E+02	1.000E-01	2.000E+03	1.001E-05	1.000E-01	4.675E-02	5.071E+01	4.675E-02	5.071E+01	
PSDF ACCE	3	21(4)	1.600065E+00	4.820225E+02	1.000E-01	2.000E+03	1.001E-05	1.000E-01	4.675E-02	5.071E+01	4.675E-02	5.071E+01	

PRINTED DATA FOR THIS CURVE FOLLOWS

ACCELERATION	CURVE	ID =	21	COMPONENT = 4	WHOLE FRAME	CARD NUMBER
		PRINT	NUMBER	X-VALUE	Y-VALUE	
		1		1.00000E-01	1.000654E-05	
		2		1.695853E-01	1.699054E-05	
		3		1.935242E-01	1.940005E-05	
		4		2.208424E-01	2.215514E-05	
		5		2.520168E-01	2.530726E-05	
		6		2.875918E-01	2.891648E-05	
		7		3.281887E-01	3.305338E-05	
		8		3.745162E-01	3.780161E-05	
		9		4.273835E-01	4.326131E-05	
		10		4.877135E-01	4.955410E-05	
		11		5.565598E-01	5.683014E-05	
		12		6.351246E-01	6.527892E-05	
		13		7.247796E-01	7.514605E-05	
		14		8.270904E-01	8.676032E-05	
		15		9.438436E-01	1.005802E-04	
		16		1.077078E+00	1.172779E-04	
		17		1.229120E+00	1.379002E-04	
		18		1.402624E+00	1.642097E-04	
		19		1.600621E+00	1.994773E-04	
		20		1.826566E+00	2.506056E-04	
		21		2.084407E+00	3.349011E-04	
		22		2.378644E+00	5.059012E-04	
		23		2.714417E+00	8.684342E-04	
		24		2.890000E+00	7.832464E-04	
		25		3.097588E+00	3.140417E-04	
		26		3.534848E+00	8.884150E-05	
		27		4.033832E+00	1.257087E-04	
		28		4.603253E+00	1.850803E-04	
		29		5.253055E+00	2.506551E-04	
		30		5.994583E+00	3.254752E-04	
		31		6.840786E+00	4.163033E-04	
		32		7.806441E+00	5.339996E-04	
		33		8.908408E+00	6.978968E-04	

34	1.016593E+01	9.471363E-04
35	1.160097E+01	1.373957E-03
36	1.323858E+01	2.245094E-03
37	1.510736E+01	4.583694E-03
38	1.723993E+01	1.196515E-02
39	1.881110E+01	1.028639E-02
40	1.967354E+01	6.065149E-03
41	2.245069E+01	1.303272E-03
42	2.561986E+01	3.384980E-04
43	2.923639E+01	2.508137E-04
44	3.336345E+01	7.144013E-04
45	3.807307E+01	2.348089E-03
46	4.344752E+01	9.533987E-03
47	4.958063E+01	4.243848E-02
48	5.071300E+01	4.675353E-02
49	5.657950E+01	2.491955E-02
50	6.456634E+01	7.942628E-03
51	7.368061E+01	3.465188E-03
52	8.408147E+01	1.850070E-03
53	9.595052E+01	3.385911E-03
54	9.937740E+01	4.908107E-03
55	1.094950E+02	6.000861E-03
56	1.249515E+02	5.446393E-03
57	1.425898E+02	7.260158E-03
58	1.627180E+02	9.372263E-03
59	1.642780E+02	8.833766E-03
60	1.856875E+02	1.574419E-03
61	2.118994E+02	1.918801E-03
62	2.418114E+02	7.528340E-03
63	2.454030E+02	7.835794E-03
64	2.759458E+02	3.646449E-03
65	3.148987E+02	1.452769E-03
66	3.427550E+02	1.725633E-03
67	3.593502E+02	1.939246E-03
68	4.100766E+02	1.869810E-03
69	4.563340E+02	1.362967E-03

70	4.679636E+02	1.008262E-03
71	5.340219E+02	4.748981E-04
72	5.861420E+02	9.060759E-04
73	6.094052E+02	8.340693E-04
74	6.954296E+02	3.860666E-04
75	7.321820E+02	4.078427E-04
76	7.935974E+02	4.625834E-04
77	8.944570E+02	4.116622E-04
78	9.056227E+02	3.796798E-04
79	1.033462E+03	3.247239E-04
80	1.072970E+03	3.727491E-04
81	1.179347E+03	2.670722E-04
82	1.267730E+03	2.413176E-04
83	1.345826E+03	2.560866E-04
84	1.478750E+03	2.163787E-04
85	1.535803E+03	1.740408E-04
86	1.706030E+03	1.378282E-04
87	1.752600E+03	1.148255E-04
88	1.949590E+03	3.762462E-05
89	1.999999E+03	2.808617E-05

X Y - O U T P U T S U M M A R Y (A U T O R P S D F)

PLOT TYPE	CURVE FRAME TYPE	CURVE NO.	RMS VALUE	NO. POSITIVE CROSSINGS	XMIN FOR ALL DATA	XMAX FOR ALL DATA	YMIN FOR ALL DATA	YMAX FOR ALL DATA	X FOR YMIN	X FOR YMAX
PSDF	ACCE	4	1.270671E+00	3.535369E+02	1.000E-01	2.000E+03	1.759E-06	2.000E+03	2.000E+03	3.365E-02
PSDF	ACCE	4	1.270671E+00	3.535369E+02	1.000E-01	2.000E+03	1.759E-06	2.000E+03	2.000E+03	3.365E-02

P R I N T E D D A T A F O R T H I S C U R V E F O L L O W S

ACCELERATION	CURVE ID =	41	COMPONENT =	4	WHOLE FRAME	CARD NUMBER
	PRINT NUMBER	X-VALUE	Y-VALUE			
	1	1.000000E-01	1.002072E-05			
	2	1.695853E-01	1.705998E-05			
	3	1.935242E-01	1.950341E-05			

4	2.208424E-01	2.230905E-05
5	2.520168E-01	2.553661E-05
6	2.875918E-01	2.925853E-05
7	3.281887E-01	3.356408E-05
8	3.745162E-01	3.856518E-05
9	4.273835E-01	4.440512E-05
10	4.877135E-01	5.127174E-05
11	5.565598E-01	5.941795E-05
12	6.351246E-01	6.919471E-05
13	7.247796E-01	8.110567E-05
14	8.270904E-01	9.590168E-05
15	9.438436E-01	1.147516E-04
16	1.077078E+00	1.395709E-04
17	1.229120E+00	1.736990E-04
18	1.402624E+00	2.234302E-04
19	1.600621E+00	3.019001E-04
20	1.826566E+00	4.406059E-04
21	2.084407E+00	7.316643E-04
22	2.378644E+00	1.533849E-03
23	2.714417E+00	4.417322E-03
24	2.890000E+00	5.594744E-03
25	3.097588E+00	3.375574E-03
26	3.534848E+00	7.723867E-04
27	4.033832E+00	2.383149E-04
28	4.603253E+00	8.763697E-05
29	5.253055E+00	3.404092E-05
30	5.994583E+00	1.396403E-05
31	6.840786E+00	8.843655E-06
32	7.806441E+00	1.310886E-05
33	8.908408E+00	2.716237E-05
34	1.016593E+01	5.788370E-05
35	1.160097E+01	1.278658E-04
36	1.323858E+01	3.183736E-04
37	1.510736E+01	1.026767E-03
38	1.723993E+01	4.563009E-03
39	1.881110E+01	5.949841E-03

40	1.967354E+01	4.467333E-03
41	2.245069E+01	2.264674E-03
42	2.561986E+01	1.700204E-03
43	2.923639E+01	1.694206E-03
44	3.336345E+01	2.147092E-03
45	3.807307E+01	3.570730E-03
46	4.344752E+01	9.288543E-03
47	4.958063E+01	3.152433E-02
48	5.071300E+01	3.364690E-02
49	5.657950E+01	1.629535E-02
50	6.456634E+01	5.303599E-03
51	7.368061E+01	2.874346E-03
52	8.408147E+01	2.439108E-03
53	9.595052E+01	2.636858E-03
54	9.937740E+01	2.146386E-03
55	1.094950E+02	5.177153E-04
56	1.249515E+02	4.392473E-04
57	1.425898E+02	1.616685E-03
58	1.627180E+02	6.730694E-03
59	1.642780E+02	6.995435E-03
60	1.856875E+02	4.662532E-03
61	2.118994E+02	4.055460E-03
62	2.418114E+02	6.490529E-03
63	2.454030E+02	6.338595E-03
64	2.759458E+02	2.280380E-03
65	3.148987E+02	9.618525E-04
66	3.427550E+02	5.585217E-04
67	3.593502E+02	3.131037E-04
68	4.100766E+02	3.058975E-04
69	4.563340E+02	6.868762E-04
70	4.679636E+02	6.783892E-04
71	5.340219E+02	4.802923E-04
72	5.861420E+02	5.269774E-04
73	6.094052E+02	4.181088E-04
74	6.954296E+02	1.461673E-04
75	7.321820E+02	9.944786E-05

10	4.877135E-01	5.328601E-05
11	5.565598E-01	6.247029E-05
12	6.351246E-01	7.384842E-05
13	7.247796E-01	8.825873E-05
14	8.270904E-01	1.070163E-04
15	9.438436E-01	1.322763E-04
16	1.077078E+00	1.677591E-04
17	1.229120E+00	2.203099E-04
18	1.402624E+00	3.035816E-04
19	1.600621E+00	4.478472E-04
20	1.826566E+00	7.306873E-04
21	2.084407E+00	1.396848E-03
22	2.378644E+00	3.495114E-03
23	2.714417E+00	1.255756E-02
24	2.890000E+00	1.799159E-02
25	3.097588E+00	1.263929E-02
26	3.534848E+00	4.072838E-03
27	4.033832E+00	1.924042E-03
28	4.603253E+00	1.203926E-03
29	5.253055E+00	9.027548E-04
30	5.994583E+00	7.724725E-04
31	6.840786E+00	7.363735E-04
32	7.806441E+00	7.740895E-04
33	8.908408E+00	8.975070E-04
34	1.016593E+01	1.160699E-03
35	1.160097E+01	1.720856E-03
36	1.323858E+01	3.096802E-03
37	1.510736E+01	7.596618E-03
38	1.723993E+01	2.661652E-02
39	1.88110E+01	3.011461E-02
40	1.967354E+01	2.110604E-02
41	2.245069E+01	8.865859E-03
42	2.561986E+01	5.639499E-03
43	2.923639E+01	4.879724E-03
44	3.336345E+01	5.528630E-03
45	3.807307E+01	8.517895E-03

46	4.344752E+01	2.145202E-02
47	4.958063E+01	7.446928E-02
48	5.071300E+01	8.031060E-02
49	5.657950E+01	4.221560E-02
50	6.456634E+01	1.650981E-02
51	7.368061E+01	1.220444E-02
52	8.408147E+01	1.710064E-02
53	9.595052E+01	4.175624E-02
54	9.937740E+01	4.531268E-02
55	1.094950E+02	2.410263E-02
56	1.249515E+02	1.106838E-02
57	1.425898E+02	1.267786E-02
58	1.627180E+02	2.484878E-02
59	1.642780E+02	2.477396E-02
60	1.856875E+02	1.095306E-02
61	2.118994E+02	7.688598E-03
62	2.418114E+02	1.250297E-02
63	2.454030E+02	1.242521E-02
64	2.759458E+02	5.884504E-03
65	3.148987E+02	4.965364E-03
66	3.427550E+02	5.778200E-03
67	3.593502E+02	4.495428E-03
68	4.100766E+02	2.230779E-03
69	4.563340E+02	2.098106E-03
70	4.679636E+02	1.785425E-03
71	5.340219E+02	8.110069E-04
72	5.861420E+02	9.148708E-04
73	6.094052E+02	8.030036E-04
74	6.954296E+02	5.944904E-04
75	7.321820E+02	5.923391E-04
76	7.935974E+02	4.116127E-04
77	8.944570E+02	3.697859E-04
78	9.056227E+02	3.608479E-04
79	1.033462E+03	2.611535E-04
80	1.072970E+03	2.391048E-04
81	1.179347E+03	1.427786E-04

82	1.267730E+03	1.341281E-04
83	1.345826E+03	1.260633E-04
84	1.478750E+03	9.241141E-05
85	1.535803E+03	6.018558E-05
86	1.706030E+03	3.137242E-05
87	1.752600E+03	4.122525E-05
88	1.949590E+03	5.267349E-05
89	1.999999E+03	4.016862E-05

* * * END OF JOB * * *

APPENDIX C

STDCE EXPERIMENT PACKAGE

- Eigenvalue Analysis, Input (Abridged)
- Eigenvalue Analysis, Output (Abridged)
- Correlation Analysis, Input (Abridged)
- Correlation Analysis, Output (Abridged)

```

SOL 103
TIME 10
CEND
TITLE = STDCE EXPERIMENT PACKAGE - AS BUILT FLIGHT HARDWARE
SUBTITLE = NORMAL MODES ANALYSIS - STATIC CONDESATION EMPLOYED
ECHO = SORT
SPC = 41
VECTOR(PLOT) = ALL
METHOD=1
DYNRED=2
BEGIN BULK
EIGR   1      SINV   0.    200.        100          +      A
+      A MASS
DYNRED  2      200.
$ DOF ASSOCIATED WITH ACCELEROMETER LOCATIONS/DOF
ASET1  123    603    744    536    149
ASET1  23     224
ASET1  2      159    12
$ PARAMETERS ASSOCIATED WITH EFFECTIVE MASS CALCULATIONS
PARAM  KEPRT  1
PARAM  EFWGT  2
PARAM  CHKSTIF 1
PARAM  CHKMASS 1
$
$ BEGINNING OF EXPERIMENT PACKAGE STRUCTURE (C200)
$
#####
#
# DUE TO ITS VOLUMINOUS NATURE, THE BULK DATA INPUT FOR THE
# EXPERIMENT PACKAGE MODEL HAS BEEN OMITTED. THE COMPLETE MODEL
# CAN BE OBTAINED FROM THE AUTHOR.
#
#####
$ PARAMETERS ASSOCIATED WITH THE MODAL SOLUTION
PARAM  AUTOSPC  YES
PARAM  COUPMASS  1
PARAM  GRDPNT  0
PARAM  K6ROT  1000.
PARAM  WTMASS  1.
ENDDATA

```


S
 * 1.000000E+00 0.000000E+00 0.000000E+00 *
 * 0.000000E+00 1.000000E+00 0.000000E+00 *
 * 0.000000E+00 0.000000E+00 1.000000E+00 *

DIRECTION
 MASS AXIS SYSTEM (S) MASS X-C.G. Y-C.G. Z-C.G.
 X 7.071376E-01 -8.341835E-18 1.209131E+01 1.537560E+01
 Y 7.071376E-01 -3.534285E-01 -1.610920E-18 1.537560E+01
 Z 7.071376E-01 -3.534285E-01 1.209131E+01 1.010355E-17

I(S)
 * 1.329014E+02 -1.182628E-01 -5.062192E+00 *
 * -1.182628E-01 1.141557E+02 6.661880E+00 *
 * -5.062192E+00 6.661880E+00 5.527565E+01 *

I(Q)
 * 1.148893E+02 *
 * 1.332355E+02 *
 * 5.420799E+01 *

Q
 * -2.411051E-02 -9.976601E-01 6.397712E-02 *
 * -9.937487E-01 1.693974E-02 -1.103471E-01 *
 * 1.090052E-01 -6.623770E-02 -9.918318E-01 *

NUMBER OF EIGENVALUES EXTRACTED 8
 NUMBER OF TRIANGULAR DECOMPOSITIONS 9
 TOTAL NUMBER OF VECTOR ITERATIONS 99

REASON FOR TERMINATION: ALL EIGENVALUES FOUND IN RANGE.

MODE NO.	EXTRACTION ORDER	EIGENVALUE	R E A L E I G E N V A L U E S			GENERALIZED MASS	GENERALIZED STIFFNESS
			RADIANS	CYCLES	GENERALIZED MASS		
1	1	1.744163E+05	4.176318E+02	6.646817E+01	1.000000E+00	1.744163E+05	
2	6	1.993209E+05	4.464537E+02	7.105531E+01	1.000000E+00	1.993209E+05	
3	4	3.066401E+05	5.537509E+02	8.813219E+01	1.000000E+00	3.066401E+05	
4	5	4.630260E+05	6.804601E+02	1.082986E+02	1.000000E+00	4.630260E+05	
5	3	5.015862E+05	7.082275E+02	1.127179E+02	1.000000E+00	5.015862E+05	
6	2	5.898927E+05	7.680447E+02	1.222381E+02	1.000000E+00	5.898927E+05	
7	8	1.051898E+06	1.025621E+03	1.632326E+02	1.000000E+00	1.051898E+06	
8	7	1.375257E+06	1.172714E+03	1.866431E+02	1.000000E+00	1.375257E+06	

 *** MATRIX EFMFRACT IS THE FRACTION OF THE EFFECTIVE WEIGHT FOR EACH MODE
 *** (ONCE AGAIN, FOR THE ASSEMBLY)

MATRIX EFMFRACT (GTNO NAME 101) IS A DB PREC 8 COLUMN X 6 ROW RECTANG MATRIX.


```

COLUMN 1 ROWS 1 THRU 6 -----
ROW
1) 1.0572D-02 -1.5857D-01 1.9509D-01 2.9864D-01 6.1923D-03 -4.6712D-05
COLUMN 2 ROWS 1 THRU 6 -----
ROW
1) -1.8622D-03 -8.6358D-02 1.9686D-04 4.2645D-02 -1.5363D-03 1.5238D-03
COLUMN 3 ROWS 1 THRU 6 -----
ROW
1) -1.6312D-02 -4.3318D-03 5.9459D-01 3.2675D-01 2.6021D-05 1.7120D-03
COLUMN 4 ROWS 1 THRU 6 -----
ROW
1) 6.2845D-03 2.5882D-01 2.1721D-01 4.5786D-04 1.5457D-04 -1.4230D-03
COLUMN 5 ROWS 1 THRU 6 -----
ROW
1) 5.0579D-01 5.1680D-03 2.8428D-04 -4.2029D-03 7.7285D-01 -4.0086D-01
COLUMN 6 ROWS 1 THRU 6 -----
ROW
1) 1.1985D-03 -4.5809D-04 7.5042D-05 4.9650D-06 1.1337D-03 -4.0530D-04
COLUMN 7 ROWS 1 THRU 6 -----
ROW
1) 6.3712D-01 -5.0890D-03 1.5057D-04 3.2806D-04 3.9838D-01 -1.0584D+00
COLUMN 8 ROWS 1 THRU 6 -----
ROW
1) 1.6855D-03 -1.0553D-01 9.8327D-03 1.3541D-01 -8.8131D-02 1.0215D-02
THE NUMBER OF NON-ZERO TERMS IN THE DENSEST COLUMN = 6
THE DENSITY OF THIS MATRIX IS 100.00 PERCENT.

```

*** END OF JOB ***

SOL 103
TIME 10

#####

CORRELATION DMAP ALTER IS INSERTED HERE

#####

CEND
SET 100 = 603, 744, 536, 224, 149, 159, 12
TITLE = STDCE EXPERIMENT PACKAGE - AS BUILT FLIGHT HARDWARE
SUBTITLE = NORMAL MODES ANALYSIS WITH CROSS ORTHOGONALITY CHECK
SEALL = ALL
SUPER = ALL
ECHO = SORT
SPC = 41
VECTOR = 100
METHOD=1
DYNRED=2
BEGIN BULK
#####

REMAINDER OF INPUT REMAINS UNCHANGED BUT
HAS BEEN OMITTED HERE FOR BREVITY

#####

DMI	PSD	0	2	1	0	16	5	
DMI	PSD	1	1	.0301	3.0142	.0010	.0165	.0002
		.0191	.0010	.0049	.1540	.0012	.0083	.4217
		.8254	.1957	.1695				
DMI	PSD	2	1	.0147	.0013	.0021	.0196	.2488
		.0249	.0866	.0054	.0590	.4642	.0049	.1695
		.0442	.0287	.4217				
DMI	PSD	3	1	.0169	.2738	.0026	.0020	.0178
		.0249	.0909	.0065	.0464	.5109	.0054	.1695
		.0402	.0301	.4870				
DMI	PSD	4	1	.0562	.0649	.1287	.0316	.0001
		.0029	.0075	.9085	1.9573	.0075	1.1007	.3318
		.1540	.2260	.1334				
DMI	PSD	5	1	.0162	.0442	.0079	.0000	.0001
		.0037	.0044	.1957	.0909	.0054	.3625	.0590
		.2054	.0301	.0422				
DMI	QUAL	0	2	1	0	16	5	
DMI	QUAL	1	1	1.9545	195.727	.0649	1.0714	.0130
		1.2403	.0065	.3182	10.0000	.0779	.5390	27.3831
		53.5974	12.7078	11.0065				
DMI	QUAL	2	1	1.5474	.1368	.2211	2.0632	26.1895
		2.6211	9.1158	.5684	6.2105	48.8632	.5158	17.8421
		4.6526	3.0211	44.3895				
DMI	QUAL	3	1	1.7789	28.8211	.2737	.2105	1.8737
		2.6211	9.5684	.6842	4.8842	53.7789	.5684	17.8421
		4.2316	3.1684	51.2632				
DMI	QUAL	4	1	2.9119	3.3627	6.6684	1.6373	.0001

	.1503	.3886	47.0725	101.415	.3886	57.0311	17.1917	2.6218
	7.9793	11.7098	6.9119					
DMI	QUAL	5	1	.7902	2.1561	.3854	.0000	.0046
	.1805	.2146	9.5463	4.4341	.2634	17.6829	2.8780	.1805
	10.0195	1.4683	2.0585					

DTI,MODELST,0
 DTI,MODELST,1,1
 DTI,MODELST,2,3
 DTI,MODELST,3,4
 DTI,MODELST,4,5
 DTI,MODELST,5,7
 PARAM,NMODES,5
 PARAM,NTEST,16
 PARAM,NMAX,8
 PARAM,GRAV,386.4
 PARAM NEWSEQ -1
 ENDDATA

S

	*	1.000000E+00	0.000000E+00	0.000000E+00	0.000000E+00	*
	*	0.000000E+00	1.000000E+00	0.000000E+00	0.000000E+00	*
	*	0.000000E+00	0.000000E+00	1.000000E+00	1.000000E+00	*

DIRECTION

DIRECTION	MASS	X-C.G.	Y-C.G.	Z-C.G.
MASS AXIS SYSTEM (S)				
X	7.071376E-01	-8.425758E-18	1.209131E+01	1.537560E+01
Y	7.071376E-01	-3.534285E-01	-1.653681E-18	1.537560E+01
Z	7.071376E-01	-3.534285E-01	1.209131E+01	1.023682E-17

I(S)

	*	1.329014E+02	-1.182628E-01	-5.062192E+00	*
	*	-1.182628E-01	1.141557E+02	6.661880E+00	*
	*	-5.062192E+00	6.661880E+00	5.527565E+01	*

I(Q)

	*	1.148893E+02	*	*
	*		1.332355E+02	*
	*			5.420799E+01

Q

	*	-2.411051E-02	-9.976601E-01	6.397712E-02	*
	*	-9.937487E-01	1.693974E-02	-1.103471E-01	*
	*	1.090052E-01	-6.623770E-02	-9.918318E-01	*

E I G E N V A L U E A N A L Y S I S S U M M A R Y (S T U R M I N V E R S E P O W E R)

NUMBER OF EIGENVALUES EXTRACTED 8
 NUMBER OF TRIANGULAR DECOMPOSITIONS 10
 TOTAL NUMBER OF VECTOR ITERATIONS 103

REASON FOR TERMINATION: ALL EIGENVALUES FOUND IN RANGE.

120

MODE NO.	EXTRACTION ORDER	EIGENVALUE	R E A L E I G E N V A L U E S			GENERALIZED STIFFNESS
			RADIANS	CYCLES	GENERALIZED MASS	
1	1	1.744163E+05	4.176318E+02	6.646817E+01	1.000000E+00	1.744163E+05
2	6	1.993209E+05	4.464537E+02	7.105531E+01	1.000000E+00	1.993209E+05
3	3	3.066401E+05	5.537509E+02	8.813219E+01	1.000000E+00	3.066401E+05
4	4	4.630260E+05	6.804601E+02	1.082986E+02	1.000000E+00	4.630260E+05
5	5	5.015862E+05	7.082275E+02	1.127179E+02	1.000000E+00	5.015862E+05
6	2	5.898927E+05	7.680447E+02	1.222381E+02	1.000000E+00	5.898927E+05
7	8	1.051898E+06	1.025621E+03	1.632326E+02	1.000000E+00	1.051898E+06
8	7	1.375257E+06	1.172714E+03	1.866431E+02	1.000000E+00	1.375257E+06

MATRIX PSD (GJNO NAME 101) IS A DB PREC 5 COLUMN X 16 ROW RECTANG MATRIX.

COLUMN ROW	1	ROWS 1 THRU 16	5 COLUMN X 16 ROW RECTANG MATRIX.
1)	3.0100D-02	3.0142D+00	1.0000D-03 1.6500D-02 2.0000D-04 1.9100D-02 1.0000D-03 4.9000D-03 1.5400D-01 1.2000D-03
11)	8.3000D-03	4.2170D-01	9.0000D-04 8.2540D-01 1.9570D-01 1.6950D-01

```

COLUMN 2 ROWS 1 THRU 16 -----
ROW
1) 1.4700D-02 1.3000D-03 2.1000D-03 1.9600D-02 2.4880D-01 2.4900D-02 8.6600D-02 5.4000D-03 5.9000D-02 4.6420D-01
11) 4.9000D-03 1.6950D-01 5.6230D-01 4.4200D-02 2.8700D-02 4.2170D-01
COLUMN 3 ROWS 1 THRU 16 -----
ROW
1) 1.6900D-02 2.7380D-01 2.6000D-03 2.0000D-03 1.7800D-02 2.4900D-02 9.0900D-02 6.5000D-03 4.6400D-02 5.1090D-01
11) 5.4000D-03 1.6950D-01 6.1900D-01 4.0200D-02 3.0100D-02 4.8700D-01
COLUMN 4 ROWS 1 THRU 16 -----
ROW
1) 5.6200D-02 6.4900D-02 1.2870D-01 3.1600D-02 1.0000D-04 2.9000D-03 7.5000D-03 9.0850D-01 1.9573D+00 7.5000D-03
11) 1.1007D+00 3.3180D-01 5.0600D-02 1.5400D-01 2.2600D-01 1.3340D-01
COLUMN 5 ROWS 1 THRU 16 -----
ROW
1) 1.6200D-02 4.4200D-02 7.9000D-03 0.0000D+00 1.0000D-04 3.7000D-03 4.4000D-03 1.9570D-01 9.0900D-02 5.4000D-03
11) 3.6250D-01 5.9000D-02 3.7000D-03 2.0540D-01 3.0100D-02 4.2200D-02

```

MATRIX QUAL (GINO NAME 102) IS A DB PREC 5 COLUMN X 16 ROW RECTANG MATRIX.

```

COLUMN 1 ROWS 1 THRU 16 -----
ROW
1) 1.9545D+00 1.9573D+02 6.4900D-02 1.0714D+00 1.3000D-02 1.2403D+00 6.5000D-03 3.1820D-01 1.0000D+01 7.7900D-02
11) 5.3900D-01 2.7383D+01 5.8400D-02 5.3597D+01 1.2708D+01 1.1007D+01
COLUMN 2 ROWS 1 THRU 16 -----
ROW
1) 1.5474D+00 1.3680D-01 2.2110D-01 2.0632D+00 2.6190D+01 2.6211D+00 9.1158D+00 5.6840D-01 6.2105D+00 4.8863D+01
11) 5.1580D-01 1.7842D+01 5.9189D+01 4.6526D+00 3.0211D+00 4.4389D+01
COLUMN 3 ROWS 1 THRU 16 -----
ROW
1) 1.7789D+00 2.8821D+01 2.7370D-01 2.1050D-01 1.8737D+00 2.6211D+00 9.5684D+00 6.8420D-01 4.8842D+00 5.3779D+01
11) 5.6840D-01 1.7842D+01 6.5158D+01 4.2316D+00 3.1684D+00 5.1263D+01
COLUMN 4 ROWS 1 THRU 16 -----
ROW
1) 2.9119D+00 3.3627D+00 6.6684D+00 1.6373D+00 1.0000D-04 1.5030D-01 3.8860D-01 4.7072D+01 1.0142D+02 3.8860D-01
11) 5.7031D+01 1.7192D+01 2.6218D+00 7.9793D+00 1.1710D+01 6.9119D+00
COLUMN 5 ROWS 1 THRU 16 -----

```

ROW
 1) 7.9020D-01 2.1561D+00 3.8540D-01 0.0000D+00 4.6000D-03 1.8050D-01 2.1460D-01 9.5463D+00 4.4341D+00 2.6340D-01
 11) 1.7683D+01 2.8780D+00 1.8050D-01 1.0019D+01 1.4683D+00 2.0585D+00

TABLE MODELST LINES CONTAINING BINARY ZERO HAVE BEEN DELETED.

RECORD NO.	0	MODE	LST	
1)				END OF 2 WORD RECORD.
RECORD NO.	1		1	
1)				END OF 1 WORD RECORD.
RECORD NO.	2		3	
1)				END OF 1 WORD RECORD.
RECORD NO.	3		4	
1)				END OF 1 WORD RECORD.
RECORD NO.	4		5	
1)				END OF 1 WORD RECORD.
RECORD NO.	5		7	
1)				END OF 1 WORD RECORD.
RECORD NO.	6			

MATRIX KANIL (GINO NAME 101) IS A DB PREC 16 COLUMN X 16 ROW SYMMETRIC MATRIX.

COLUMN	1	ROWS	1 THRU	16
ROW				
1)	3.8671D+03	-2.0657D+01	-7.3996D+01	-7.4112D+00
11)	3.3613D+02	4.2935D+01	3.4230D+02	8.7708D+00
COLUMN	2	ROWS	1 THRU	16
ROW				
1)	3.8671D+03	-2.0657D+01	-7.3996D+01	-7.4112D+00
11)	3.3613D+02	4.2935D+01	3.4230D+02	8.7708D+00

1) 3.8671D+03 -2.0657D+01 -7.3996D+01 -7.4112D+00 5.1865D+00 1.9035D+01 -2.3374D+01 3.1034D+01 -5.9529D+01 -4.5280D+02
 11) 3.3613D+02 4.2935D+01 3.4230D+02 8.7708D+00 9.7407D+01 2.1891D+01

1)	-2.0657D+01	1.1612D+06	5.6098D+04	-4.4039D+03	-3.5291D+02	1.6954D+04	2.8885D+04	-3.4433D+04	8.4153D+02	-3.5928D+04
11)	2.4570D+03	2.5181D+03	2.7903D+04	4.4918D+02	-5.4554D+02	2.5468D+03				
COLUMN	3	ROWS	1 THRU	16						
ROW										
1)	-7.3996D+01	5.6098D+04	6.6848D+05	-5.3680D+02	-7.6624D+02	-1.6434D+05	-3.4315D+04	9.7597D+04	-2.9133D+03	7.8853D+04
11)	-1.9072D+02	-5.7651D+03	-8.3565D+04	-9.9919D+02	1.1514D+04	-9.1975D+03				
COLUMN	4	ROWS	1 THRU	16						
ROW										
1)	-7.4112D+00	-4.4039D+03	-5.3680D+02	6.1152D+04	5.4529D+01	-6.7732D+00	4.7967D+02	9.2308D+01	-1.4662D+02	-2.4044D+03
11)	6.0953D+02	-3.6998D+01	-8.8820D+02	3.2007D+01	4.5661D+02	-1.2759D+02				
COLUMN	5	ROWS	1 THRU	16						
ROW										
1)	5.1865D+00	-3.5291D+02	-7.6624D+02	5.4529D+01	3.7159D+03	-3.4397D+02	3.2681D+02	-1.6049D+02	1.2256D+01	1.0354D+02
11)	-7.6812D+01	-2.0134D+01	1.3845D+02	-1.0126D+01	-4.5209D+02	1.1936D+02				
COLUMN	6	ROWS	1 THRU	16						
ROW										
1)	1.9035D+01	1.6954D+04	-1.6434D+05	-6.7732D+00	-3.4397D+02	3.6545D+05	6.7727D+04	-1.2481D+04	1.5790D+02	-3.1010D+03
11)	-5.2188D+02	7.4158D+02	1.6002D+04	8.9645D+01	-2.5177D+03	1.5953D+03				
COLUMN	7	ROWS	1 THRU	16						
ROW										
1)	-2.3374D+01	2.8885D+04	-3.4315D+04	4.7967D+02	3.2681D+02	6.7727D+04	9.0132D+04	-4.3566D+03	-1.3932D+03	-1.4157D+04
11)	5.1488D+02	-8.4996D+02	-3.7928D+03	7.0838D+01	7.2565D+02	-6.0361D+02				
COLUMN	8	ROWS	1 THRU	16						
ROW										
1)	3.1034D+01	-3.4433D+04	9.7597D+04	9.2308D+01	-1.6049D+02	-1.2481D+04	-4.3566D+03	1.2474D+06	-1.7072D+04	-5.4062D+05
11)	-1.1210D+06	3.3808D+04	4.7816D+05	2.2641D+03	-4.3674D+04	6.3870D+04				
COLUMN	9	ROWS	1 THRU	16						
ROW										
1)	-5.9529D+01	8.4153D+02	-2.9133D+03	-1.4662D+02	1.2256D+01	1.5790D+02	-1.3932D+03	-1.7072D+04	4.1165D+04	1.6283D+04
11)	1.6305D+04	-1.3414D+04	4.1969D+03	2.3854D+03	1.5578D+04	-1.5196D+04				
COLUMN	10	ROWS	1 THRU	16						
ROW										
1)	-4.5280D+02	-3.5928D+04	7.8853D+04	-2.4044D+03	1.0354D+02	-3.1010D+03	-1.4157D+04	-5.4062D+05	1.6283D+04	8.7135D+05
11)	4.9368D+05	-2.4685D+04	-7.5362D+05	1.4740D+04	1.0351D+05	-5.9858D+04				
COLUMN	11	ROWS	1 THRU	16						
ROW										

```

1) 3.3613D+02 2.4570D+03 -1.9072D+02 6.0953D+02 -7.6812D+01 -5.2188D+02 5.1488D+02 -1.1210D+06 1.6305D+04 4.9368D+05
11) 1.2568D+06 -3.5982D+04 -4.5721D+05 -1.6238D+04 -3.7406D+04 -3.7624D+04
COLUMN 12 ROWS 1 THRU 16
ROW
1) 4.2935D+01 2.5181D+03 -5.7651D+03 -3.6998D+01 -2.0134D+01 7.4158D+02 -8.4996D+02 3.3808D+04 -1.3414D+04 -2.4685D+04
11) -3.5982D+04 7.1406D+04 -4.9610D+04 -1.6680D+03 -3.5564D+04 7.9086D+04
COLUMN 13 ROWS 1 THRU 16
ROW
1) 3.4230D+02 2.7903D+04 -8.3565D+04 -8.8820D+02 1.3845D+02 1.6002D+04 -3.7928D+03 4.7816D+05 4.1969D+03 -7.5362D+05
11) -4.5721D+05 -4.9610D+04 9.2113D+05 -1.7488D+04 3.3436D+04 -1.2285D+05
COLUMN 14 ROWS 1 THRU 16
ROW
1) 8.7708D+00 4.4918D+02 -9.9919D+02 3.2007D+01 -1.0126D+01 8.9645D+01 7.0838D+01 2.2641D+03 2.3854D+03 1.4740D+04
11) -1.6238D+04 -1.6680D+03 -1.7488D+04 2.0310D+04 7.8234D+03 2.8202D+03
COLUMN 15 ROWS 1 THRU 16
ROW
1) 9.7407D+01 -5.4554D+02 1.1514D+04 4.5661D+02 -4.5209D+02 -2.5177D+03 7.2565D+02 -4.3674D+04 1.5578D+04 1.0351D+05
11) -3.7406D+04 -3.5564D+04 3.3436D+04 7.8234D+03 3.0858D+05 -1.3776D+05
COLUMN 16 ROWS 1 THRU 16
ROW
1) 2.1891D+01 2.5468D+03 -9.1975D+03 -1.2759D+02 1.1936D+02 1.5953D+03 -6.0361D+02 6.3870D+04 -1.5196D+04 -5.9858D+04
11) -3.7624D+04 7.9086D+04 -1.2285D+05 2.8202D+03 -1.3776D+05 1.8628D+05

```

124

MATRIX MAN1 (GINO NAME 102) IS A DB PREC 16 COLUMN X 16 ROW SYMMETRIC MATRIX.

```

COLUMN 1 ROWS 1 THRU 16
ROW
1) 2.1498D-04 1.1474D-05 3.4248D-05 -7.3988D-06 -1.1946D-05 -4.7151D-06 9.4154D-06 -6.5352D-07 3.3069D-05 1.9741D-04
11) -1.1337D-04 -4.7335D-05 -1.2346D-04 1.4512D-05 -2.6013D-05 1.9260D-06
COLUMN 2 ROWS 1 THRU 16
ROW
1) 1.1474D-05 8.6888D-02 -3.3489D-02 -4.3884D-03 1.2517D-03 7.9264D-03 7.5349D-03 1.4136D-02 7.7877D-04 1.5528D-02
11) 1.4323D-04 -2.9089D-03 -1.1613D-02 -3.4713D-05 9.0842D-04 -5.6998D-04
COLUMN 3 ROWS 1 THRU 16
ROW
1) 3.4248D-05 -3.3489D-02 1.4913D-01 2.0343D-03 3.1252D-03 -3.2952D-02 -1.6788D-02 -2.5516D-02 -1.9537D-03 -2.3435D-02

```

11) -2.1915D-03 5.8976D-03 2.3711D-02 1.5904D-04 -4.1198D-03 1.2964D-03
 COLUMN 4 ROWS 1 THRU 16 -----
 ROW
 1) -7.3988D-06 -4.3884D-03 2.0343D-03 1.0323D-01 -2.8328D-05 -3.5922D-03 -6.5172D-03 -6.5542D-04 -2.8206D-04 -3.6276D-03
 11) 4.1680D-04 -1.0015D-04 -1.1278D-03 3.5936D-05 4.1441D-04 -1.4184D-04
 COLUMN 5 ROWS 1 THRU 16 -----
 ROW
 1) -1.1946D-05 1.2517D-03 3.1252D-03 -2.8328D-05 1.8593D-02 -5.2408D-05 -2.6952D-04 1.1403D-04 5.3151D-05 3.3964D-04
 11) 5.9529D-05 6.5182D-05 2.4741D-04 3.2685D-05 8.7125D-04 -2.1359D-04
 COLUMN 6 ROWS 1 THRU 16 -----
 ROW
 1) -4.7151D-06 7.9264D-03 -3.2952D-02 -3.5922D-03 -5.2408D-05 7.5134D-02 1.5327D-02 4.4501D-03 2.6133D-04 1.0073D-03
 11) 4.8323D-04 -6.8106D-04 -6.4003D-03 -7.7844D-06 8.6458D-04 -3.6762D-04
 COLUMN 7 ROWS 1 THRU 16 -----
 ROW
 1) 9.4154D-06 7.5349D-03 -1.6788D-02 -6.5172D-03 -2.6952D-04 1.5327D-02 2.9972D-02 2.1831D-03 5.2307D-04 5.6888D-03
 11) -1.0471D-04 1.1866D-03 9.8319D-04 -2.8679D-05 -5.6658D-05 3.4798D-04
 COLUMN 8 ROWS 1 THRU 16 -----
 ROW
 1) -6.5352D-07 1.4136D-02 -2.5516D-02 -6.5542D-04 1.1403D-04 4.4501D-03 2.1831D-03 7.3821D-02 1.4427D-02 1.1456D-02
 11) 2.7883D-02 -2.8773D-02 -1.4322D-02 -3.5552D-03 3.5539D-03 1.5541D-03
 COLUMN 9 ROWS 1 THRU 16 -----
 ROW
 1) 3.3069D-05 7.7877D-04 -1.9537D-03 -2.8206D-04 5.3151D-05 2.6133D-04 5.2307D-04 1.4427D-02 9.0869D-02 4.3707D-05
 11) 2.8452D-02 -2.1364D-02 -1.8016D-02 -2.5306D-03 -2.1041D-03 4.1713D-03
 COLUMN 10 ROWS 1 THRU 16 -----
 ROW
 1) 1.9741D-04 1.5528D-02 -2.3435D-02 -3.6276D-03 3.3964D-04 1.0073D-03 5.6888D-03 1.1456D-02 4.3707D-05 1.6865D-01
 11) -4.8164D-02 -8.1359D-04 -3.5273D-02 4.4427D-03 -1.3826D-02 8.9411D-03
 COLUMN 11 ROWS 1 THRU 16 -----
 ROW
 1) -1.1337D-04 1.4323D-04 -2.1915D-03 4.1680D-04 5.9529D-05 4.8323D-04 -1.0471D-04 2.7883D-02 2.8452D-02 -4.8164D-02
 11) 9.8396D-02 -2.4335D-02 5.3628D-02 4.4527D-03 8.4815D-03 -2.0186D-03
 COLUMN 12 ROWS 1 THRU 16 -----
 ROW
 1) -4.7335D-05 -2.9089D-03 5.8976D-03 -1.0015D-04 6.5182D-05 -6.8106D-04 1.1866D-03 -2.8773D-02 -2.1364D-02 -8.1359D-04

```

11) -2.4335D-02 1.2638D-01 3.7316D-03 1.9650D-03 9.2482D-05 -8.6108D-03
COLUMN 13 ROWS 1 THRU 16 -----
ROW
1) -1.2346D-04 -1.1613D-02 2.3711D-02 -1.1278D-03 2.4741D-04 -6.4003D-03 9.8319D-04 -1.4322D-02 -1.8016D-02 -3.5273D-02
11) 5.3628D-02 3.7316D-03 1.9667D-01 1.7474D-04 1.1483D-02 -5.3984D-02
COLUMN 14 ROWS 1 THRU 16 -----
ROW
1) 1.4512D-05 -3.4713D-05 1.5904D-04 3.5936D-05 3.2685D-05 -7.7844D-06 -2.8679D-05 -3.5552D-03 -2.5306D-03 4.4427D-03
11) 4.4527D-03 1.9650D-03 1.7474D-04 3.6820D-02 -6.4626D-03 -2.5253D-03
COLUMN 15 ROWS 1 THRU 16 -----
ROW
1) -2.6013D-05 9.0842D-04 -4.1198D-03 4.1441D-04 8.7125D-04 8.6458D-04 -5.6658D-05 3.5539D-03 -2.1041D-03 -1.3826D-02
11) 8.4815D-03 9.2482D-05 1.1483D-02 -6.4626D-03 5.0436D-02 2.5864D-03
COLUMN 16 ROWS 1 THRU 16 -----
ROW
1) 1.9260D-06 -5.6998D-04 1.2964D-03 -1.4184D-04 -2.1359D-04 -3.6762D-04 3.4798D-04 1.5541D-03 4.1713D-03 8.9411D-03
11) -2.0186D-03 -8.6108D-03 -5.3984D-02 -2.5253D-03 2.5864D-03 1.0898D-01

```

MATRIX PHIANL (GINO NAME 103) IS A DB PREC 8 COLUMN X 16 ROW RECTANG MATRIX.

```

COLUMN 1 ROWS 1 THRU 16 -----
ROW
1) -2.0390D-02 -2.9741D-03 6.0337D-03 -2.6834D-02 5.7581D-01 5.1606D-02 -1.4163D-01 -2.8924D-03 2.5953D-01 -5.3506D-01
11) -1.2321D-03 2.0291D+00 -5.4832D-01 7.9818D-01 -4.1638D-01 -1.8812D+00
COLUMN 2 ROWS 1 THRU 16 -----
ROW
1) 1.6751D-02 -4.2170D-03 -1.6228D-02 9.9353D-03 -7.3013D+00 -2.5647D-02 5.4394D-02 -1.0754D-02 3.7587D-03 2.2656D-02
11) -1.2500D-02 1.8885D-01 1.7963D-02 7.8973D-02 -6.2965D-02 -1.1801D-01
COLUMN 3 ROWS 1 THRU 16 -----
ROW
1) -1.3929D-02 1.0017D-02 -5.0975D-02 -5.6374D-02 -2.3845D-01 1.3200D-01 -4.4590D-01 1.2146D-01 1.4153D+00 -1.3640D+00
11) 6.4580D-02 -7.2944D-01 -1.4184D+00 -1.1010D+00 1.1620D-01 -9.1261D-01
COLUMN 4 ROWS 1 THRU 16 -----
ROW
1) 6.6384D-02 -2.6449D-03 7.2103D-03 -2.7374D-02 6.3013D-02 -1.2620D-01 4.6273D-01 1.2371D-01 2.8147D+00 9.4575D-01
11) 9.7476D-02 1.1681D+00 9.2036D-01 -1.1112D+00 -6.2654D-02 6.9132D-01

```

```

COLUMN 5      ROWS 1 THRU 16 -----
ROW
1) -7.3509D-02 2.3418D-02 -1.0242D-01 -7.8287D-02 -1.0766D-02 -2.6540D-02 2.3503D-02 6.2523D-01 7.1045D-01 -3.3952D-02
11) 6.9329D-01 -3.1868D-01 6.9396D-02 4.5793D+00 -2.4138D-02 4.6949D-02 -----
COLUMN 6      ROWS 1 THRU 16 -----
ROW
1) 5.6387D-03 7.5389D-03 1.0231D-02 3.0995D+00 1.5636D-02 1.1812D-02 -1.7484D-01 -1.1712D-02 1.2787D-01 4.9934D-02
11) -6.7468D-03 3.0439D-02 5.7459D-02 1.1632D-01 -1.3166D-02 5.2326D-02 -----
COLUMN 7      ROWS 1 THRU 16 -----
ROW
1) 3.3307D-01 -1.3593D-01 5.7308D-01 -7.6579D-02 -1.5671D-02 1.5244D-01 -1.1059D-01 -1.9456D+00 1.2244D+00 -7.2994D-02
11) -1.8957D+00 -7.2654D-01 -6.2958D-03 1.4223D+00 -7.7325D-01 3.6275D-01 -----
COLUMN 8      ROWS 1 THRU 16 -----
ROW
1) -2.7057D-01 -7.4609D-02 2.5817D-01 -8.3060D-02 -1.5591D-01 2.0087D-01 -4.4668D-01 -1.8755D-01 -3.7695D-02 -8.3594D-01
11) 2.4506D-01 1.2866D+00 -2.8782D-01 8.7656D-01 1.7506D+00 1.9821D+00 -----

```

MATRIX LAMAT (GJNO NMME 104) IS A REAL 5 COLUMN X 8 ROW RECTANG MATRIX.

```

COLUMN 1      ROWS 1 THRU 8 -----
ROW
1) 1.7442E+05 1.9932E+05 3.0664E+05 4.6303E+05 5.0159E+05 5.8989E+05 1.0519E+06 1.3753E+06
COLUMN 2      ROWS 1 THRU 8 -----
ROW
1) 4.1763E+02 4.4645E+02 5.5375E+02 6.8046E+02 7.0823E+02 7.6804E+02 1.0256E+03 1.1727E+03
COLUMN 3      ROWS 1 THRU 8 -----
ROW
1) 6.6468E+01 7.1055E+01 8.8132E+01 1.0830E+02 1.1272E+02 1.2224E+02 1.6323E+02 1.8664E+02
COLUMN 4      ROWS 1 THRU 8 -----
ROW
1) 1.0000E+00 1.0000E+00 1.0000E+00 1.0000E+00 1.0000E+00 1.0000E+00 1.0000E+00 1.0000E+00
COLUMN 5      ROWS 1 THRU 8 -----
ROW
1) 1.7442E+05 1.9932E+05 3.0664E+05 4.6303E+05 5.0159E+05 5.8989E+05 1.0519E+06 1.3753E+06

```

MATRIX LAMDA (GINO NAME 101) IS A REAL 5 COLUMN X 5 ROW SQUARE MATRIX.

COLUMN	ROWS	1 THRU	5			
ROW						
1)	1	1.7442E+05	3.0664E+05	4.6303E+05	5.0159E+05	1.0519E+06
COLUMN	ROWS	1 THRU	5			
ROW						
1)	1	4.1763E+02	5.5375E+02	6.8046E+02	7.0823E+02	1.0256E+03
COLUMN	ROWS	1 THRU	5			
ROW						
1)	1	6.6468E+01	8.8132E+01	1.0830E+02	1.1272E+02	1.6323E+02
COLUMN	ROWS	1 THRU	5			
ROW						
1)	1	1.0000E+00	1.0000E+00	1.0000E+00	1.0000E+00	1.0000E+00
COLUMN	ROWS	1 THRU	5			
ROW						
1)	1	1.7442E+05	3.0664E+05	4.6303E+05	5.0159E+05	1.0519E+06

MATRIX PHURED (GINO NAME 102) IS A DB PREC 16 COLUMN X 16 ROW RECTANG MATRIX.

COLUMN	ROWS	1 THRU	16								
ROW											
1)	1	-2.0390D-02	-2.9741D-03	6.0337D-03	-2.6834D-02	5.7581D-01	5.1606D-02	-1.4163D-01	-2.8924D-03	2.5953D-01	-5.3506D-01
11)	1	-1.2321D-03	2.0291D+00	-5.4832D-01	7.9818D-01	-4.1638D-01	-1.8812D+00				
COLUMN	ROWS	1 THRU	16								
ROW											
1)	1	-1.3929D-02	1.0017D-02	-5.0975D-02	-5.6374D-02	-2.3845D-01	1.3200D-01	-4.4590D-01	1.2146D-01	1.4153D+00	-1.3640D+00
11)	1	6.4580D-02	-7.2944D-01	-1.4184D+00	-1.1010D+00	1.1620D-01	-9.1261D-01				
COLUMN	ROWS	1 THRU	16								
ROW											
1)	1	6.6384D-02	-2.6449D-03	7.2103D-03	-2.7374D-02	6.3013D-02	-1.2620D-01	4.6273D-01	1.2371D-01	2.8147D+00	9.4575D-01
11)	1	9.7476D-02	1.1681D+00	9.2036D-01	-1.1112D+00	-6.2654D-02	6.9132D-01				
COLUMN	ROWS	1 THRU	16								
ROW											
1)	1	-7.3509D-02	2.3418D-02	-1.0242D-01	-7.8287D-02	-1.0766D-02	-2.6540D-02	2.3503D-02	6.2523D-01	7.1045D-01	-3.3952D-02
11)	1	6.9329D-01	-3.1868D-01	6.9396D-02	4.5793D+00	-2.4138D-02	4.6949D-02				
COLUMN	ROWS	1 THRU	16								

ROW
 1) 3.3307D-01 -1.3593D-01 5.7308D-01 -7.6579D-02 -1.5671D-02 1.5244D-01 -1.1059D-01 -1.9456D+00 1.2244D+00 -7.2994D-02
 11) -1.8957D+00 -7.2654D-01 -6.2958D-03 1.4223D+00 -7.7325D-01 3.6275D-01

MATRIX NDIR (GINO NAME 101) IS A DB PREC 5 COLUMN X 16 ROW RECTANG MATRIX.
 COLUMN 1 ROWS 1 THRU 16

ROW
 1) -1.0000D+00 -1.0000D+00 1.0000D+00 -1.0000D+00 1.0000D+00 1.0000D+00 -1.0000D+00 -1.0000D+00 1.0000D+00 -1.0000D+00
 11) -1.0000D+00 1.0000D+00 -1.0000D+00 1.0000D+00 -1.0000D+00 -1.0000D+00 1.0000D+00 -1.0000D+00

COLUMN 2 ROWS 1 THRU 16

ROW
 1) -1.0000D+00 1.0000D+00 -1.0000D+00 -1.0000D+00 1.0000D+00 -1.0000D+00 1.0000D+00 -1.0000D+00 1.0000D+00 -1.0000D+00
 11) 1.0000D+00 -1.0000D+00 -1.0000D+00 -1.0000D+00 1.0000D+00 -1.0000D+00 -1.0000D+00

COLUMN 3 ROWS 1 THRU 16

ROW
 1) 1.0000D+00 -1.0000D+00 1.0000D+00 1.0000D+00 -1.0000D+00 1.0000D+00 -1.0000D+00 1.0000D+00 1.0000D+00 1.0000D+00
 11) 1.0000D+00 1.0000D+00 1.0000D+00 -1.0000D+00 -1.0000D+00 -1.0000D+00 1.0000D+00

COLUMN 4 ROWS 1 THRU 16

ROW
 1) -1.0000D+00 1.0000D+00 -1.0000D+00 -1.0000D+00 -1.0000D+00 1.0000D+00 -1.0000D+00 1.0000D+00 1.0000D+00 -1.0000D+00
 11) 1.0000D+00 -1.0000D+00 1.0000D+00 1.0000D+00 -1.0000D+00 -1.0000D+00 1.0000D+00

MATRIX ACCEL (GINO NAME 101) IS A DB PREC 5 COLUMN X 16 ROW RECTANG MATRIX.
 COLUMN 1 ROWS 1 THRU 16

ROW
 1) -2.8729D+03 -2.8770D+05 9.5422D+01 -1.5749D+03 1.9099D+01 1.8231D+03 -3.0198D+01 -4.6771D+02 1.4699D+04 -1.1452D+02
 11) -7.9224D+02 4.0250D+04 -8.5872D+01 7.8782D+04 -1.8679D+04 -1.6178D+04

COLUMN 2 ROWS 1 THRU 16

ROW
 1) -2.0571D+03 1.8189D+02 -2.9389D+02 -2.7427D+03 -3.4816D+04 3.4844D+03 -1.2118D+04 7.5563D+02 8.2561D+03 -6.4957D+04

```

11) 6.8568D+02 -2.3719D+04 -7.8685D+04 -6.1851D+03 4.0161D+03 -5.9010D+04
COLUMN 3 ROWS 1 THRU 16
ROW
1) 2.6215D+03 -4.2472D+04 4.0332D+02 -3.1022D+02 2.7611D+03 -3.8625D+03 1.4100D+04 1.0083D+03 7.1976D+03 7.9251D+04
11) 8.3763D+02 2.6293D+04 9.6019D+04 -6.2358D+03 -4.6691D+03 7.5543D+04
COLUMN 4 ROWS 1 THRU 16
ROW
1) -6.2398D+03 7.2058D+03 -1.4289D+04 -3.5085D+03 -1.5425D+00 -3.2203D+02 8.3272D+02 1.0087D+05 2.1732D+05 -8.3272D+02
11) 1.2221D+05 -3.6839D+04 5.6181D+03 1.7098D+04 -2.5092D+04 1.4811D+04
COLUMN 5 ROWS 1 THRU 16
ROW
1) 2.1001D+03 -5.7302D+03 1.0242D+03 0.0000D+00 -1.2589D+01 4.7969D+02 -5.7038D+02 -2.5371D+04 1.1784D+04 -7.0005D+02
11) -4.6995D+04 -7.6488D+03 -4.7969D+02 2.6628D+04 -3.9022D+03 5.4708D+03

```

```

^^^CALCULATION OF STATIC MODE SHAPE = 1
^^^EIGENVALUE = 1.744163E+05
^^^CALCULATION OF STATIC MODE SHAPE = 3
^^^EIGENVALUE = 3.066401E+05
^^^CALCULATION OF STATIC MODE SHAPE = 4
^^^EIGENVALUE = 4.630260E+05
^^^CALCULATION OF STATIC MODE SHAPE = 5
^^^EIGENVALUE = 5.015862E+05
^^^CALCULATION OF STATIC MODE SHAPE = 7
^^^EIGENVALUE = 1.051898E+06

```

MATRIX PHITST (GINO NAME 101) IS A DB PREC 5 COLUMN X 16 ROW RECTANG MATRIX.

```

COLUMN 1 ROWS 1 THRU 16
ROW
1) -1.1470D-02 -2.0486D-01 2.1794D-01 1.2585D-01 -7.7756D-01 8.0133D-02 -1.5914D-01 -2.8153D-01 3.0109D-01 -3.2671D-01
11) -1.7262D-01 1.9754D+00 -1.8255D-01 1.7751D+00 -4.5812D-01 -1.4264D+00
COLUMN 2 ROWS 1 THRU 16
ROW
1) -2.5013D-02 1.0259D-02 -5.1080D-02 -6.8619D-02 -2.4554D-01 1.5431D-01 -5.2616D-01 6.6025D-02 5.8618D-01 -1.5778D+00
11) 1.3066D-02 -1.0289D+00 -1.6358D+00 -6.5633D-01 1.3180D-01 -1.0479D+00

```



```

COLUMN      3      ROWS      1 THRU      16      -----
ROW
1) 4.4640D-02 -7.0581D-02 7.8078D-02 -1.8496D-02 5.1734D-02 -8.0252D-02 3.2179D-01 7.6714D-02 2.7574D+00 9.2387D-01
11) 9.5708D-02 1.1566D+00 9.8107D-01 -1.4519D+00 -7.3473D-02 6.5690D-01
COLUMN      4      ROWS      1 THRU      16      -----
ROW
1) -1.5584D-01 5.7639D-02 -2.3027D-01 -1.5662D-02 -1.0518D-03 -5.4184D-02 2.5632D-02 1.1572D+00 3.3581D-01 4.2169D-02
11) 1.2048D+00 -2.1624D-01 1.2601D-01 3.8738D+00 4.4765D-04 -2.2371D-01
COLUMN      5      ROWS      1 THRU      16      -----
ROW
1) 3.5479D-01 -1.1745D-01 4.0653D-01 -6.4960D-02 1.2444D-02 9.5565D-02 -2.0904D-02 -1.9133D+00 1.2195D+00 -3.0744D-02
11) -1.9641D+00 -6.6454D-01 -1.1082D-01 1.4979D+00 -6.7011D-01 4.1274D-01

```

MATRIX COC (GINO NAME 101) IS A DB PREC 5 COLUMN X 5 ROW SQUARE MATRIX.

```

COLUMN      1      ROWS      1 THRU      5      -----
ROW
1) 9.3348D-01 -1.8541D-01 9.4840D-03 1.2227D-01 1.7024D-01
COLUMN      2      ROWS      1 THRU      5      -----
ROW
1) -7.5754D-09 9.5914D-01 -2.8186D-01 1.2019D-02 1.4342D-02
COLUMN      3      ROWS      1 THRU      5      -----
ROW
1) 2.7085D-08 4.5976D-08 9.9551D-01 -6.6078D-02 -4.4689D-03
COLUMN      4      ROWS      1 THRU      5      -----
ROW
1) 2.6309D-08 -3.0715D-08 1.5382D-08 9.5514D-01 -2.8113D-01
COLUMN      5      ROWS      1 THRU      5      -----
ROW
1) -9.0502D-09 9.4404D-09 -4.5419D-09 -4.1090D-09 9.9406D-01

```

^^CROSS ORTHOGONALITY COMPUTATION COMPLETE

*** END OF JOB ***

REPORT DOCUMENTATION PAGE

Form Approved
OMB No. 0704-0188

Public reporting burden for this collection of information is estimated to average 1 hour per response, including the time for reviewing instructions, searching existing data sources, gathering and maintaining the data needed, and completing and reviewing the collection of information. Send comments regarding this burden estimate or any other aspect of this collection of information, including suggestions for reducing this burden, to Washington Headquarters Services, Directorate for Information Operations and Reports, 1215 Jefferson Davis Highway, Suite 1204, Arlington, VA 22202-4302, and to the Office of Management and Budget, Paperwork Reduction Project (0704-0188), Washington, DC 20503.

1. AGENCY USE ONLY (Leave blank)	2. REPORT DATE November 1994	3. REPORT TYPE AND DATES COVERED Technical Memorandum	
4. TITLE AND SUBTITLE Correlation of Finite Element Free Vibration Predictions Using Random Vibration Test Data		5. FUNDING NUMBERS WU-None	
6. AUTHOR(S) Jeffrey A. Chambers		7. PERFORMING ORGANIZATION NAME(S) AND ADDRESS(ES) National Aeronautics and Space Administration Lewis Research Center Cleveland, Ohio 44135-3191	
8. PERFORMING ORGANIZATION REPORT NUMBER E-9243		9. SPONSORING/MONITORING AGENCY NAME(S) AND ADDRESS(ES) National Aeronautics and Space Administration Washington, D.C. 20546-0001	
10. SPONSORING/MONITORING AGENCY REPORT NUMBER NASA TM-106787		11. SUPPLEMENTARY NOTES This report was submitted as a dissertation in partial fulfillment of the requirements for the degree Master of Science in Engineering Mechanics to Cleveland State University, Cleveland, Ohio, June 1994. Responsible person, Jeffrey A. Chambers, organization code 4320, (216) 433-8612.	
12a. DISTRIBUTION/AVAILABILITY STATEMENT Unclassified - Unlimited Subject Category 39		12b. DISTRIBUTION CODE	
13. ABSTRACT (Maximum 200 words) Finite element analysis is regularly used during the engineering cycle of mechanical systems to predict the response to static, thermal, and dynamic loads. The finite element model (FEM) used to represent the system is often correlated with physical test results to determine the validity of analytical results provided. Results from dynamic testing provide one means for performing this correlation. One of the most common methods of measuring accuracy is by classical modal testing, whereby vibratory mode shapes are compared to mode shapes provided by finite element analysis. The degree of correlation between the test and analytical mode shapes can be shown mathematically using the cross orthogonality check. A great deal of time and effort can be exhausted in generating the set of test acquired mode shapes needed for the cross orthogonality check. In most situations response data from vibration tests are digitally processed to generate the mode shapes from a combination of modal parameters, forcing functions, and recorded response data. An alternate method is proposed in which the same correlation of analytical and test acquired mode shapes can be achieved without conducting the modal survey. Instead a procedure is detailed in which a minimum of test information, specifically the acceleration response data from a random vibration test, is used to generate a set of equivalent local accelerations to be applied to the reduced analytical model at discrete points corresponding to the test measurement locations. The static solution of the analytical model then produces a set of deformations that once normalized can be used to represent the test acquired mode shapes in the cross orthogonality relation. The method proposed has been shown to provide accurate results for both a simple analytical model as well as a complex space flight structure.			
14. SUBJECT TERMS Random vibration; Modal analysis; Vibration; Vibration testing; Loads and vibration; Structures		15. NUMBER OF PAGES 145	
17. SECURITY CLASSIFICATION OF REPORT Unclassified		16. PRICE CODE A07	
18. SECURITY CLASSIFICATION OF THIS PAGE Unclassified	19. SECURITY CLASSIFICATION OF ABSTRACT Unclassified	20. LIMITATION OF ABSTRACT	